Investigating the Effects of Hybrid Fibres on the Structural Behaviour of Two-Way Slabs

By

© Ramin Pourreza, B.Sc. (Eng.), M.Sc. (Eng.)

A thesis submitted to the School of Graduate Studies in partial fulfillment of the requirements for the degree of Master of Engineering

FACULTY OF ENGINEERING AND APPLIED SCIENCE

MEMORIAL UNIVERSITY OF NEWFOUNDLAND

May 2014

St. John's Newfoundland Canada

“In god we trust”

To my parents;

Abstract

This research is conducted to examine the effects of hybrid fibres on the performance of two-way slabs. The hybrid fibres were a cocktail of steel and macro-synthetic fibres. An experimental investigation was carried out to examine the structural behaviour of hybrid-fibre-reinforced concrete (HFRC) two-way slabs under static loading conditions.

A literature review was carried out on slab-column connections made with steel-fibre-reinforced concrete (SFRC). The major experimental findings of previous research were discussed and the data were collected into a databank. The review of the results revealed a large scatter in the data. Nonetheless, there was an apparent size effect in the specimens. The expressions proposed to predict the capacity of the SFRC slabs gave a significant degree of scatter when evaluated using all the test results in the database.

In the current study, eight full-scale interior slab-column connections with side dimensions of 1900 mm were prepared and tested. The slabs were all simply supported along four edges and loaded through a 250 × 250 mm central column. The steel fibre

volume fraction (0 to 0.96%) and the slab thickness (200 and 250 mm) were the main variables. The structural behaviour of the test slabs was investigated with regard to load-deflection characteristics, deflection profiles, steel reinforcement and concrete strains, crack patterns, modes of failure, and punching-shear capacity.

The test results revealed that an increase in fibre content enhanced the stiffness, energy-absorption, and the capacity of the test specimens. The results also confirmed that using HFRC caused a decrease in the steel strain due to the contribution of HFRC in tension. The addition of hybrid fibres, up to 0.96%, increased the shear strength of the 200 and 250 mm-thick slabs, by 32 and 20%, respectively, compared to the reference slabs. The addition of hybrid fibres caused a ductile punching failure in the slabs. The ductility increased by 154 and 157% with the addition of fibres up to 0.96% for the 200 and 250 mm-thick slabs, respectively. The experimental observations confirmed that the contribution of fibres in the 200 mm-thick slabs was more pronounced than in the case of the 250 mm-thick ones. The results revealed that as the thickness of the test slabs increased, the fibres had less effect on enhancing the capacity of the slabs.

Finally, the existing equations for predicting the capacity of SFRC two-way slabs were evaluated using the experimental results from this research. In general, the equations produced a small scatter in the predicted results. The equation proposed by Narayanan and Darwish gave a reasonably safe prediction with least scatter compared to the prediction of Hiroshi Higashiyama et al. which gave the safest prediction, however, it had a large scatter.

Acknowledgement

The author wishes to express his deep appreciation to his supervisors Dr. A. Hussein and Dr. H. Marzouk for their excellent supervision, keen guidance, and financial support. Partial funding from Mitacs is gratefully appreciated. The completion of this thesis would not have been possible without the patience and invaluable help of the technical staff of the structural laboratory at Memorial University, specifically S. Organ and M. Curtis.

Sincere thanks are due to the Concrete Products, especially Doug Tipton, for donating all the concrete used in the study.

At the end, profound appreciation is extended to all the author's family members, especially his father and mother, and to his friends for their encouragement and support.

Table of Contents

List of Figures

List of Tables

Chapter 1

Introduction

1.1. General

Concrete has been successfully used for centuries because of its desirable characteristics, including strength, durability, and constructability. Reinforced-concrete elements, containing steel bars as the reinforcement to enhance concrete against tensile stresses, have been used since the 19th century.

Flat plates in buildings, walls of tanks and shell panels in the offshore structures, and bridge decks are all samples of popular and prevalent reinforced-concrete structural systems, which are always subjected to specific types of loads that cause large deformations, displacements, cracks, and other types of erosion in harsh environments. Because of their ease of construction and simple formwork, flat plates and slab-column connections are also frequently used in concrete structures.

One of the major possible failure modes for such structural systems, however, is the punching failure. Distinguished by its undesirable catastrophic result, the punching failure occurs suddenly and with little or sometimes no warning. The insufficient concrete cover, poor design or workmanship, and presence of large amounts of aggressive agents that penetrate through the cracks, which results in the corrosion of steel-reinforcement will also cause the failure of reinforced-concrete plates. Since the cracks cause a decrease in the stiffness of the elements, which may cause a failure in shear, flexure, or torsion, the conventional concrete might not be suitable for such applications.

Nonetheless, numerous methods are proposed here to enhance the punching-shear capacity of the slabs. Distribution of the principal stresses in a larger area around the column in slab-column connections results in a reduction in stresses; consequently, using drop panels, column capitals, larger columns, or any combination of these factors are used to improve the punching-shear capacity of two-way slabs. In addition, using shear reinforcement, bent-up bars on column heads, and stirrups are all mentioned as other methods to enhance the shear capacity of slabs and flat plates. Some of these methods slow down the construction, however, and cause the formwork to become more complicated and expensive.

Additionally, increasing the tensile strength of the concrete is another alternative to enhance the punching-shear capacity of concrete flat plates, as proposed in the literature. Fibre-reinforced concrete (FRC) was offered as an effective material to improve the punching failure and significantly increase the ductility and energy-absorption property of such structural systems, by increasing the tensile strength of the concrete.

Using FRC, then, leads to a transformation from a brittle type of failure to a ductile one; fibres not only delay the formation of the diagonal shear cracks, but also bridge the cracks and prevent their excessive opening when undergoing the pull-out process to prevent the cracks' propagation. As such, adding fibres to the concrete causes a reduction in the corrosion of reinforcement by reducing the cracks widths and propagation. Hence, using fibres decreases the rate of corrosion in the steel-reinforcement, prevents the loss of stiffness by bridging the cracks, and improves the ultimate shear-strength of the concrete, which ultimately all lead to minimising the probability of failure in the structural elements.

1.2. Scope of Research

As mentioned, increasing the tensile strength of the concrete by adding fibres to the concrete mixture is one of the proposed methods, which causes an improvement in the punching-shear capacity of fibre-reinforced concrete (FRC) flat plates. A more recent type of FRC is called hybrid-fibre-reinforced concrete (HFRC), in which two or more different types of fibres with various shapes, materials, and strengths are combined together. Using HFRC, moreover, leads to a multifunctional material as a result of the synergetic effects of the various added fibres.

This research is conducted as a master's thesis to examine the effects of hybrid fibres on structural behaviour and performance of one-to-one, full-scale, reinforced-concrete two-way slabs under static loading conditions. The combination of steel and macro-synthetic fibres is added to the concrete, and the effects on the punching-shear

capacity of concrete slabs are observed. Besides evaluating the punching-shear capacity, other structural behaviour such as load-deflection relationship, strains in concrete and steel-reinforcement, cracking patterns, ductility and energy-absorption, post-punching behaviour, and modes of failure are investigated.

The specimens are designed, prepared and tested, in order to estimate the effects of slab thickness and fibre volume fraction as the significant variables on the structural behaviour of the elements. As mentioned earlier, the test specimens are designed as one-to-one, full-scale slabs to avoid size effects on the results.

Consequently, a complete databank is prepared from all of the previously tested two-way slabs, mentioned in the literature, and the results of this study are added to the databank. To evaluate the performance of the fibres, test specimens are compared with the reference slabs. Additionally, the accuracy of the existing prediction equations, proposed by different researchers, for FRC Plates is evaluated.

Building upon the expertise in the area of structure sustainability, the results of this research are shared with industry to continue the strong partnership between it and Memorial University. Moreover, the local concrete industry plays an important role in this development. Over the past ten years, the collaboration between industry and Memorial University has helped foster tremendous research that has translated into important, real-life applications.

1.3. Research Objectives

The main objectives of the current investigation are summarized as follows:

1. To prepare a complete databank containing the tested two-way slabs, in order to be able to compare the results and find better solutions to design the FRC structures by analyzing available data.

2. To carry out an experimental program to investigate the structural behaviour of HFRC plates, with significant variables such as fibre volume fraction and slab thickness.

3. To examine the effects of hybrid fibres on the ductility and deformation characteristics, such as deflection profiles, and concrete and steel-reinforcement strains of HFRC two-way slabs, in comparison to traditional reinforced-concrete two-way slabs with different thicknesses.

4. To evaluate the accuracy of the proposed rational prediction equations, to predict the punching-shear capacity of hybrid-fibre-reinforced Concrete (HFRC) two-way slabs.

1.4. Thesis Outline

This thesis is divided into five chapters: the introduction, the review of literature, the experimental program, test results and discussion, and the conclusions.

Chapter 1 covers the introduction and significance of the study, containing a brief description of the differences between the structural behaviour of FRC and traditional concrete, as the statement of the problem.

The review of the previous theoretical studies and investigations on the fibre-reinforced concrete slabs, existing prediction equations, and the related code expressions are noted in Chapter 2.

Chapter 3, meanwhile, presents the experimental methods and work done, including the details of test specimens and properties of used materials. As well, the test set-up and equipment used in the experimental program are also described in the chapter.

Observed test results in terms of load-deflection relationship, as well as the effects of the main variables such as effective depth and fibre volume fraction on structural behaviour of the test specimens are discussed completely in Chapter 4. Accordingly, an evaluation on the accuracy of the existing prediction equations is carried out and explained.

Finally, the conclusions according to the test results are mentioned, and recommendations for future researches are summarized in Chapter 5.

Chapter 2

Review of Literature

2.1. Introduction

Punching-shear failure of slab-column connections occurs suddenly with little or sometimes no warning and produces catastrophic results. The inverse relation between the strength and the ductility, when using high-strength concrete, causes more significant problems.

Fibre-reinforced concrete (FRC) can prevent the punching failure and increase the ductility and energy-absorption properties of slab-column connections, by enhancing the tensile strength of the concrete. Hence, the presence of fibres increases the ultimate shear capacity of FRC structural elements in comparison to the conventional concrete elements. Such use could also, ultimately, transforms the mode of failure from a brittle type to a ductile one.

Several experimental programs are available on the effect of various parameters such as reinforcement-ratio, fibre content, and concrete compressive-strength on the punching-shear capacity of slab-column connections and the associated modes of failure. Based on the results of those investigations, some researchers proposed equations to predict the punching-shear capacity of FRC slab-column connections.

A literature review is carried out on slab-column connections with FRC and the major experimental findings are discussed. The existing results are collected into a databank. The values are screened and only the results that represent realistic slab-column connections are kept in the databank. The existing equations that were proposed to predict the punching-shear capacity of FRC slabs are evaluated using the collected databank. The results of the predictions are presented and discussed.

2.2. Fibre-Reinforced Concrete (FRC)

Fibre-reinforced concrete (FRC) was offered as an effective alternative in the 1970s to efficiently enhance the weakness of concrete in resisting tensile stresses. The addition of fibres improves the characteristics of concrete, such as ductility, energy-absorption, residual strength, and flexural toughness. As such, the presence of fibres in the concrete mixture produces ductile failures in reinforced-concrete plates [2-4]. Two different types of fibres, such as steel and hybrid fibres, are added to the concrete mixtures. The main characteristics and applications of various types of used fibres in concrete are presented in this section.

2.2.1. Steel-Fibre-Reinforced Concrete (SFRC)

The behaviour of steel-fibre-reinforced concrete (SFRC) is affected by shape, length and slenderness, and also the distribution of the fibres in the mixture. Hence, fibres with greater aspect-ratios, which equal length to diameter ratios of fibers, and different deformed shapes, which have higher bond characteristics, improve the flexural strength of SFRC elements more than other types of fibres [6]. Steel fibres are, in addition, used for various applications such as pavements, slabs, tunnel linings, and numerous types of concrete repair. Furthermore, they are used as a partial replacement for the steel-reinforcement [2-4]. The high-modulus steel fibres, consequently, increase service load, first cracking load, and the ultimate capacity of the concrete plates.

The improvement of the load-carrying capacity, caused by the addition of fibres, depends on the relative values of the elastic modulus of adopted fibres and elastic modulus of the concrete matrix [7-9]. Fibres with higher elastic modulus than the concrete matrix, then, have a greater contribution to improve the concrete tensile behaviour and could produce ductile shear failures in reinforced-concrete plates. Also, an increase in toughness because of the use of fibres minimizes cracking due to temperature changes, relative humidity, and other natural causes.

Steel fibres do not require any special mixing technique and the fibre-reinforced concrete can be prepared easily, as plain concrete. Based on the environment in which concrete members are being used, however, corrosion of steel fibres close to the concrete surface might occur. Nonetheless, some researchers found that the corrosion does not affect the structural integrity of the members [6].

Different types of steel fibres are available such as round, flat, crimped, and hooked, as shown in Figure 2.1, with a wide range of tensile strengths of about 280-2800 MPa, depending on the type of steel and the production technique.

Figure 2.1. Different types of steel fibres

Table 2.1 presents the characteristics of different types of steel fibres used in fibre-reinforced concrete.

Table 2.1. Characteristics of different types of steel fibres

Fibre shape	Fibre length (mm)	Fibre diameter (mm)	Fibre aspect ratio (length / diameter)	Ultimate tensile strength (MPa)
Corrugated	25 - 50	-	-	1200
Crimped	30 - 50	0.3 - 0.5	90 - 100	1200 - 1820
Hooked	30 - 60	0.38 - 1.05	48 - 100	1000 - 2300

2.2.2. Synthetic-Fibre-Reinforced Concrete (SyFRC)

As one of the innovative approaches to improve the behaviour of concrete, synthetic fibres are frequently used in small contents and offer the advantages of evenly-

distributed and high-corrosion resistance. Synthetic fibres can be used as secondary reinforcement to delay the formation of initial cracks, and are normally useful when early-age properties are needed to be improved [7-9].

Synthetic fibres enhance the load-bearing capacity in the post-crack zone. As well, they improve the impact resistance, flexural toughness, fracture properties, and ductility. Due to the low modulus of elasticity of synthetic fibres, however, the overall modulus is not significantly affected by these types of fibres.

Synthetic fibres can also be mixed with concrete using conventional facilities, without any need to use special techniques. The fibres are manufactured in various shapes, modulus of elasticity, and tensile strengths. Some of the main applications of synthetic fibres are shotcreting and piling operations.

2.2.3. Hybrid-Fibre-Reinforced Concrete (HFRC)

A more recent type of FRC is called hybrid-fibre-reinforced concrete (HFRC). Two or more different types of fibres are rationally combined together and added to the concrete. HFRC derives benefits from each one of the individual fibres and then exhibits a synergetic response. Thus, hybrid fibres provide a matrix in which each type of specific fibres has its own benefits for mechanical and physical performances of concrete, making it a multifunctional material.

Fibres that are stronger and stiffer, such as steel fibres, improve first-crack stress and ultimate strength, and also increase ductility and toughness. The synthetic fibres with lower modulus of elasticity are more flexible and enhance the early-age properties of the

mixture and control the cracking [7-9]. Fibres with different lengths and diameters can be combined. This provides a hybrid combination in which smaller fibres bridge micro-cracks and larger ones prevent the propagation of macro-cracks, which ultimately leads to an improvement in the toughness of the concrete material [7-9].

2.3. Previous Experimental Research on SFRC Two-Way Slabs

As mentioned in the previous section, the addition of steel or hybrid fibres improves the performance of the concrete. In the following section, previous experimental studies on the structural performance of SFRC and HFRC two-way slabs are presented, and the major results of those investigations that are related to this study are highlighted.

2.3.1. Previous Experimental Research on SFRC Members

Ito et al. [10] examined the effects of using steel-fibre-reinforced concrete on the punching-shear strength of two-way slabs under static and repeated loading. The test specimens were 900 × 900 mm and had thickness between 40 to 80 mm. The researchers concluded that a reduction in the slab thickness by 15% could be substituted by adding 1%, by volume, of steel fibres in the concrete mixture of the test slabs.

Swamy and Ali [2] tested 19 slab-column connections. The specimens were one-to-one, full-scale models of a typical floor, with a column spacing of 4 m in both directions. The effects of fibre reinforcement on deformation and strength characteristics were investigated. The specimens were 1800 × 1800 × 125 mm and had an average

effective depth of 100 mm. The slabs were loaded centrally through a 150 × 150 mm stub column. The test variables were the fibre volume (0 to 1.2%), fibre location (entire specimen, 3h and 3.5h from the column face and for a thickness of 60 mm, only of the tension side of the specimen), flexural reinforcement distribution (uniform and banded), fibre type (crimped, hooked, and plain), reinforcement reduction and variation of shear reinforcement. Three slabs contained fibres in the entire specimen. From the research, the authors concluded that the use of fibres led to the reduction of the deformations at all stages of loading, especially after initial cracking. Furthermore, the maximum load carried by the slab and the deformation sustained at failure were all enhanced by the use of fibres, which also caused an increase in the punching-shear capacity up to about 40%. Also, the ductility and energy absorption increased by 100 and 300%, respectively. It was observed that the failure surface was pushed away from the column face. The addition of fibres of about 1% transformed the brittle-type failure to a gradual and ductile one, with a corresponding reduction of about 30 to 40% in the flexural reinforcement.

Walraven et al. [11], meanwhile, tested 24 circular concrete slabs to investigate the use of steel fibres as punching-shear reinforcement. The diameter of the slabs was 1750 mm and the thickness was 140 mm. The slabs were loaded through a cylindrical stub with a diameter of 250 mm. The main variables were the steel fibre volume fraction (0 to 1.25%), flexural reinforcement ratio (0.09, 1 and 1.84%), type of concrete (normal weight and light weight), and the existence of compressive membrane action (presence of the ring around the sample). No details were provided for the test specimens to show the arrangement of the flexural reinforcement. The authors concluded that steel fibres increased the punching-shear resistance of the slabs and also enhanced the residual post

peak punching strength, especially for the light weight concrete slabs. It was also concluded that, for the light-weight concrete, the fibres can act as the shear reinforcement; however, for the normal-weight concrete, the fibres only enhance the punching-shear capacity.

Narayanan and Darwish [12] investigated the behaviour and strength characteristics of steel-fibre-reinforced micro-concrete slabs subjected to punching-shear. Twelve 780 × 780 mm square slabs were tested with a thickness of 60 mm. The span length was 700 mm and the slabs were loaded through a 100 mm square-column stub at the center of the slab. The main variables were the steel fibre volume fraction (0.25 to 1.25%), the flexural reinforcement ratio (1.79 to 2.69%), and the cube compressive strength of concrete (37.2 to 66.3 MPa). The results showed a gradual and ductile failure of the test slabs. There was a considerable increase in the post ultimate ductility and residual load capacity of the slabs with a high volume fraction of fibres. The results revealed that increasing the fibre content caused a decrease in the critical punching-shear perimeter around the loaded area. This observation contradicts the findings of Swamy and Ali [2]. The slabs used in the experimental program were small micro-slabs, with a thickness equal to 60 mm. Thus, the tested slabs were too thin and the results may not be suitable to establish the effects of fibres on the structural behaviour of realistic slab-column connections.

Theodorakopoulos and Swamy [3] investigated the effects of adding steel fibres to light weight concrete slab column connections. The authors tested 20 slabs that represented one-to-one, full-scale models of a prototype flat-plate structure with a column spacing of 4 m center-to-center in both directions. The slabs were 1800 × 1800 × 125 mm

and had an average depth of 100 mm. The specimens were loaded centrally through a column stub. The test variables were the fibre reinforcement volume (0 to 1 %), types of fibres (two types of crimped fibres, Japanese, hooked and paddle), loading area (stub column size 100, 150, and 200 mm), concrete cube compressive strength (about 18 to 58 MPa), and the reduction of the flexural steel-reinforcement ratio (from 0.37 to 0.55%). The results revealed that the incorporation of 1% steel fibres enhanced the first-crack load, yield load, and punching-shear strength by about 30 to 45% and increased the serviceability load by 15 to 40%. The presence of fibres delayed the formation of diagonal cracks and also transformed the sudden punching into a ductile and gradual failure. No loss of concrete cover and no loss in structural continuity were observed. By preserving the continuity and integrity of slabs, the fibres enhanced the residual strength and increased the ductility and energy-absorption of the slabs.

Alexander and Simmonds [4] investigated the effect of adding corrugated steel fibres to concrete on the shear capacity by testing six slab-column specimens to failure. Each specimen, 155 mm thick and 2750 mm square, was loaded using a 200 mm square-column stub placed at the center of the slab. Normal-weight concrete was used for all specimens. The concrete clear cover (11 and 38 mm) and the fibre volume fraction (0, 0.4, and 0.8%) were selected as the main variables. The observations showed that the failure of the test slabs could be described as shear failures. Addition of steel fibres increased the punching-shear capacity of the slab-column connections by 20 to 30% depending on cover and fibre content. The presence of fibres also enhanced the ductility, and it was concluded that fibres were a viable way to increase the punching-shear capacity.

Tan and Paramasivam [13] tested 14 specimens to investigate the punching-shear behaviour of steel-fibre-reinforced concrete slabs. The slabs were simply supported on all four edges. The main variables were the effective span-to-depth ratio (20.5 to 65.2), steel-fibre volume fraction (0.31 to 2%), slab thickness (22 to 70 mm), concrete cubic compressive strength (35, 50, and 65 MPa), and size of the loaded area (100, 150, and 200 mm). The load-deflection curves of the SFRC slabs showed four distinct regions: initial elastic un-cracked, crack developing, post-yielding, and post-peak region. An increase in steel-fibre volume fraction, slab thickness, concrete compressive strength, and size of the loaded area led to an increase in cracking load, yield load, ultimate load, and ductility of the SFRC test slabs. The authors found a reasonable agreement between the experimental results and the code predictions of BS-CP110. The thicknesses of the test specimens were between 35 and 70 mm, which seem to be too small to be considered as actual two-way slabs used in construction.

Shaaban and Gesund [14] tested 13 slabs to investigate the effects of adding steel fibres on the punching-shear strength of slabs. The steel fibre volume fraction (0 to 1.95% by volume) was chosen as the main variable. The slabs were 1600 mm square with a thickness of 82.5 mm and were loaded using a 63.5 mm square-column stub at the center of each specimen. The concrete clear cover was 13 mm and the fibres used were 25 mm long with a nominal tensile strength of 1200 MPa. An air bag was used to apply the load on the specimen. It was concluded that the addition of fibres increased the punching-shear capacity of the slab. Based on the test results, the authors proposed an equation to predict the punching-shear capacity of SFRC two-way slabs. The proposed equation is mentioned later in this chapter.

Harajli et al. [15] investigated the effects of steel fibres on the punching-shear strength of flat slabs, by testing 12 small-scale 650 mm square slab-column connections. The specimens were cast in two main groups with different thicknesses (55 and 75 mm). Each group contained specimens with various fibre types (hooked, collated hooked, and long monofilament polypropylene) and volume fractions (0 to 2%) as the main variables. A reinforcement ratio equal to 1.12% was selected for all specimens to ensure that the shear failure occurred before reaching the nominal flexural resistance. From the results, it was concluded that the addition of steel fibres up to 2% by volume increased the punching-shear capacity of the slabs by about 36%. The addition of fibres decreased the angle of failure and thus pushed the failure surface away from column face. It was also found that the angle of failure was independent of the length and aspect ratio of fibres. The addition of fibres not only improved ductility and energy absorption of the specimens in the post-failure range, but also modified the failure mode from punching to a flexural or to a ductile punching mode.

McHarg et al. [16] tested six two-way slab column connections. The authors investigated the effects of the location of fibres and concentration of slab reinforcement on the punching-shear capacity, negative moment cracking, and stiffness of the slabs. The full-scale slabs represented the 2.3 × 2.3 m column-strip region around the interior columns of a prototype flat-plate structure, with 4.75 × 4.75 m bays. The slab thickness was 150 mm with a 25 mm clear concrete cover around the top and bottom reinforcement, and the interior columns were 225 mm squares. It was found that providing 0.5% of fibres in the vicinity of the column resulted in a significant improvement in the performance. The punching-shear resistance increased by about 38% and 26% for uniform and banded

distributed bars, respectively. There was also an increase in ductility and post-cracking stiffness. The crack widths decreased by about 25% and 20% inside and outside the column region, respectively, at the service load level. In general, it was found that providing fibre-reinforced concrete cover caused a gain in the punching-shear capacity and a better crack control.

Hanai and Holanda [18] investigated the influence of steel fibres on the punching strength of flat slabs and shear strength of concrete beams. The objective of the research was to examine any similarities that could provide an insight into the ductility of the connections. The main variables were the steel fibre volume fraction (0 to 2%), fibre type (hooked-end fibres with circular and rectangular sections with different aspect ratios), and concrete compressive strength (23.1 to 59.7 MPa). The results of the investigation revealed that theoretical strength models based upon a linear dependence on fibre content was sufficient to predict the effect of fibres.

Yang et al. [19] evaluated the effects of high-strength steel-reinforcement on punching-shear behaviour of two-way slabs. In their research, six flat-plate specimens were tested with dimensions of 2300 × 2300 × 150 mm. The specimens had 225 mm square column stubs at the center. The main variables were the flexural reinforcement ratio (0.64, 1.18, 1.36, and 2.15%), the type of bars (normal and high-strength), the distribution of the reinforcement (uniform and banded), and the use of steel fibres (0.5% by volume). The fibres were used only within the immediate column region and to a distance of about 500 mm from the column face. Replacing the normal reinforcement with high-strength steel-reinforcement with the same area caused a 27% increase in the punching-shear capacity. The use of high-strength reinforcement with the same flexural

resistance caused wider cracks and lower stiffness, which ultimately produced the same punching-shear resistance. Increasing the reinforcement ratio in slabs resulted in higher post-cracking stiffness, more uniform distribution of the strains in the flexural reinforcement, and smaller cracks. This was more evident in the test slabs with the banded distribution of reinforcement.

Nguyen-Minh et al. [20] investigated the cracking behaviour and resistance of steel-fibre-reinforced concrete flat slabs under punching loads. Twelve small-scale specimens, consisting of nine steel-fibre-reinforced slabs and three reference slabs, were tested. All slabs were 125 mm thick and had flexural reinforcement ratio of 0.66%. The specimens were divided into three groups, with each group having three SFRC and one control slab. Group A slabs were 900 mm square, Group B slabs were 1200 mm, and Group C slabs were 1500 mm. Fibre volume fraction in each group was also considered as a variable (about 0, 0.25, 0.35, and 0.45% by volume). It was found that steel fibres enhanced the punching-shear resistance of the slabs between 9% to 39.8%, and also reduced cracks widths up to approximately 70% at serviceability limit state. Also, the steel fibres enhanced the stiffness of the slabs and also improved ductility and integrity of the connections.

Cheng and Parra-Montesinos [21] evaluated the effectiveness of steel fibres to increase the punching-shear resistance of two-way slabs subjected to a monotonically increased concentrated load. The authors tested ten slabs representing isolated interior slab-column connections, with dimensions of 1520 × 1520 × 152 mm. The slabs had a square-column stub at the center. The main variables were the fibre type (regular hooked, high-strength hooked, and twisted), fibre ultimate strength (1100, 1800, and 2300 MPa),

fibre volume fraction (1 and 1.5%), and the flexural reinforcement ratio (0.56 and 0.83%). Only four slabs contained fibres in the entire specimen and two slabs were made with mortar instead of concrete. Ultimately, the investigation revealed that addition of fibres resulted in an enhancement in the punching-shear resistance of the slab up to 55% and an increase in deformation capacity. The use of fibres changed the mode of failure from punching to a ductile punching, or even flexural yielding, in one of the slabs.

Using hooked-end-type steel fibres, Higashiyama et al. [22] tested 12 SFRC slabs. The main variables were the fibre volume (0.63 to 1.03% by volume), slab thickness (100, 140, and 180 mm), flexural reinforcement ratio (0.4 to 0.91%), and concrete compressive strength (21.6 to 42.4 MPa). The slabs were 1200 mm square and were simply supported along four edges with a span length of 1000 mm. A design equation was proposed, as well, using the test data collected from the literature. The authors claimed that the proposed equation reasonably predicted the punching-shear capacity of SFRC slabs, considering 50 slabs from the literature.

2.3.2. Previous Experimental Research on HFRC Members

Perumal and Thanukumari [23] investigated the effects of using hybrid-fibre-reinforced concrete on beam-column connections under earthquake loading. Different proportions of steel and polypropylene fibre combinations were examined. The results showed higher displacements without developing wider cracks in the hybrid-reinforced beams. It was also concluded that the addition of polypropylene fibres increased the energy-dissipation capacity and ultimate load for both types of concrete.

Ding et al. [24] evaluated the effects of fibre types (macro-steel fibre and macro-plastic fibre) on the shear strength and shear toughness of reinforced-concrete beams. The upper bounds of fibre dosages were based on the workability of self-compacting concrete. Compared to the beams without fibres, hybrid fibres improved the shear strength and load-bearing capacity in the post-peak region. The authors concluded that conventional transverse ties can be partly replaced by the fibre cocktail of steel and plastic fibres. It was observed that there was a decrease in crack widths and spacing due to the failure-pattern change and multi-crack formation.

Noghabai [25] investigated the shear and bending of HFRC beams. The main variables were the fibre volume fraction, types of fibres (metallic and non-metallic), and the effective depth of the test specimens. The author concluded that the addition of fibres improved the tensile resistance of the concrete, and the HFRC beams were observed to have the same capacity as the reference specimens.

To increase the load carrying capacity, Kutzing and Konig [26] used fibre cocktail in the column head of slab-column connections. The results showed an increase in the ultimate load capacity. The load-deflection curves showed an enhancement in the system ductility. In addition, the authors also concluded that the cracking patterns of the specimen with hybrid-fibre-reinforced concrete were more distributed than the conventional ones without fibres.

Mu and Meyer [27] investigated the effects of fibre type (AR-Glass, PVA, and Polypropylene), fibre form (distributed short fibres or continuous Woven and Knitted fibre mesh), and fibre volume fraction on two-way bending behaviour and punching-shear capacity of glass concrete slabs. It was found that fibre mesh was more effective than

short distributed fibres in two-way bending, which the authors attributed to the enhanced interfacial bond between the mesh and concrete. It was observed that short distributed fibres improved flexural capacity, ductility, and shear capacity of the test slabs.

Ostertag and Blunt [28] investigated bridge-approach slabs made with hybrid-fibre-reinforced concrete. The fibres were used to improve the service life of the specimens and to control the cracking. Fibre hybridization showed control of initiation and propagation of micro-cracks and delaying macro-cracks propagation. Hybrid-fibre-reinforced concrete showed enhanced crack resistance, flexural behaviour, and an increase of the post crack flexural stiffness in comparison to the reference specimens.

Hadi [29] compared the ductility and load-carrying capacity of five concrete two-way slabs. Four FRC slabs had different types of fibres (steel and polypropylene) and one reference slab without fibres. The slabs were 820 × 820 × 80 mm and had 0.5% and 1% fibre volume fractions of each type of fibres. The results showed that the presence of fibres increased the strength of concrete, ultimate deflection, final collapse load, ductility, and energy absorption of the slabs. The steel fibres, nevertheless, still had better performance than polypropylene ones.

2.4. Predicting the Punching-Shear Capacity of SFRC Slabs

In this section, the equations proposed in the literature to predict the punching-shear capacity of SFRC two-way slabs are presented. It should be noted that there are no equations developed to predict the punching-shear capacity of HFRC two-way slabs in the literature.

Narayanan and Darwish [12] proposed an empirical equation to predict the ultimate shear capacity as follows:

$$V_{uf} = {}_{s}(0.24 f_{spf} + 16\rho + 0.41\ F)\ b_{pf}\ d \quad (2\text{-}1)$$

where is the average fibre interfacial bond stress with an average value of 4.15 MPa; b_{pf} is the critical punching-shear perimeters calculated as ($4c + 3\ h$) (1 -kF); f_{spf} is the split cylinder strength of fibre-reinforced concrete, which can be calculated as $\frac{f_{cuf}}{20-\sqrt{F}} + 0.7 + \sqrt{F}$; f_{cuf} is the cubic compressive strength; k is a non-dimensional factor, which is equal to 0.55; F is the fibre factor, which is calculated by $\frac{L}{D} V_f d_f$; L and D are length and diameter of the fibres; d_f is the bond factor; and ξ_s is considered as 1.6-0.002h.

Shaaban and Gesund [14] developed an equation to predict the punching-shear capacity of flat plates containing corrugated steel fibres as follows:

$$V_c = \frac{(0.3W_f + 6.8)}{12} \sqrt{f_c}\ b_o d \quad (2\text{-}2)$$

where W_f is the percent of fibres by weight, which is calculated as $\frac{7850 V_f}{W_c}$ and is less than 8%; W_c is the unit weight of plain concrete (kg/m^3); b_o is the punching perimeter and is equal to 4($b + d$) for a square column; and b is the column side dimension.

Harajli et al. [15] provided an equation to predict the ultimate punching-shear of concrete slabs due to the addition of steel fibres. A linear equation was proposed based on the experimental results obtained in their study. The equation was expressed as follows:

$$P_u = (0.54 + 0.09 V_f)\ \sqrt{f_c}\ b_o d \quad (2\text{-}3)$$

where V_f is the volume fraction of fibres in %; b_o is the perimeter of the critical shear surface in mm; d is the depth to the center of reinforcing steel in mm; and f_c is the cylindrical concrete compressive strength in MPa.

Based on their experimental results, Hanai and Holanda [18] developed an equation to design FRC slabs for punching shear. The equation is a modification of the ACI 318 expression, which is as follows:

$$P_u = 0.6266(0.06V_f + 0.53)\ \sqrt{f_c}\ b_o d \quad (2\text{-}4)$$

where b_o is the punching perimeter, which equals to $4(c + d)$; c is the column side dimension; f_c is the compressive strength of concrete in MPa; and V_f is the fibre volume fraction in %. However, the equation contains a safety-factor and can only be used for design and not for predicting the punching-shear capacity.

Higashiyama et al. [22] developed an equation that is based on the Japan Society of Civil Engineers (JSCE) equation for punching-shear capacity of traditional slabs. The code equation was empirically modified by defining a fibre factor, and the proposed equation was expressed as follows:

$$V_u = \sqrt[4]{\frac{1000}{d}}\ \sqrt[3]{100\rho}\ \left(1+\frac{1}{1+\frac{0.25u}{d}}\right)(0.2\ \sqrt{f_c} + 0.41\ F)(u + d)(1\text{-}kF)\ d \quad (2\text{-}5)$$

where F is the fibre factor and can be calculated by $\frac{L}{D}V_f d_f$; L and D are the length and diameter of the fibres; d_f is the bond factor; τ is the average fibre interfacial bond stress, which is equal to 4.15 MPa; u is the perimeter of the loading pad and equals to $4c$; the terms $0.2\ \sqrt{f_c}$, $\sqrt[4]{\frac{1000}{d}}$, and $\sqrt[3]{100\rho}$ should be less than 1.2, 1.5, and 1.5, respectively,

Based on the results of 12 SFRC slabs in their study, the factor *k* was derived to be equal to 0.32.

2.5. Analysis of the Available Data in the Literature

A literature review on the punching shear of SFRC slabs was carried out and the results were collected into a databank. In total, the results of 173 specimens were collected. Due to the use of circular shapes, light-weight concrete, and shear reinforcement in the test specimens, 82 slabs were omitted and only 91 slabs were chosen to be used and analyzed in the database of this study. The detailed results are presented in Table A.1 of Appendix A.

In addition, 24 specimens were used as reference slabs as they contained no fibres. Those slabs are not used in the comparisons and are not included in the graphs. Hence, the remaining 67 slabs are used in the following discussion. All of the specimens are made with SFRC and there are no slabs available in the literature that contains HFRC.

Based on the collected data, different ranges for the dimensions of the test specimens, reinforcement ratios, fibre volume fractions, and concrete compressive-strength are investigated. The distribution of the specimens, depending on those parameters, is presented. The ranges of the parameters are shown in Figures 2.2 to 2.7.

Figure 2.2 shows that among the slabs, which are selected in the databank, about 51% of them have an effective depth less than 80 mm. This is a small thickness for a slab-column connection that is used in actual construction. Slabs with an effective depth between 80 and 100 mm were 9% of the database. Approximately, 40% of the slabs had

an effective depth greater than 100 mm. According to the design codes, the minimum thickness of two-way slabs should be equal to 100 mm. Hence, the specimens with thickness less than 100 mm do not have any practical application in buildings. Only 13% of the slabs have thicknesses more than 120 mm. Figure 2.3 shows that 74% of the slabs were cast with normal-strength concrete, with compressive strength less than 40 MPa.

Different ranges for reinforcement ratio, from less than 0.5% to more than 2.5% were used in the test specimens, as shown in Figure 2.4. Most of the slabs were designed to fail in punching-shear. In 14 slabs, which are 21% of the specimens, the observed ductile punching failure could be attributed to the low-reinforcement ratio, less than 0.6%, and not due to the addition of fibres. Nonetheless, these specimens are included in the databank.

Figure 2.5 shows the distribution of fibre volume fractions, from less than 0.5% for 21% of the test specimens, to more than 1% of fibres for 42% of the test slabs. As shown in Figures 2.6, 45% of the slabs failed in punching-shear. It should be noted that 50% of the slabs had a reinforcement-ratio more than 1% and were designed to fail in punching-shear.

Figure 2.7 shows that 58% of the used fibres are hooked-type fibres. The slabs in the database included, only, specimens with fibres in the entire test specimen and not only concentrated in a specific region around the column area.

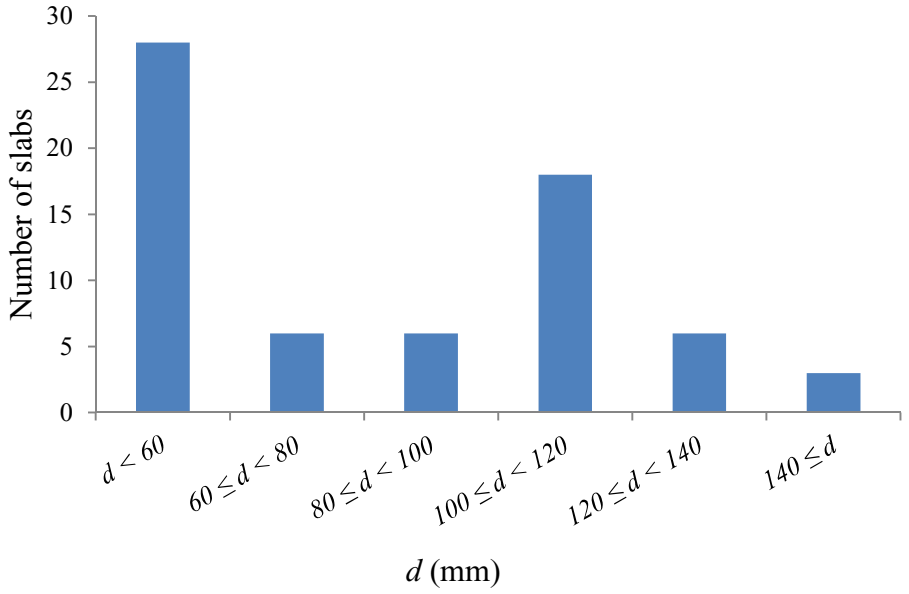

Figure 2.2. Distribution of the slabs by effective depth

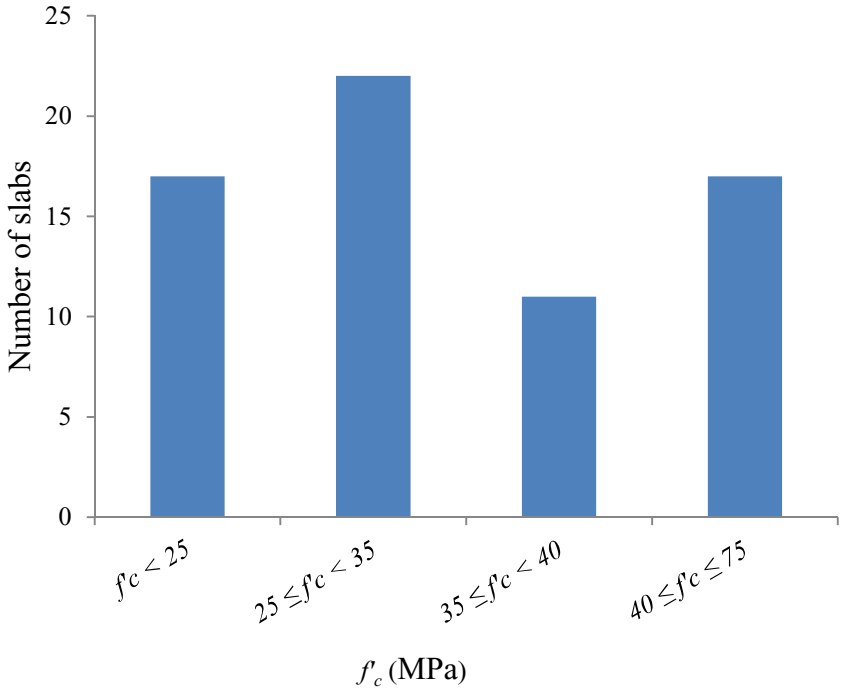

Figure 2.3. Distribution of the slabs by concrete compressive strength

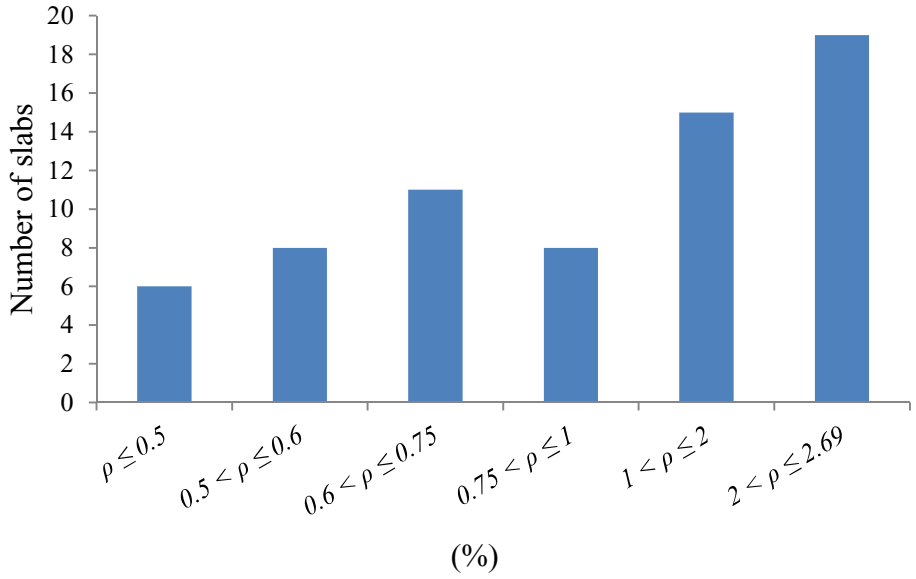

Figure 2.4. Distribution of the slabs by reinforcement ratio

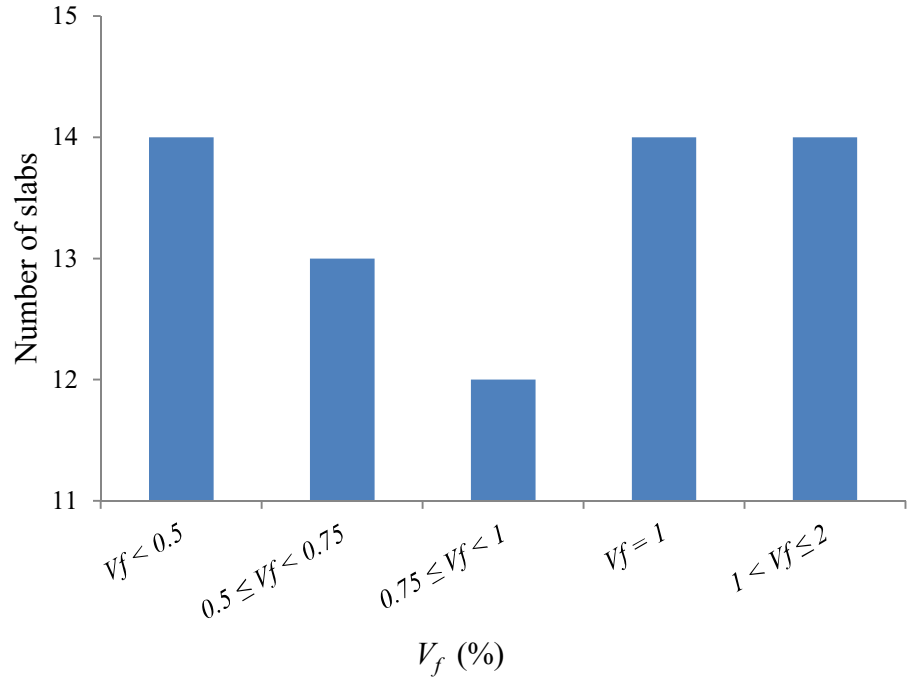

Figure 2.5. Distribution of the slabs by fibre volume fraction

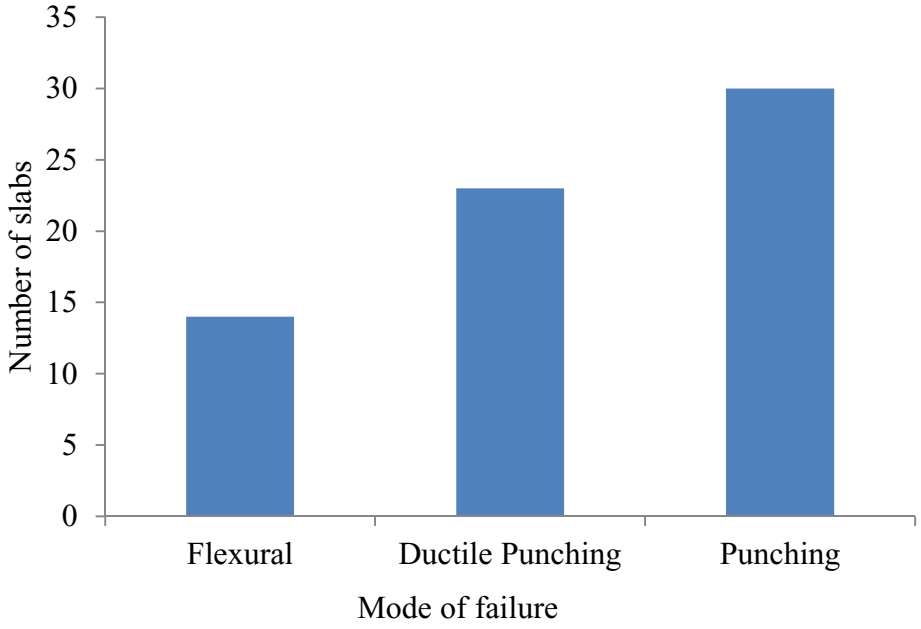

Figure 2.6. Distribution of the slabs by mode of failure

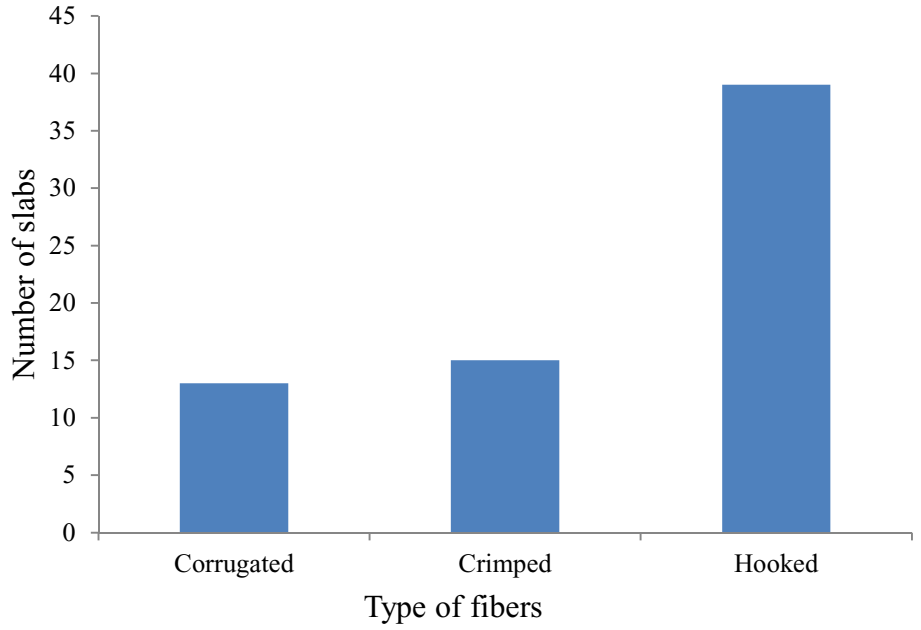

Figure 2.7. Distribution of the slabs by type of fibres

The effects of fibre volume fraction, average effective depth, concrete compressive strength, and reinforcement ratio on the punching-shear capacity of the 67 selected two-way slabs in the database are presented in the next paragraphs. The values of the shear strength, normalized by $\sqrt{f'_c}$, are plotted versus each of the above mentioned variables. The results are shown in Figures 2.8 to 2.11.

According to the plots, almost all of the normalized shear strengths are larger than 0.33 and 0.38, as required in the ACI 318-11 [30] and CSA 23.3-04 [31] code equations, respectively. However, the code equations are to be used in the design of reinforced-concrete specimens containing no fibres. Hence, the traditional code equations are not suitable to estimate the punching-shear capacity of FRC slabs.

Figures 2.8 to 2.11 do not follow any pattern and there is no specific trend in the capacity of the slabs in relation to the different parameters. Nonetheless, and according to Figure 2.9, it is clear that as the effective depth of the slab increases, the normalized shear strength decreases. This trend seems to be true for all of the slabs containing different amount of fibres. The importance of this observation is that there could be a size effect, and the effectiveness of the fibres may not be the same as the slab depth increases.

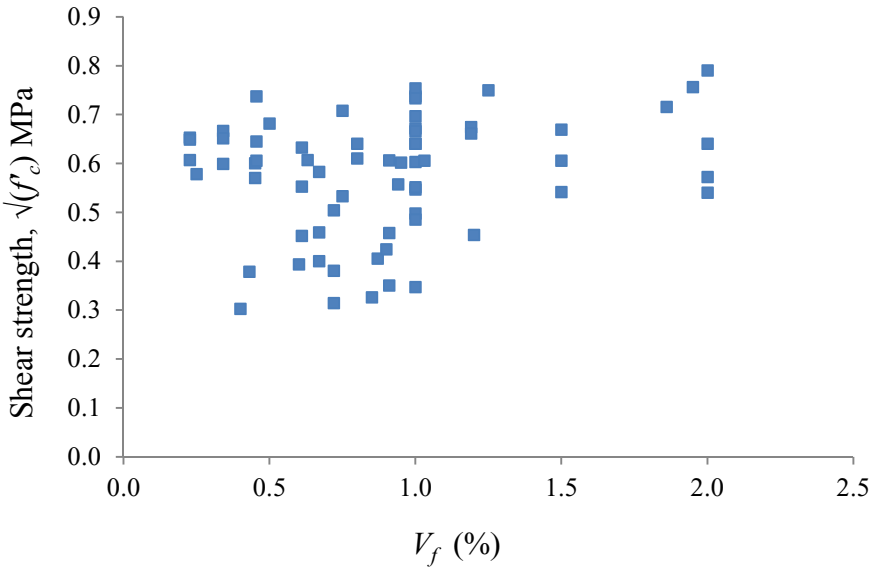

Figure 2.8. Normalized shear strength w.r.t. $\overline{f_c}$ vs. fibre volume fraction

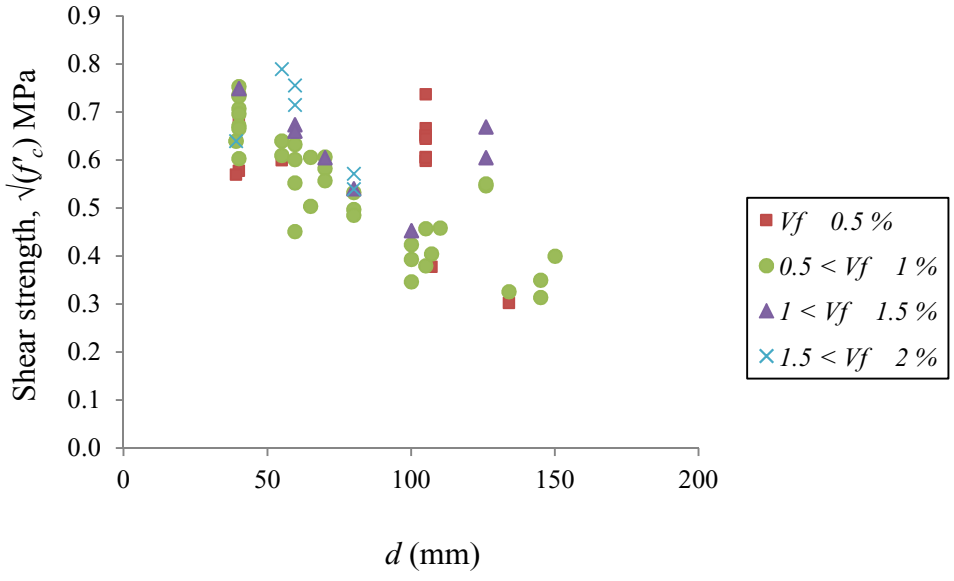

Figure 2.9. Normalized shear strength w.r.t. $\overline{f_c}$ vs. average effective depth

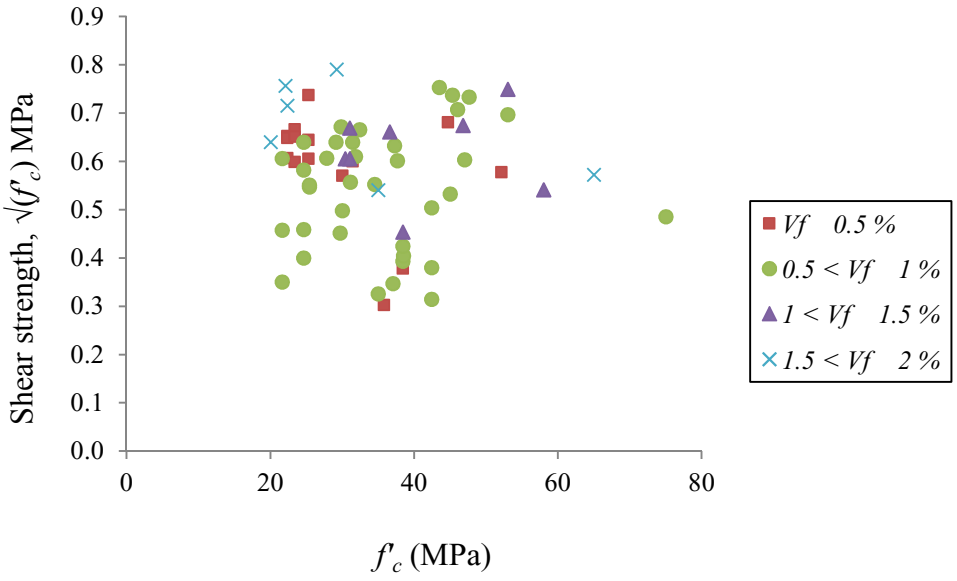

Figure 2.10. Normalized shear strength w.r.t. $\overline{f_c}$ vs. compressive strength

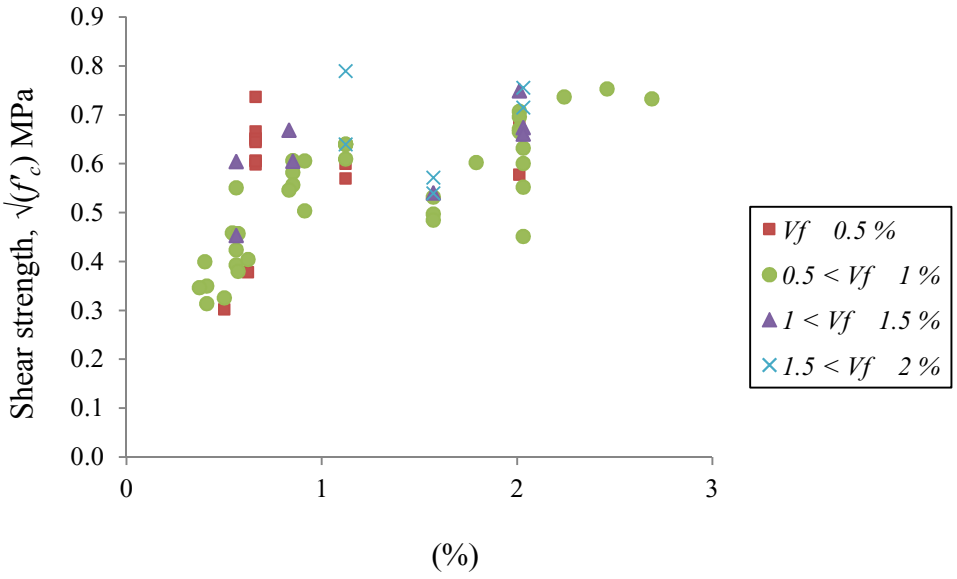

Figure 2.11. Normalized shear strength w.r.t. $\overline{f_c}$ vs. reinforcement ratio

2.6. Prediction of the Capacity of the Slabs in the Database

As mentioned earlier, equations were developed by some researchers to predict the punching-shear capacity of SFRC slabs. The punching-shear capacity of the slabs in the database is compared to the predictions of those equations. The values of V(test)/V(predicted) are given in Figures 2.12 to 2.15. The detailed test results of the slabs are given in Table A.2 of Appendix A. The collected data is used to assess the strength predictions according to the equations proposed by Narayanan and Darwish [12], Shaaban and Gesund [14], Harajli et al. [15], and Higashiyama et al. [22]. The proposed equations used for the comparison were mentioned earlier in this chapter. The predictions of these equations show a significant degree of scatter when compared to the test results.

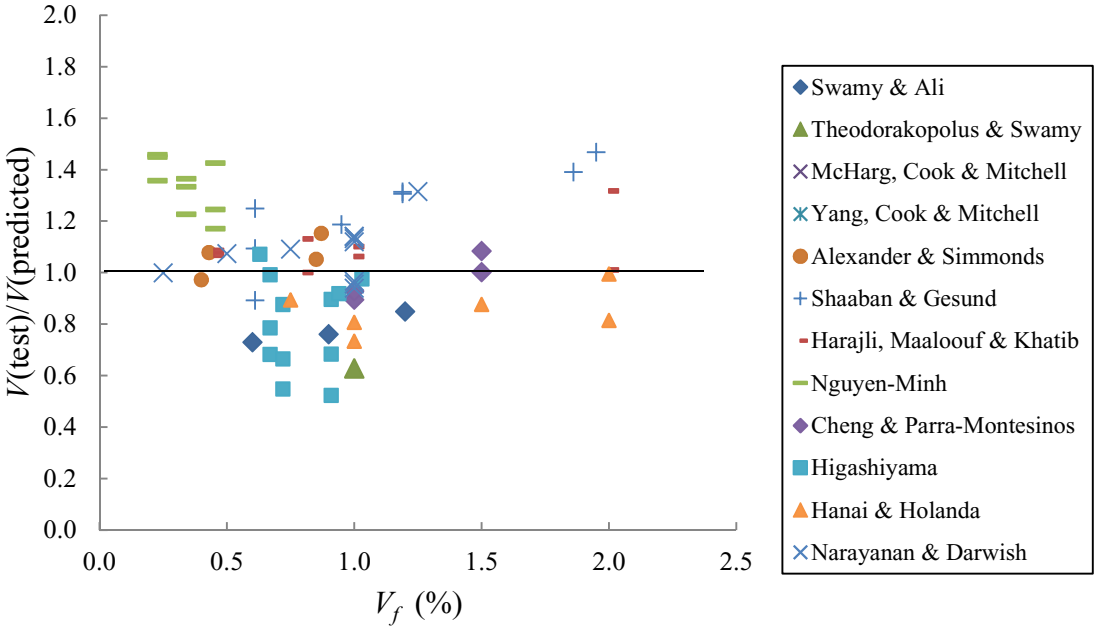

Figure 2.12. $V_{(T.)}/V_{(P.)}$ vs. V_f(%) using Narayanan & Darwish [12]

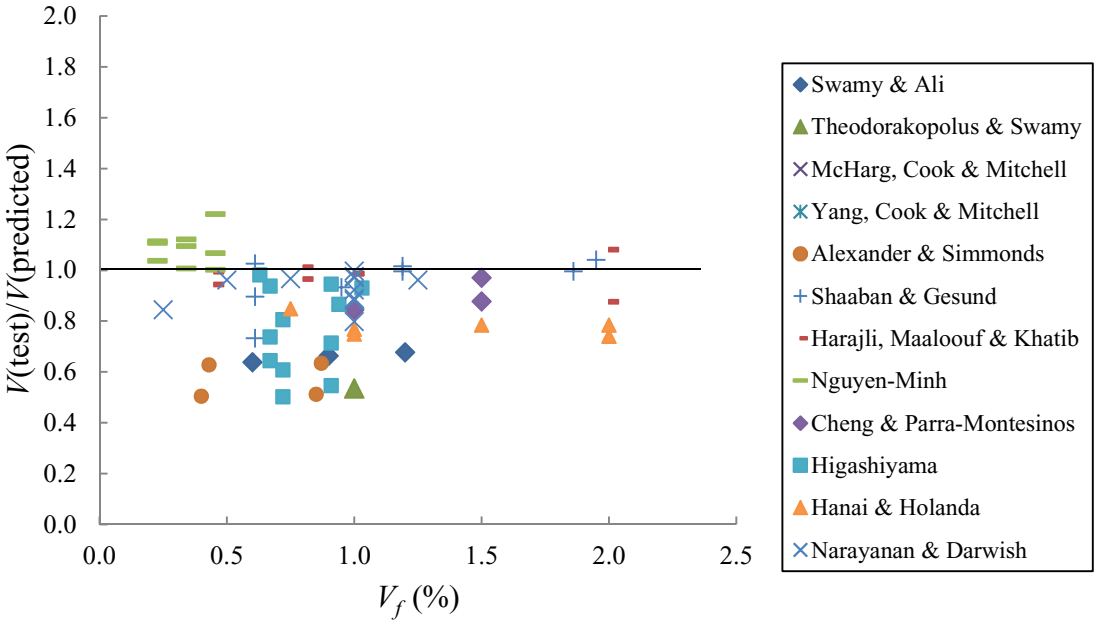

Figure 2.13. $V_{(T.)}/V_{(P.)}$ vs. V_f(%) using Shaaban & Gesund [14]

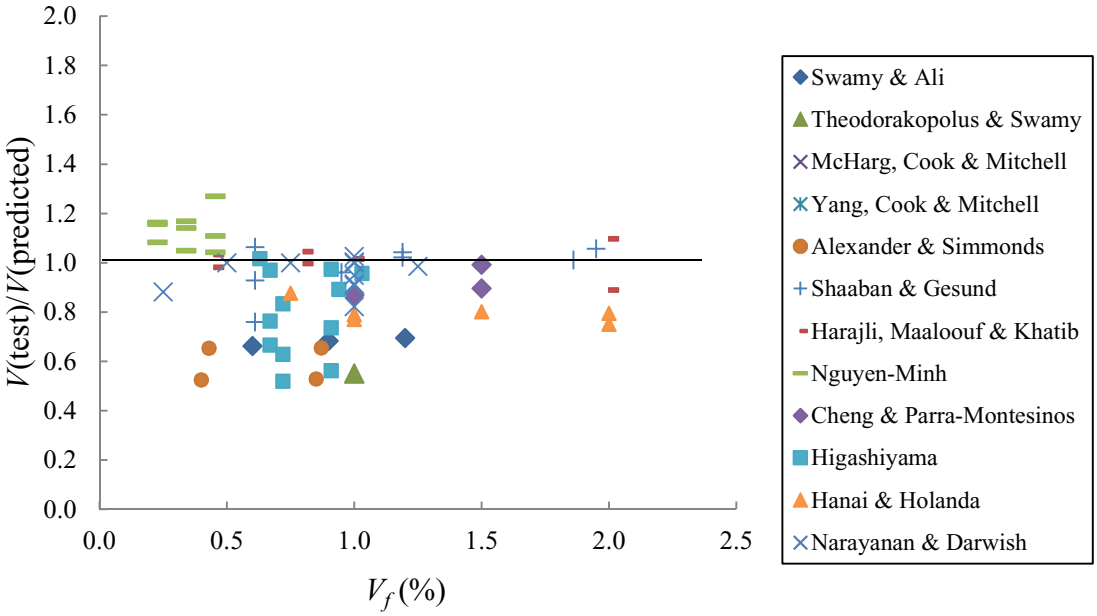

Figure 2.14. $V_{(T.)}/ V_{(P.)}$ vs. V_f(%) using Harajli, Maalouf & Khatib [15]

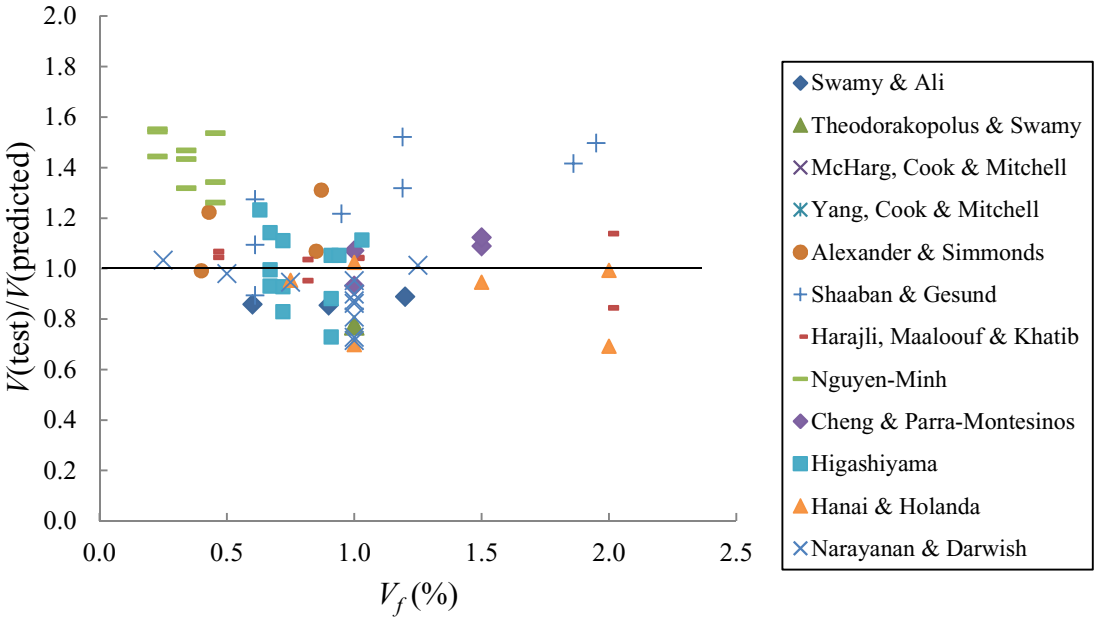

Figure 2.15. $V_{(T.)}/V_{(P.)}$ vs. V_f(%) using Hiroshi Higashiyama et al. [22]

According to Figures 2.13 and 2.14, the equations proposed by Shaaban and Gesund [14], and Harajli, Maalouf and Khatib [15] give unsafe predictions as they overestimate the capacity of 74 and 66% of the slabs, respectively. Figure 2.15 indicate that the equation provided by Hiroshi Higashiyama et al. [22] underestimates the punching capacity of 58% of the slabs. This equation contains fibre factors, and is based on the Japanese code equation. The equation seems to have reasonable correlation with the punching-shear capacity of the test slabs.

The equation proposed by Narayanan and Darwish [12] is the most conservative equation, as it underestimates 59% of the tested slabs. According to the results of comparisons, the mean value of the ratios, V(test)/V(predicted), the standard deviations, and also the coefficient of variation are calculated and given in Table 2.2.

The results, presented in Table 2.2, show that the equation by Narayanan and Darwish [12] gives the closest predictions, with a mean value of V(test)/V(predicted) equal to 1.07 and standard deviation of 0.26. The equation proposed by Higashiyama et al. [22] gives also reasonable predictions, with a mean value of V(test)/V(predicted) equal to 1.10 and standard deviation equal to 0.25.

Table 2.2. Mean, standard deviation, and coefficient of variation of V(test)/V(predicted)

Values	Narayanan & Darwish [12]	Shaaban & Gesund [14]	Harajli, Maalouf & Khatib [15]	Hiroshi Higashiyama et al. [22]
Mean	1.07	0.85	0.88	1.10
Standard deviation	0.26	0.18	0.18	0.25
Coefficient of variation	0.24	0.21	0.21	0.22

The analysis of the results in the database revealed that an increase in the effective depth caused a decrease in the normalized shear strength, as shown in Figure 2.9. Hence, the predictions of the proposed equations were further examined based on the depth of the slabs.

A depth of 100 mm is the smallest depth that could be used in an actual slab-column connection. In the collected database, 41% of the specimens had an effective depth higher than 100 mm. Hence, the slabs in the database divided into two groups with depths smaller and greater than 100 mm. The results of the different prediction equations based on that division of the slabs are shown in Figures 2.16 to 2.19.

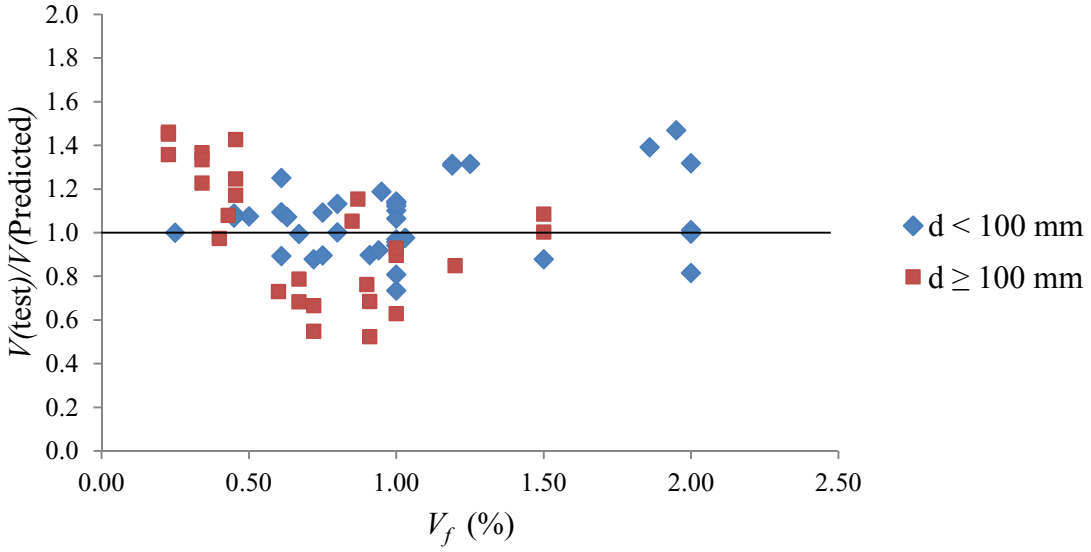

Figure 2.16. $V_{(T.)}/V_{(P.)}$ vs. V_f(%) using Narayanan & Darwish [12]

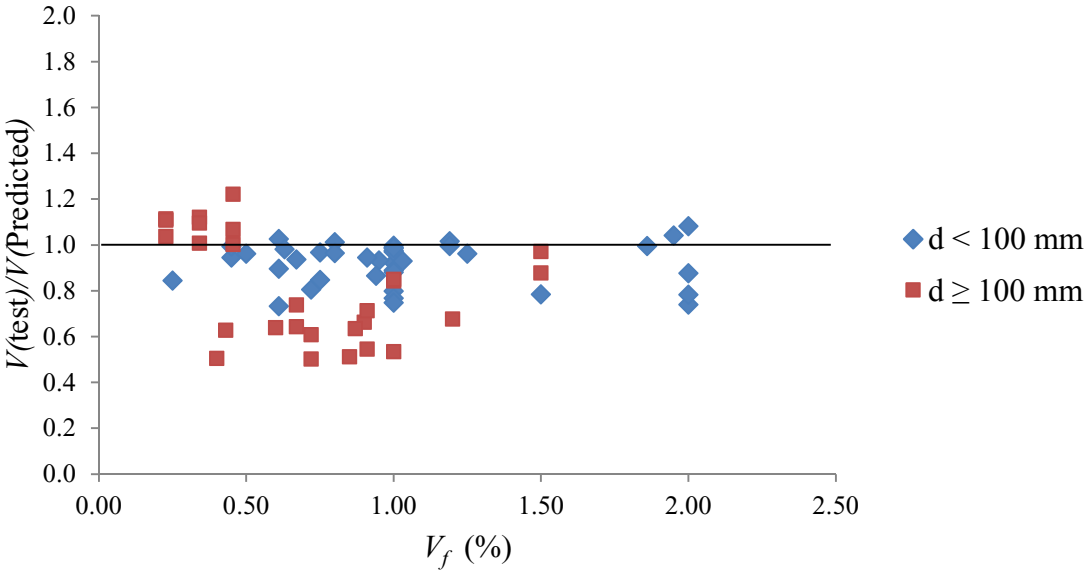

Figure 2.17. $V_{(T.)}/V_{(P.)}$ vs. V_f(%) using Shaaban & Gesund [14]

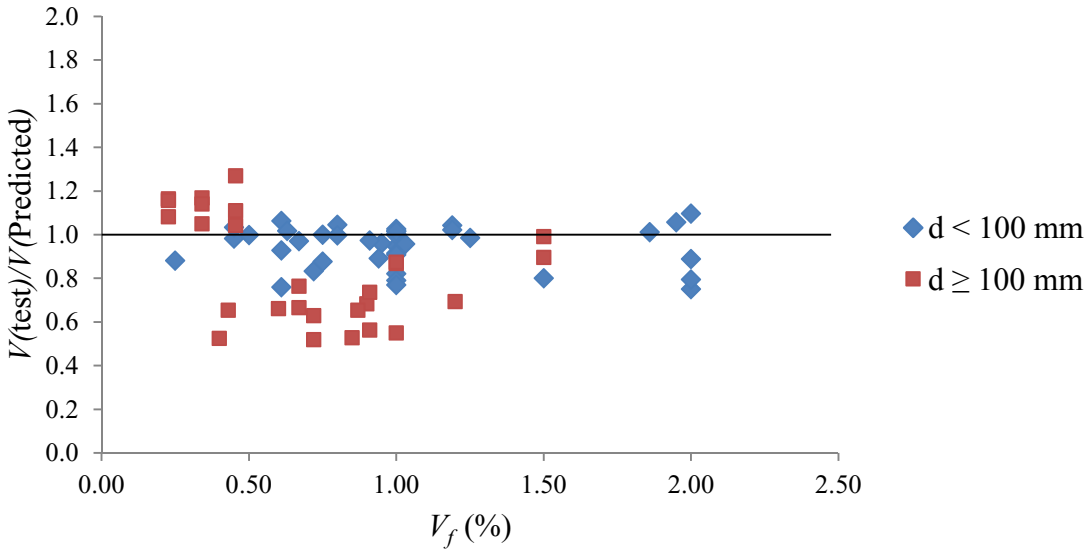

Figure 2.18. $V_{(T.)}/V_{(P.)}$ vs. V_f(%) using Harajli, Maalouf & Khatib [15]

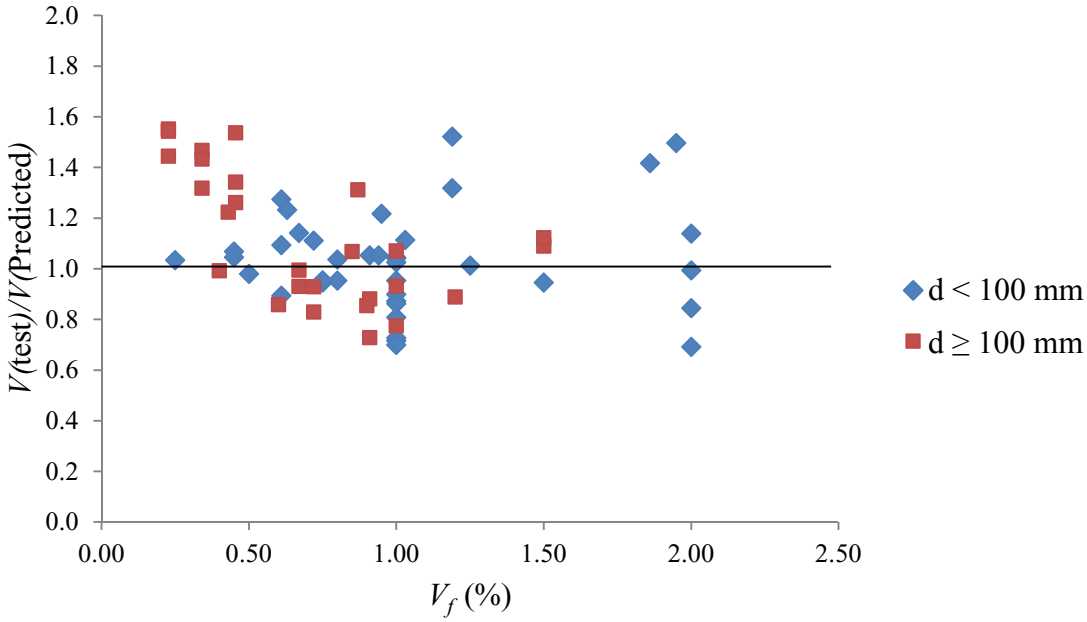

Figure 2.19. $V_{(T.)}/V_{(P.)}$ vs. V_f(%) using Hiroshi Higashiyama et al. [22]

According to the Figures 2.16 to 2.19, the equations by Shaaban and Gesund [14] and Harajli, Maalouf and Khatib [15] over-estimate 67% of the tested slabs with effective depths higher than 100 mm. The equation proposed by Higashiyama et al. [22] and Narayanan and Darwish [12], meanwhile, underestimates the punching-shear capacity of 59 and 52% of the thick slabs, respectively.

The main objective of presenting Figures 2.16 to 2.19, then, is to show that the existing prediction equations are able to predict the shear strength of thin slabs more reasonably than the thick slabs. As the effective depths of the slabs increase the specimens are mostly in the unsafe region of the graphs or become close to that region.

2.7. Research on the Structural Behaviour of HFRC Slabs

In the current chapter, different types of FRC were introduced, along with previous research and proposed equations to predict the punching-shear capacity of SFRC two-way slabs. According to the literature review, very limited publications are available on the structural behaviour of HFRC two-way slabs, as mentioned in part 2.3.2.

Almost all of the FRC two-way slabs contained steel fibres, and most of the test specimens had small thicknesses. Consequently, there is little experimental research that examines the effects of hybrid fibres on the structural behaviour of full-scale HFRC two-way slabs. In addition, very little data are available on thick SFRC slabs to examine the effects of fibres on their punching-shear strength.

In this study, an experimental program is carried out to investigate the structural behaviour of HFRC two-way slabs. The investigated structural behaviour covered the

punching-shear capacity, ductility, energy absorption, and mode of failure. The test specimens are designed as full-scale two-way slabs. Two different thicknesses of 200 and 250 mm were tested. The objective of the research was to investigate the structural behaviour of slabs that better represent actual slab-column connections that are used in real construction.

Chapter 3

Experimental Program

3.1. Introduction

This chapter presents a detailed description of the experimental program that was carried out at the structural laboratory of Memorial University of Newfoundland (MUN). The main objective of the program was to investigate the structural behaviour of hybrid-fibre-reinforced concrete (HFRC) two-way slabs.

The experimental program consisted of preparing, casting, testing, and evaluating the structural behaviour of six HFRC slabs and two reinforced-concrete slabs with no fibres, as reference slabs. Details of the preparation of the formworks, reinforcement mats, and instrumentation that was used to measure the deformations and strains are given in the chapter. The test set-up, loading frame, and data-acquisition system are also described in this chapter.

3.2. Material Properties

3.2.1. Hybrid-Fibre-Reinforced Concrete (HFRC)

The hybrid-fibre-reinforced concrete (HFRC) mix that was used to construct all specimens was obtained from a local ready-mix supplier. The targeted compressive strength was 60 MPa. The mix proportions for the test specimens are given in Table 3.1.

Table 3.1. Mix proportions for one cubic meter of the HFRC mix

Coarse aggregate	kg	1170
Fine aggregate	kg	630
Cement	kg	460
W/C ratio	kg	0.34
Super plasticizer	lit	2
Water reducer	lit	1

Four concrete mixtures were used with different steel fibre volume fractions as 0.68, 0.8, and 0.96%. The concrete containing no fibres used in the reference slabs. Also, the volume fraction of macro-synthetic fibres was 0.2% for all HFRC mixtures. There was a slight variation between the different mixtures for the purpose of proper mix design.

3.2.2. Steel and Synthetic Fibres

The steel fibres used in the specimens were hooked-type fibres. The fibres were 50 mm long and had a diameter of 1.1 mm. The ultimate tensile strength of the steel fibres was 1100 MPa.

The synthetic fibres used in this investigation were 40 mm long with an aspect ratio of 90 and tensile strength of 620 MPa. The fibres were composed of a polymer blend that partially fibrillates during mixing, which improves the mechanical characteristics of the concrete. Table 3.2 shows the properties of the used fibres, as supplied by the manufacturer.

Table 3.2. Properties of fibres as supplied by the manufacturer

Steel fibres	Fibre type	-	Hooked
	Fibre length	L_f (mm)	50
	Fibre diameter	D_f (mm)	1.1
	Ultimate tensile strength	MPa	1100
Macro synthetic fibres	Fibre length	L_f (mm)	40
	Fibre diameter	D_f (mm)	0.45
	Ultimate tensile strength	MPa	620

The HFRC mixture was used to cast the entire test slab rather than using fibre-reinforced concrete in the area around the column stubs, as was done in the previous researches such as the research done by Joo-Ha Lee et al. [17].

3.2.3. Reinforcing Bar

The reinforcing bars were cold-worked ribbed bars, CSA Grade 400, with a minimum characteristic strength of 400 MPa and the actual characteristic strength was 430 MPa. A typical stress-strain curve for a reinforcing bar, obtained from a tension test, at the structural laboratory of Memorial University of Newfoundland (MUN), is shown in Figure 3.1.

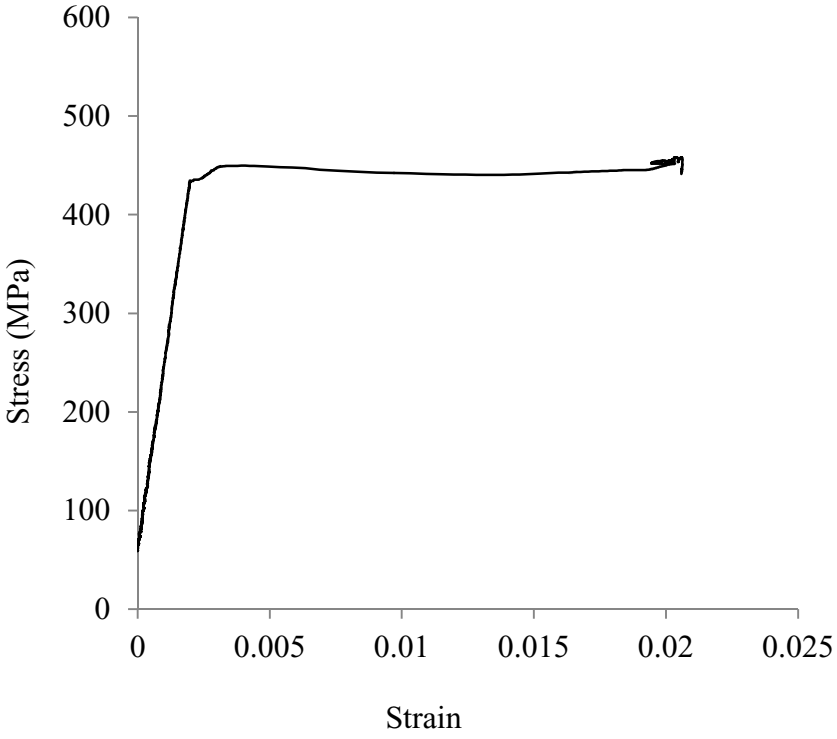

Figure 3.1. Stress-strain curve for a typical reinforcing bar

3.3. Concrete Properties

3.3.1. Compressive Strength

The compressive strength of the concrete was determined according to ASTM C39-04 standard. Six standard 150 × 300 mm cylinders for the HFRC mixtures and six 100 × 150 mm cylinders for the reference mixtures were cast at the same time of casting the slabs.

The cylinders were cured and kept at the same location as the test slabs and were also tested at the same time of testing the slabs. Before testing, the cylinders were capped

with sulphur capping compound. Figure 3.2 shows a photograph of the compression test machine. The load rate was 0.25 MPa/second, as per ASTM C39-04 standard.

Figure 3.2. Concrete compression test machine

3.3.2. Modulus of Rupture

The flexural strength of the HFRC was determined according to ASTM C1609/C1609M-05 standard. Six 100 × 100 × 400 mm prisms were cast at the same time of casting the slabs, and were cured and kept at the same location as the slabs. The prisms were tested at the same time of testing the slabs. Figure 3.3 shows a photograph of the closed-loop MTS test machine that was used to apply load on the prisms, until failure. The applied displacement rate was 0.05 mm per minute, according to the mentioned standard.

Figure 3.3. Flexural performance test machine

3.4. Compressive Strength and Flexural Performance of HFRC

The compressive and flexural tensile strengths of all mixes are presented in Table 3.3. As mentioned earlier, the mixtures were designed to have a 28 day compressive strength equal to 60 MPa. However, because of the weather conditions at the batch plant and the outdoor storage of the aggregate, the results were different than the targeted value. The lowest value, consequently, was 60 MPa and the highest value was 79 MPa.

The addition of fibres to the concrete mix caused an increase in the modulus of rupture of the concrete, as shown in Table 3.3. However, the concrete compressive strength, also, had an effect on the modulus of rupture. Hence, the values are normalized with respect to the square root of the concrete compressive strength to eliminate the effect of the compressive strength.

Table 3.3. Compressive strength and modulus of rupture of different mixtures

No.	Concrete mixtures	V_f-steel (%)	V_f-synthetic (%)	Concrete strength, f_c' (MPa)	Modulus of rupture, f_r (MPa)	$f_r / \sqrt{f_c'}$
1	Reference	0	0	70	5.45	0.65
2	HFRC–0.68	0.68	0.2	77	7.10	0.81
3	HFRC–0.8	0.80	0.2	61	7.20	0.92
4	HFRC–0.96	0.96	0.2	60	8.35	1.08

The results show that addition of fibres up to 0.68% caused a gain of 25% in the normalized flexural strength. Adding 0.8% fibres caused an increase of 42% in the modulus of rupture, compared to the reference samples. The highest value of increase in the normalized flexural strength, equal to 66%, was observed in the mixture with 0.96% of steel fibres.

Figure 3.4 shows the flexural stress versus the central deflection of the prisms. The post-cracking behaviour of the HFRC samples, in comparison to the reference samples, showed the ability of the HFRC prisms to resist the load even after the peak load was reached. This could be attributed to the presence of fibres, which were able to bridge the cracks and could improve the post-peak flexural capacity of the fibre-reinforced concrete.

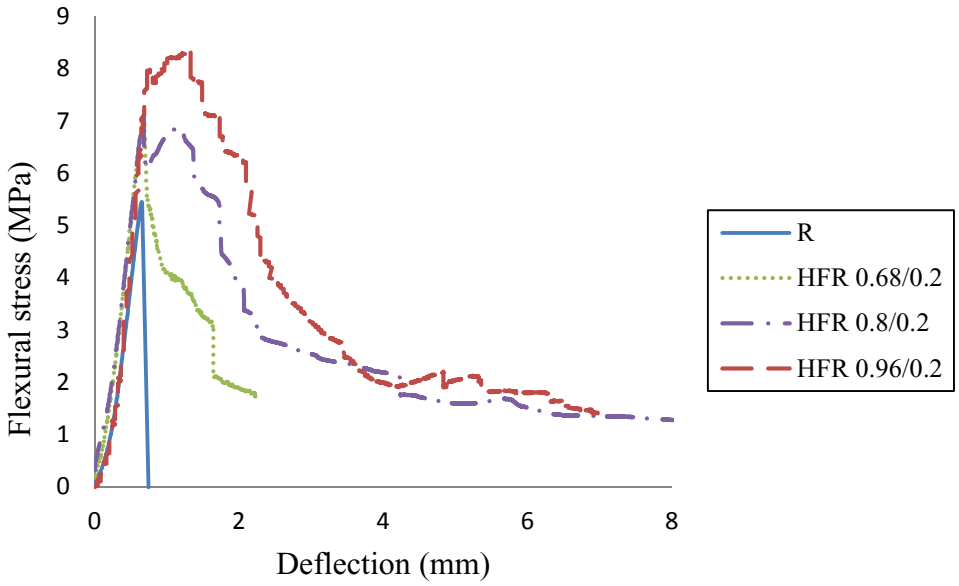

Figure 3.4. Stress-deflection characteristics of the prisms

3.5. Slab Specimens

The test program consisted of a series of tests on eight full scale two-way slabs. The test slabs had side dimensions of 1900 mm in both directions. The thickness of the slabs and the fibre volume fractions of the concrete mixtures are considered as the main variables. The slabs were centrally loaded through a 250 × 250 mm column stub. During testing, the slabs were simply supported along all four edges, with the corners free to lift.

The slabs were divided into two groups with 200 and 250 mm thickness. Each group contained different fibre volume fractions as 0, 0.68, 0.8, and 0.96%. The 0% fibre volume fraction was used in the reference slabs.

The specimens represent, with good approximation, the region of a negative bending moment around an interior column of a full-scale model of a typical flat slab

system. A prototype flat-plate-structure is shown in Figure 3.5. The points of contra-flexure are about 0.21 times the span from supports. Hence, the test specimens would represent a 4.5 × 4.5 m flat-plate structure.

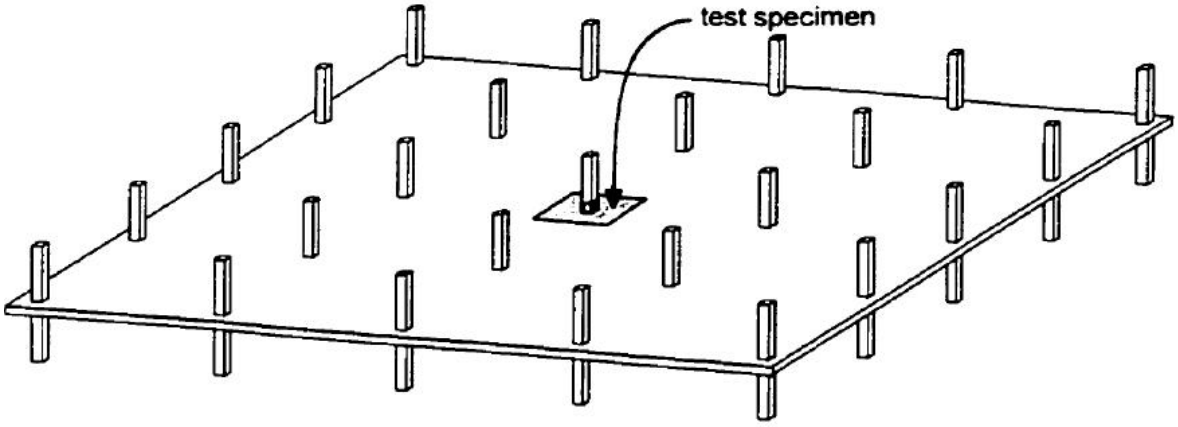

Figure 3.5. Prototype flat-plate structure (4.5 × 4.5 m bays)

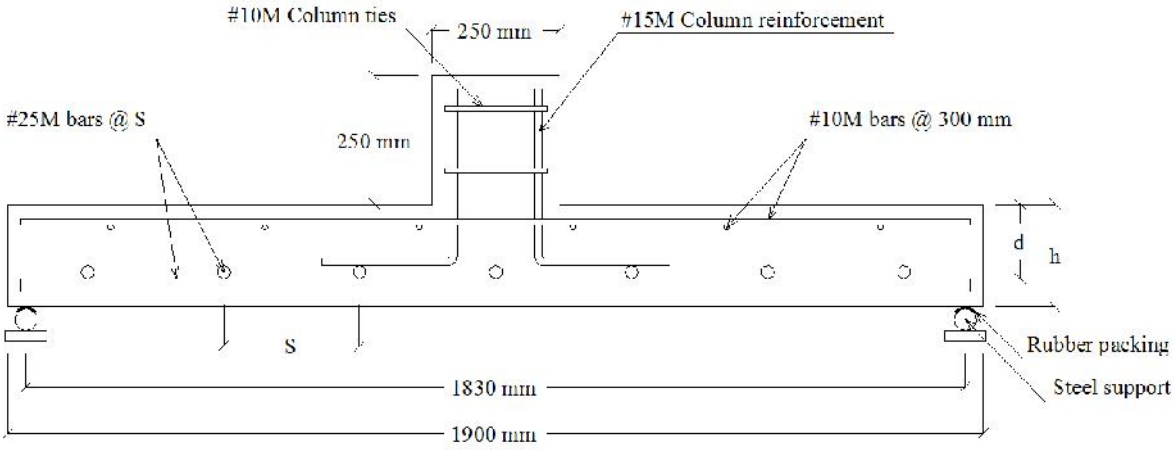

Figure 3.6. Details of a test specimen

The dimensions and reinforcement details of a typical test slab are shown in Figure 3.6. In each slab, 6-10M steel bars were used as compression reinforcement in both directions. These bars are considered to be the integrity reinforcement. The reinforcement ratio for all of the test slabs was 1.3% and the spacing was selected based on the reinforcement ratio and is given in Table 3.4.

Table 3.4. Slab specimen details

No.	Groups	Specimen	$d_{avg.}$ (mm)	(%)	V_f - steel (%)	V_f - synthetic (%)	Reinf.	Bar spacing (mm)
1	200 mm-thick slabs	R200	145	1.3	0	0	7-25M	265
2		HFR200–0.68/0.2	145	1.3	0.68	0.2	7-25M	265
3		HFR200–0.8/0.2	145	1.3	0.8	0.2	7-25M	265
4		HFR200–0.96/0.2	145	1.3	0.96	0.2	7-25M	265
5	250 mm-thick slabs	R250	195	1.3	0	0	9-25M	195
6		HFR250–0.68/0.2	195	1.3	0.68	0.2	9-25M	195
7		HFR250–0.8/0.2	195	1.3	0.8	0.2	9-25M	195
8		HFR250–0.96/0.2	195	1.3	0.96	0.2	9-25M	195

3.6. Slab Formwork and Fabrication

The test slabs were cast in a steel formwork at the concrete laboratory. The formwork used to cast the slabs was a square 2 × 2 m steel plate with 7 mm thickness, which was supported on steel beams. The beams were supported on steel W-shape columns. Four removable steel plates, along the four edges, were used as sides of the formwork.

The steel bars were cut in the same length of 1850 mm, which allowed for a clear cover of 25 mm from each side of the formwork edge. Strain gauges were mounted at specific locations on the steel bars. The bars were tied together to form the top and

bottom steel mats. The lower reinforcing mat rested on four concrete chairs with thickness of 30 mm, which was the clear concrete cover. The chairs were placed around corners far from the punching zone to eliminate any effect on the punching-shear capacity. The column stubs were reinforced with four 800 mm long 15M L-shaped steel bars. The stirrups used in the columns were 10M bars. Figure 3.7 shows the formwork and the reinforcement used in a test specimen before casting.

Figure 3.7. A reinforcement cage in the formwork for a typical slab

During casting, the concrete was vibrated using a vibrator. The top surface of the slab was levelled and finished with a steel trowel. A steel mould was used as a formwork for the column stub. The mould was placed at the center of each slab. The columns were, then, poured after 24 hours of casting. Subsequently, the slabs were kept in the formwork for a week. After the first 24 hours, water was sprayed on the specimens once a day to

keep the surface wet. The specimens were cured in such way for a week. Once removed from the formwork, the slabs were kept in the structural laboratory until the day of testing.

3.7. Test Set-up

The specimens were tested in a test setup that was designed and fabricated in the structural laboratory of Memorial University of Newfoundland (MUN). The slabs were tested in a vertical position in order to be able to detect and mark the cracks, as they develop. The transverse load was applied on the slabs through a hydraulic jack.

The test setup consisted of four retaining walls. Two walls were used to support the four steel beams that, in turn, supported the test specimen. Four 32 mm diameter rods were welded on the beams to form four sides of the slab support system. A 5 mm packing rubber was glued on the rods. The rubber packing between the rods and the slab was used to ensure uniform contact along the supports. The supporting steel beams were anchored to the retaining walls, which were anchored to the 1000 mm-thick structural floor. The other two retaining walls were used to support the hydraulic jack that applied the load directly on the column stub. The retaining wall units were restrained at the top and lower edges by self-supporting closed rigid steel frames, made with W600 sections. The function of the frames was to minimize the lateral displacement of the supporting retaining walls, and to ensure that the test setup would act as a rigid self-supporting unit. A hydraulic jack was used to apply a concentric load on the column stub in a horizontal

position. The jack had a maximum capacity of 3110 kN and a maximum displacement of 300 mm.

Test slabs were lifted and installed into the frame using a 10 ton crane, and also removed in the same way after the tests were finished. The applied load was measured using a pressure gauge, while the displacement of the jack was measured using an externally mounted linear-variable differential transducer (LVDT). A photograph of the test setup is shown in Figure 3.8.

Figure 3.8. Test set-up

3.8. Instrumentation and Measurements

3.8.1. Deflections

Five linear-variable differential transducers (LVDTs) were placed at five specific locations on the tension side of the slabs to measure the deflection of the specimens

during loading. Figure 3.9 shows the positions of the LVDTs. The readings from the LVDTs were logged into a data acquisition system.

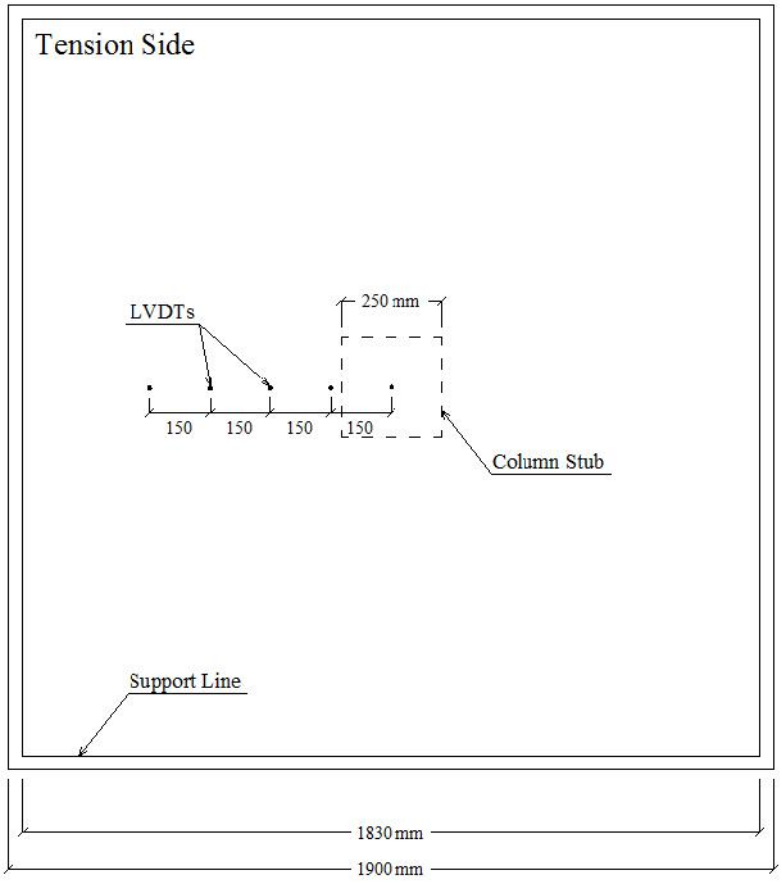

Figure 3.9. A typical arrangement of LVDTs

3.8.2. Steel Strains

Steel strains were measured at different locations by means of electrical strain gauges. The arrangement of the steel-strain gauges is shown in Figure 3.10. The strain gauges were 6 mm long, with a strain limit of approximately 5%. The grid resistance of the used strain gauge was $120 \pm 0.3\%$ in ohms at 24 degrees of

centigrade, and the gauge factor was 2.09 ± 0.5%. To protect against any possible damage by water and also during casting, the gauges were coated with a protective sealant and then covered with a plastic tape.

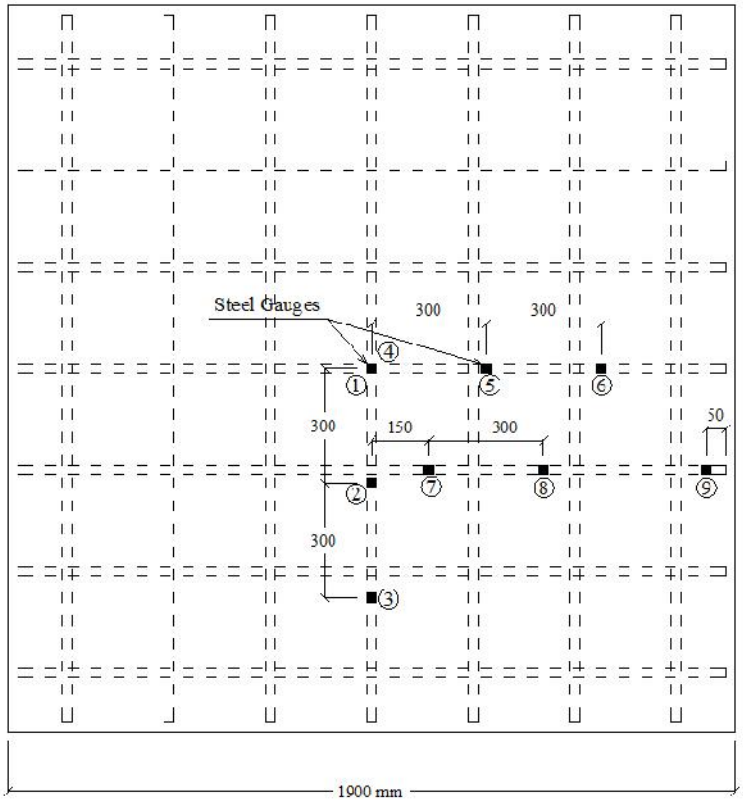

Figure 3.10. A typical arrangement of steel strain gauges

3.8.3. Concrete Strains

The concrete strains were measured at five locations on the compression side of the slabs, as shown in Figure 3.11. The strains were measured using electrical-resistance strain gauges glued to the compression side of the slab surface at various distances from the column face. The concrete surface was ground at each position, and a thin layer of

epoxy resin was placed on the location to obtain an even surface. Each strain gauge was placed in position and connected to the data acquisition system.

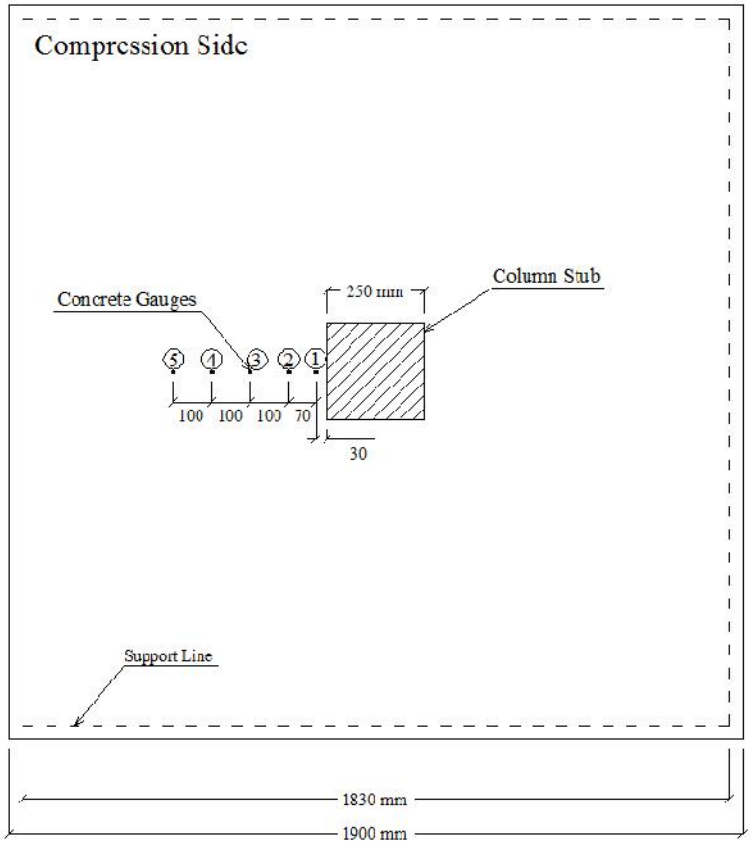

Figure 3.11. A typical arrangement of concrete strain gauges

3.8.4. Data Acquisition System

The electrical steel strain gauges mounted on the steel-reinforcement, concrete strain gauges installed on the compression side of the slabs, LVDTs, and pressure gauge readings were logged to a computerized data acquisition system. All measurements were

stored in a computer file. The software used was Lab-VIEW. The data scanning and saving rate was set to 0.5 seconds.

3.9. Test Procedure

An initial load equal to 10% of the ultimate predicted load was applied to ensure a complete contact between the slab and the supports and, also, to eliminate initial settlements of the frame and the hydraulic jack. The initial applied load was, then, released to 10 kN and the test was started. The slab was loaded at a selected load increment of 22.4 kN until first crack occurred. After marking the first crack, loading was continued at a load increment of 44.8 kN until failure. After each load increment, the slab was carefully inspected and the cracks were marked, as shown in Figure 3.12.

Figure 3.12. Marking the cracks on a typical slab

Chapter 4

Test Results and Discussion

4.1. Introduction

This chapter presents a detailed description of the results and observations obtained from testing the eight reinforced-concrete two-way slabs that were described in the previous chapter. As mentioned earlier, the slab thickness and fibre volume fraction were the main variables of the experiments. The slabs were tested in two groups with different thicknesses: the first group contained the 200 mm-thick slabs and the second group contained the specimens with 250 mm thickness. Within each group the specimens had different amounts of fibre volume fractions of 0.68, 0.8, and 0.96% in the HFRC test slabs, and 0% in the reference slabs.

The experimental data was collected and analyzed; however, due to the large amount of data, only a few representative ones are used in the presentation. The structural

behaviour of the slabs is presented in terms of load-deflection characteristics, stiffness, ductility and energy-absorption, reinforcement and concrete strains, post-punching behaviour, cracking patterns, and punching-shear capacity. The predictions of the existing design equations for SFRC slabs are compared to the test results from the current program. The results of the comparison show that the existing equations, developed for SFRC, can predict the capacity of the HFRC slabs, tested in the current study, with a reasonable accuracy.

4.2. Load-Deflection Characteristics

The applied load-versus-deflection curves for the test specimens are shown in Figures 4.1 and 4.2. As mentioned earlier, the tests were carried out using a displacement control system and the deflections were obtained from the LVDTs, which were placed at the center of each slab. During the test, the load was paused at specific intervals to inspect the cracks and map them. The first crack of each specimen was observed through visual inspection, and the corresponding load was recorded. This load is referred to as the first crack load. As a result of having the system on hold at each loading interval, the loads decreased slightly. Hence, the graphs are not very smooth. Nevertheless, the effects of the decrease on the ultimate load and deflection characteristics are negligible.

In general, the slabs behaved in a linear elastic fashion up to the formation of the first cracks. According to Figure 4.1, the load-deflection graphs show a linear behaviour up to a point that is close to the yield load in the 200 mm-thick slabs.

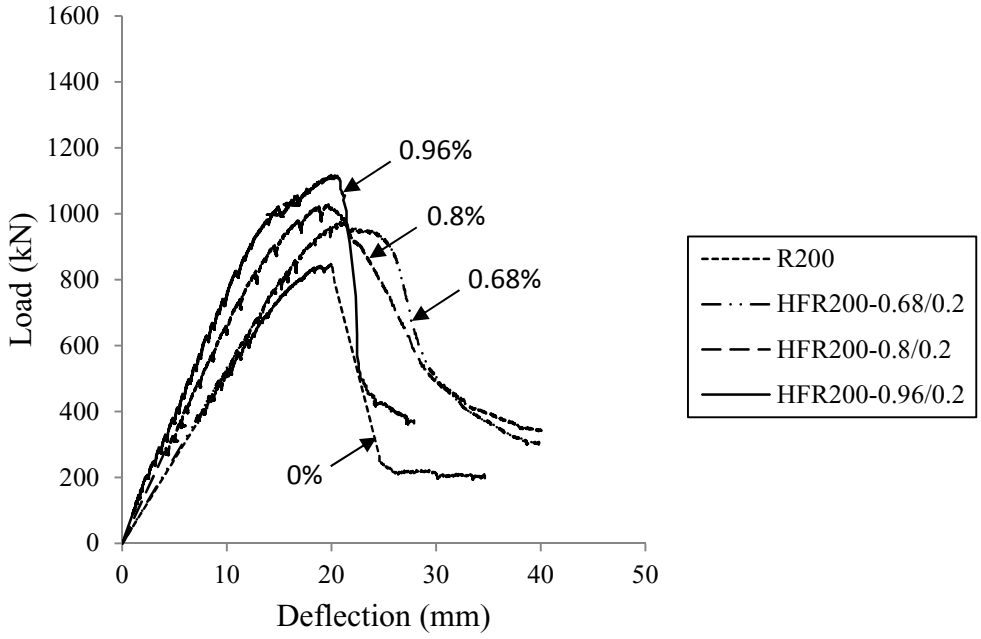

Figure 4.1. Load–deflection characteristics of the 200 mm thick slabs (Group 1)

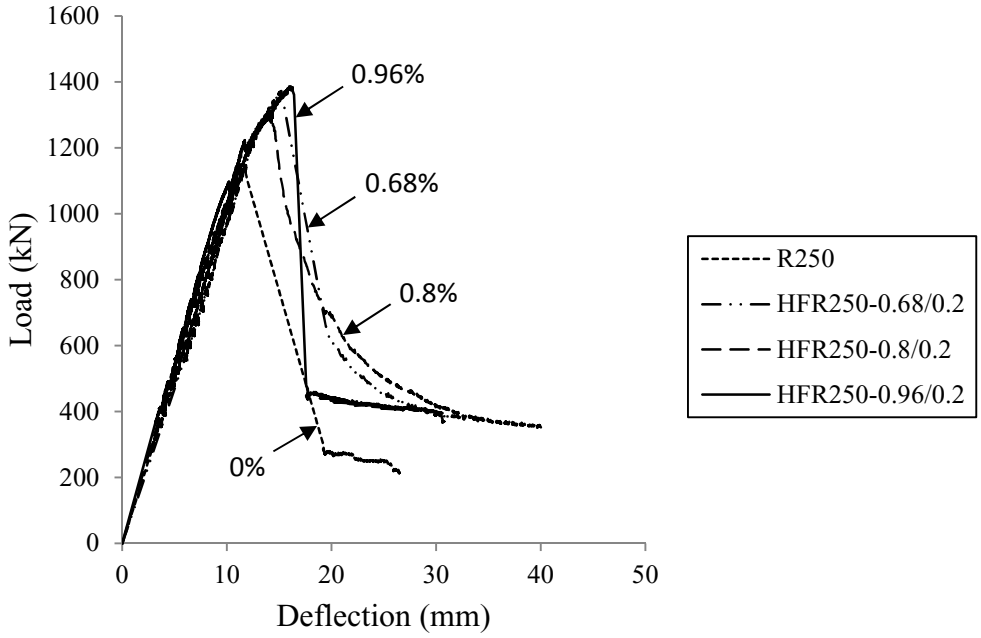

Figure 4.2. Load–deflection characteristics of the 250 mm thick slabs (Group 2)

For the 250 mm-thick slabs, and as shown in Figure 4.2, the linear load-deflection behaviour was pronounced almost up to the failure load.

The observations show that the decrease in the stiffness of the HFRC slabs is small and the stiffness does not significantly change before and after the first crack forms. In addition, the reduction in stiffness occurred very close to the peak load. This can be attributed to the addition of fibres, which are able to bridge the cracks, and resist the tensile stresses, even after cracking until the point in which the fibres start being pulled out of the concrete and the failure occurs.

The load-deflection curves could indicate the modes of failure of the test specimens. Failure modes of two-way slabs could be classified as flexural failure, punching failure, and ductile punching failure. In the condition that most of the flexural reinforcement yield before punching occurs and slab exhibits large deflections, flexural failure takes place. When the slabs have small deformations with partial yielding of the flexural reinforcement at the column head, shear failure occurs. The third type of failure, ductile-punching failure, is a transition between the first two mentioned cases [1].

According to the load-deflection curves, no flexural failure was observed in any of the test specimens, as none of the curves showed a state of steadily increasing deflections at a constant load, which means an increase in deflections with no increasing in applied load. Hence, all of the slabs failed in punching. According to Figures 4.1 and 4.2, the reference slabs, both with 200 and 250 mm thicknesses, failed in punching with a sudden decrease in the load carrying capacity after the shear capacity was reached.

However, in the slabs containing fibres, the type of failure could be classified as a ductile punching. The slabs did not have a sudden loss in the capacity after the ultimate load was reached and a gradual reduction in the load-deflection curves was observed. The 200 mm-thick slabs were still able to carry some load even after the failure occurred. This is referred to as the post-punching behaviour.

In the second group of slabs, as well, this change in the mode of failure was also observed. The mode of failure of the 250 mm-thick slabs containing 0.68 and 0.8% of fibres could be classified as ductile punching failure. However, the 250 mm-thick slab containing 0.96% of fibres had a sudden drop in the load-deflection curve, which shows a punching failure. Although having a sudden drop, the slab sustained 30% of the capacity after the peak load was reached.

While the effect of the fibres on the modes of failure is obvious, when comparing the load-deflection curves of the test specimens with different thicknesses, the load-deflection figures show that the presence of fibres in the 200 mm-thick slabs has a more significant effect on the mode of failure than in the thicker slabs.

The test specimens had similar reinforcement ratio and close compressive strengths. Consequently, the observed transition from a brittle type of failure to a ductile one could be attributed to the addition of hybrid fibres. Table 4.1 gives the values of the measured deflections at first crack, first yield of flexural reinforcement, and ultimate load.

The first crack was observed with the naked eye and, hence, it could only be determined when the crack showed on the slab surface. Consequently, the values of the first crack load may not be very accurate.

Table 4.1. Load and deflection characteristics of the test slabs

No.	Specimen	First crack load (kN)	Deflection at first crack load (mm)	Yield load (kN)	Deflection at yield load (mm)	Ultimate load (kN)	Deflection at ultimate load (mm)
1	R200	146.7	0.67	564.0	11.03	847.9	19.91
2	HFR200–0.68/0.2	100.9	0.61	504.4	9.68	978.1	21.23
3	HFR200–0.8/0.2	110.0	0.70	692.3	10.44	1029.9	16.97
4	HFR200–0.96/0.2	142.1	0.72	619.0	7.94	1117.6	19.97
5	R250	155.9	0.88	779.5	7.75	1147.6	11.66
6	HFR250–0.68/0.2	110.0	0.63	706.1	7.45	1375.5	15.19
7	HFR250–0.8/0.2	105.5	0.76	926.2	8.94	1300.2	14.12
8	HFR250–0.96/0.2	142.1	0.80	967.4	8.69	1386.5	15.97

The deflection values appear to be dependent on the volume fraction of fibres in the test slabs. For the 200 mm-thick slabs, for example, adding fibres reduced the deformations at almost all stages of loading before failure, especially at the yield and the ultimate load.

However, for the 250 mm-thick slabs, the deflection values are close at all stages of loading. Hence, it can be concluded that the contribution of fibres in the 200 mm-thick slabs is more significant than in the 250 mm-thick slabs.

4.3. Stiffness, Ductility, and Energy-Absorption

The load needed to cause a unit displacement at the center of a slab is referred to as the stiffness of the slab. Ductility represents the ratio of deflection at the point in which the load drops down to 25% of the ultimate load ($_2$) to the deflection at yield load of the flexural reinforcement ($_1$), as shown in Figure 4.3. In other words, ductility shows the deformation ability of a structural element before failure. The energy-absorption is

defined as the area under the load-deflection curve at 25% of the ultimate load in the post-peak region, as shown in Figure 4.4.

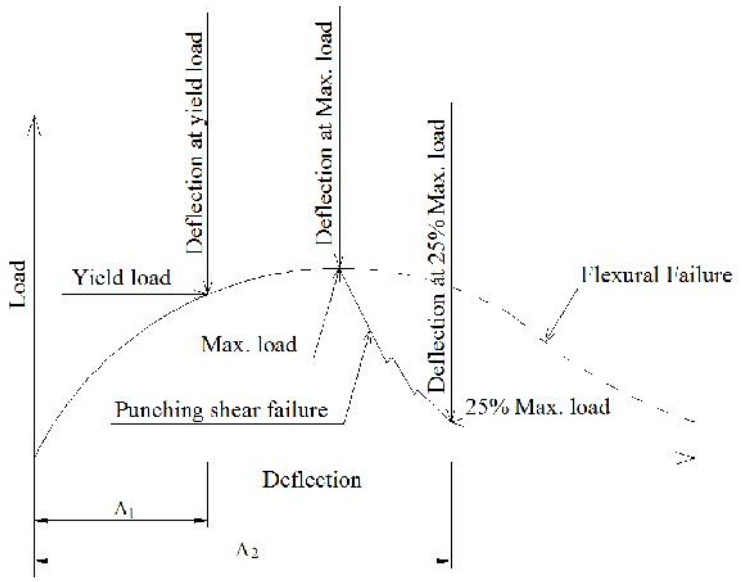

Figure 4.3. Definition of ductility

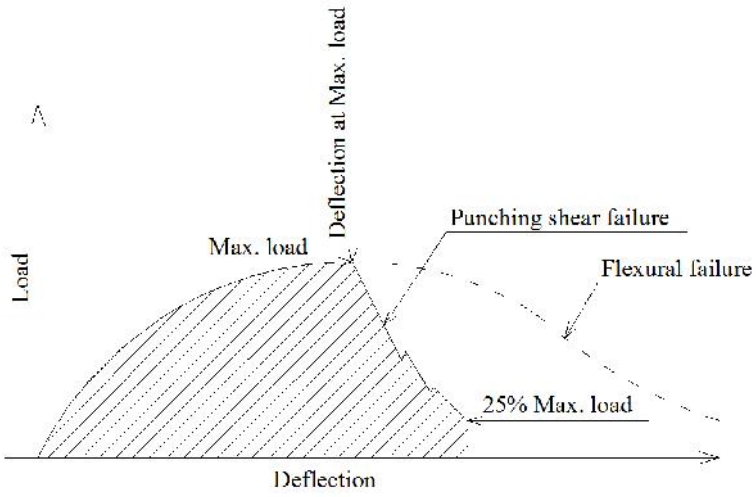

Figure 4.4. Definition of energy-absorption

According to previous experimental results, such as Swamy and Ali [2] and Theodorakopoulos and Swamy [3], adding steel fibres up to even more than 1% by volume enhances the stiffness and ductility. In the current study, it was observed that addition of fibres up to 0.96% caused a significant effect on the stiffness, ductility, and energy absorption of the test slabs, which is in agreement with the results of previous studies.

The load-deflection curves of the HFRC slabs show a different behaviour than the reference ones. As the applied load increases, cracks form and the slab experiences a gradual loss in the stiffness [1]. As mentioned earlier and shown in Figures 4.1 and 4.2, the load-deflection curves for the 200 mm-thick slabs show an almost-constant stiffness to the yield load, and at that point the stiffness of the specimens start to gradually decrease. For the 250 mm-thick slabs, the stiffness remained constant during loading and started to decrease at a point close to the shear capacity of the slabs. Table 4.2 shows the amounts of stiffness, ductility, and energy-absorption capacity of the test specimens, including reference slabs and HFRC two-way slabs.

The addition of fibres caused an increase in the stiffness of the 200 mm-thick test slabs. For example, increasing the fibre content to 0.68% by volume caused an increase of 5% in the stiffness compared to the reference slab. Also, for specimen HFR200-0.8, an increase of about 35% in the stiffness was observed. The improvement in stiffness for specimen HFR200-0.96, with the highest amount of fibre volume fraction, was 78%.

Nevertheless, the 250 mm-thick slabs did not have a significant change in the stiffness in comparison to the reference slabs. For the 250 mm-thick slabs containing 0.68% of fibres, the stiffness reduced to 5%, compared to the reference specimens.

Nonetheless, in the slabs containing 0.8, and 0.96% fibres, the increase in the stiffness was 7 and 14%, respectively. Hence, the results show that, in the 200 mm-thick slabs, the fibres have more significant effect on the stiffness compared to the 250 mm-thick slabs.

Table 4.2. Stiffness, ductility, and energy absorption capacity of the test slabs

No.	Specimen	Stiffness (kN/mm)	Ductility $_{0.25u}/\ _{y}$	Energy absorption capacity (kN.mm × 10^3)
1	R200	55.0	2.72	14.4
2	HFR200–0.68/0.2	57.5	4.71	23.2
3	HFR200–0.8/0.2	75.0	6.89	27.8
4	HFR200–0.96/0.2	97.7	6.92	31.2
5	R250	109.6	2.47	14.1
6	HFR250–0.68/0.2	102.8	4.53	21.9
7	HFR250–0.8/0.2	117.4	5.66	22.5
8	HFR250–0.96/0.2	125.2	6.34	25.8

Table 4.2 shows that, for the 200 mm-thick slabs, the ductility increased by 73% with the addition of fibres up to 0.68%. As well, the addition of 0.8 and 0.96% fibres caused an improvement equal to 153 and 154%, respectively, compared to the reference slab. The ductility also increased when the amount of fibres increased, for all of the 250 mm-thick slabs. In comparison to the reference slabs, increasing the amount of fibres to 0.68% caused an 83% enhancement in the ductility of the specimen HFR250-0.68. The improvement for the specimens HFR250-0.8 and HFR250-0.96 was equal to 129 and 157%, respectively.

In addition, the energy-absorption capacity of the HFRC slabs was also enhanced as the fibre volume fraction was increased. Increasing the amount of fibres to 0.68 and 0.8% caused an improvement of about 62 and 93% in the energy absorption of the 200

mm-thick specimens, respectively. On the other hand, for the 250 mm-thick slabs, an enhancement of 53 and 60% occurred by increasing the amount of fibres to 0.68 and 0.8%, respectively. Also, comparing the results of the different test specimens indicates that, as steel fibres were increased up to 0.96%, the energy absorption increased by 116 and 83% for the slabs with 200 and 250 mm thickness, respectively. Thus, the maximum energy absorption was observed in the slabs with the highest amount of steel fibres equal to 0.96% by volume.

Figures 4.5 to 4.8 show the load-deflection characteristics of the test specimens with different effective depths. Each plot shows a pair of slabs with the same fibre volume but with different thicknesses; namely 200 and 250 mm. According to the Figures, increasing the effective depth improved the stiffness of the slabs.

In the reference slabs, the stiffness had an enhancement of about 99% by increasing the effective depth. In the test specimens containing 0.68, 0.8, and 0.96% fibres, the stiffness of the slabs had an enhancement equal to 79, 57, and 28%, respectively. Hence, the results show that, in the slabs containing more fibres, the contribution of the effective depth in increasing the stiffness is less than other specimens containing less amounts of fibres.

Increasing the thickness of the slabs from 200 to 250 mm caused a decrease in the ductility of the specimens. For the reference slabs, the ductility had a 9% decrease by increasing the thickness. Also, for the HFRC slabs containing 0.68, 0.8, and 0.96% fibres, the ductility had a decrease equal to 4, 18, and 8%, respectively, by increasing the thickness of the slabs from 200 to 250 mm.

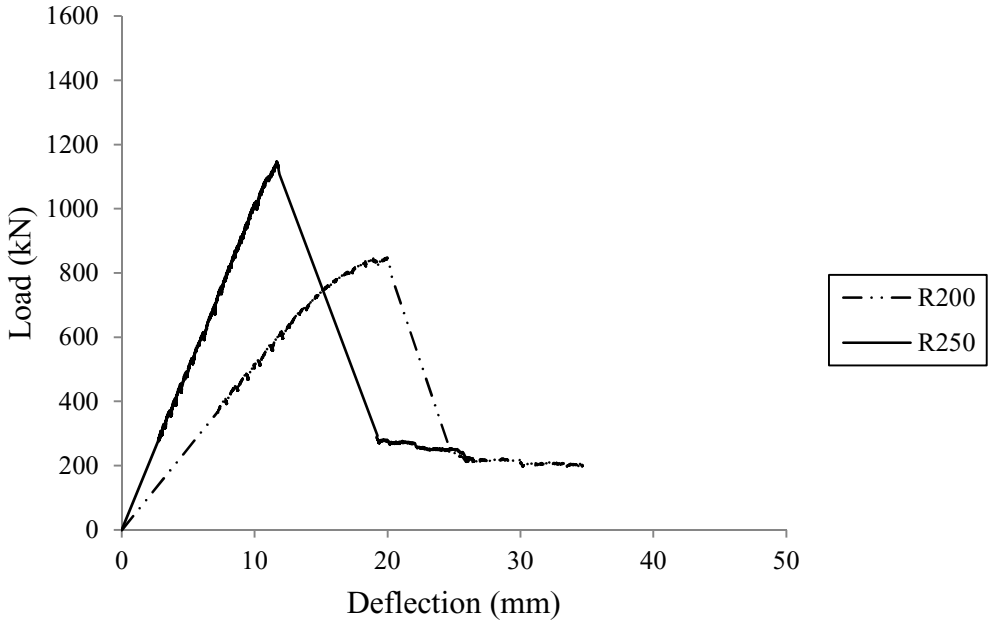

Figure 4.5. Load-deflection characteristics (reference slabs)

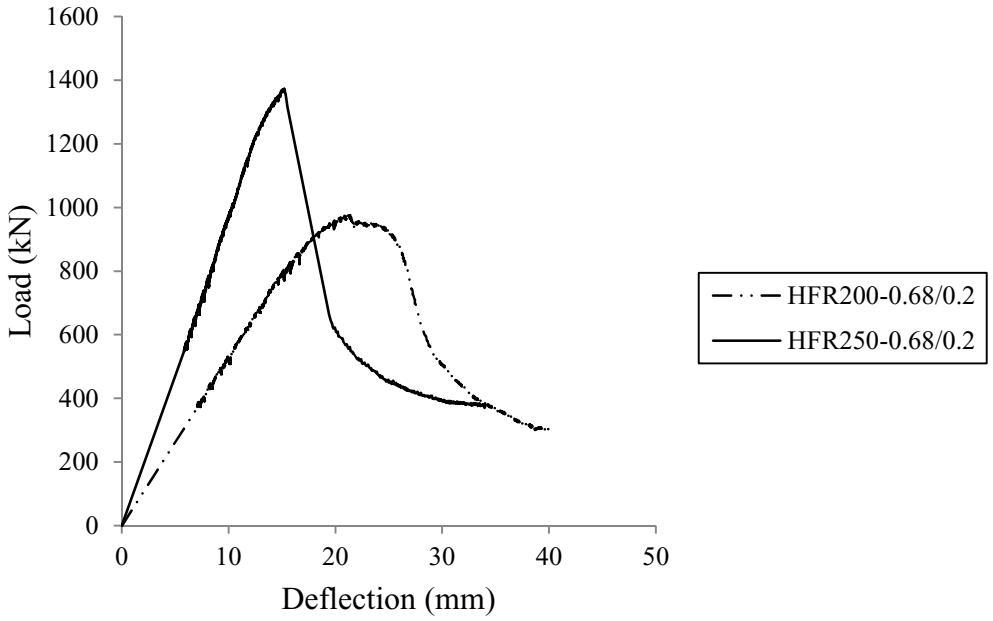

Figure 4.6. Load-deflection characteristics (V_f = 0.68%)

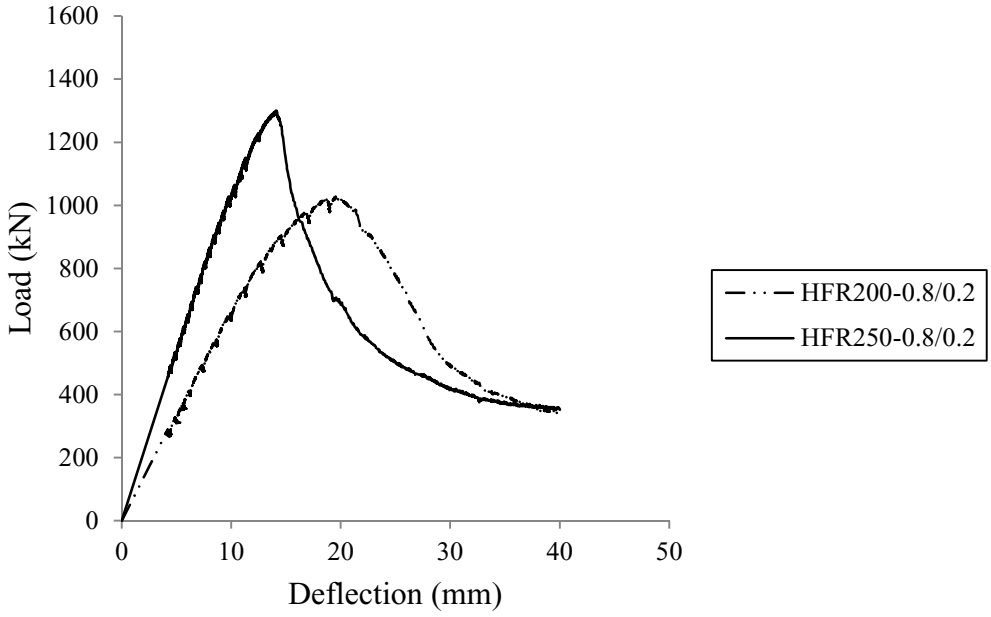

Figure 4.7. Load-deflection characteristics (V_f = 0.8%)

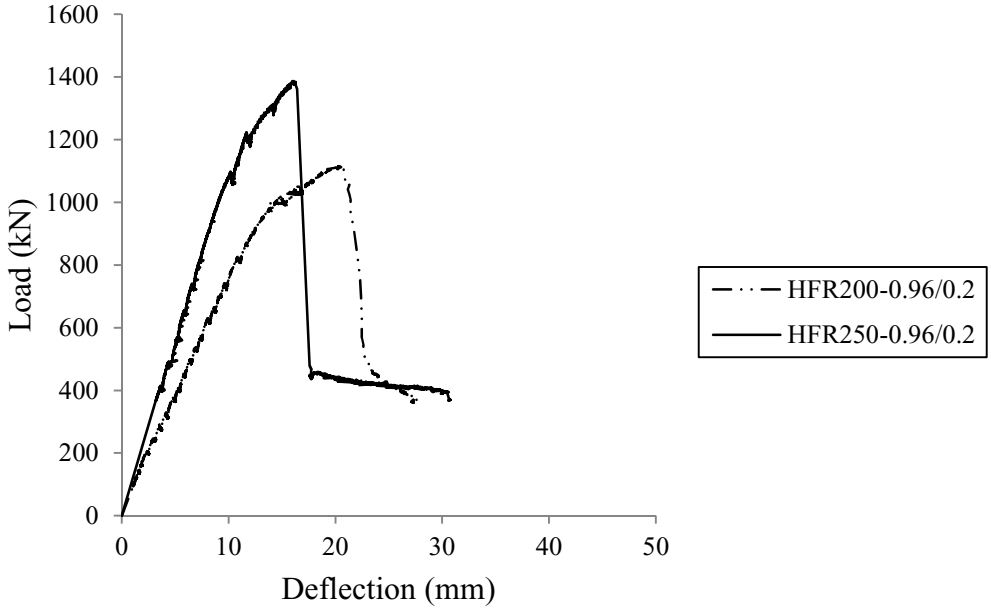

Figure 4.8. Load-deflection characteristics (V_f = 0.96%)

In addition, energy-absorption decreased with increasing the effective depth for all of the test slabs. In the reference slabs, a reduction of 2% was observed by increasing the thickness from 200 to 250 mm. In the HFRC slabs, meanwhile, the increase in the thickness caused a decrease of 6, 19, and 17%, for the slabs containing 0.68, 0.8, and 0.96% fibres, respectively.

The concrete compressive strength of the specimens was almost similar and other characteristics of the test specimens were the same. Hence, it can be concluded that the increase in the stiffness paired with the reduction in the ductility and energy-absorption could be attributed to the presence of fibres. Fibres are able to bridge the cracks and cause the concrete to sustain tensile stresses even after cracking.

4.4. Deflection Profiles

To construct the deflection profiles for the test specimens, the deflection measurements at different locations along the width of a specimen are used. The deflection profiles show the deformational responses to the applied load. As mentioned in the previous chapter, the deflection values were measured at five different locations on one side of the symmetrical specimens, as shown in Figure 3.10. The deflection profiles can be used in classifying the modes of failure, and to determine the curvature of the specimens.

It was observed in previous research that the deflection profiles depend on the type of reinforcement. Qi Zhang [32] observed that in the two-way slabs containing FRP reinforcement, the deflection profiles were almost bilinear, with a turning point occurring

at a location in which the inclined shear cracks started growing toward the tension face of the slabs. However, according to the deflection profiles shown in Figures 4.9 to 4.16, no such specific turning point is observed in any of the current test slabs. Also, no linear deflection was observed at any distances from the face of the columns. Instead, a curvature is observed in all of the test specimens. This indicates that the slabs are not rotating as a rigid body in any region, even after the formation of the shear cracks. The deflection profiles show that before the formation of the first crack, the deflections are too small at different locations away from the center of the slabs.

By adding the steel fibres to the concrete mixture and by increasing the thickness of the slabs, less deformation was observed in the deflection profiles. It appears that the flexural reinforcement and the stiffening of the concrete cover by the fibres prevent the punching cone to appear on the flexural side of the test specimens by behaving as a membrane. Hence, it is not possible to identify the punching failure by increasing the deflections around the columns in any of the deflection profiles shown in Figures 4.9 to 4.16.

This behaviour and observations are in agreement with previous studies such as those by Cheng and Parra-Montesinos [21]. Also, there is a gradual increase in the deflections in different loads from 50 kN to the failure load. This indicates that there is no sudden rise in the measured deformation at any stage of loading, which ultimately results in no discontinuities in the deformation profiles.

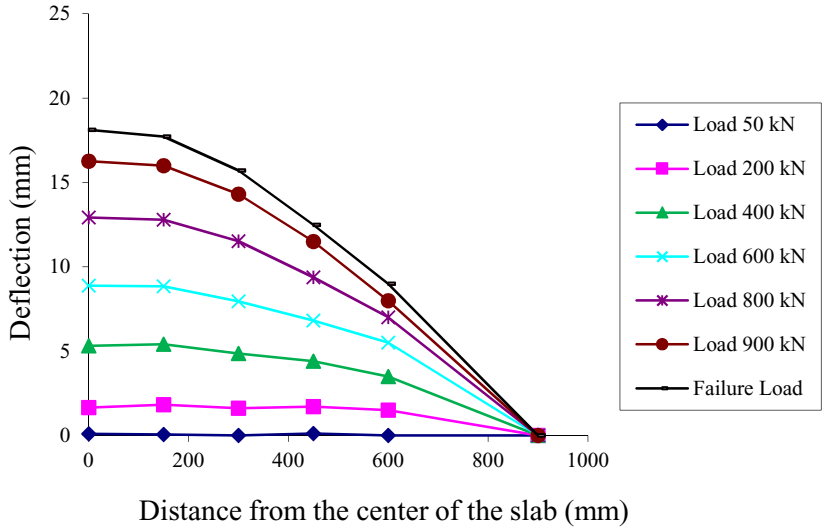

Figure 4.9. Deflection profile for R200

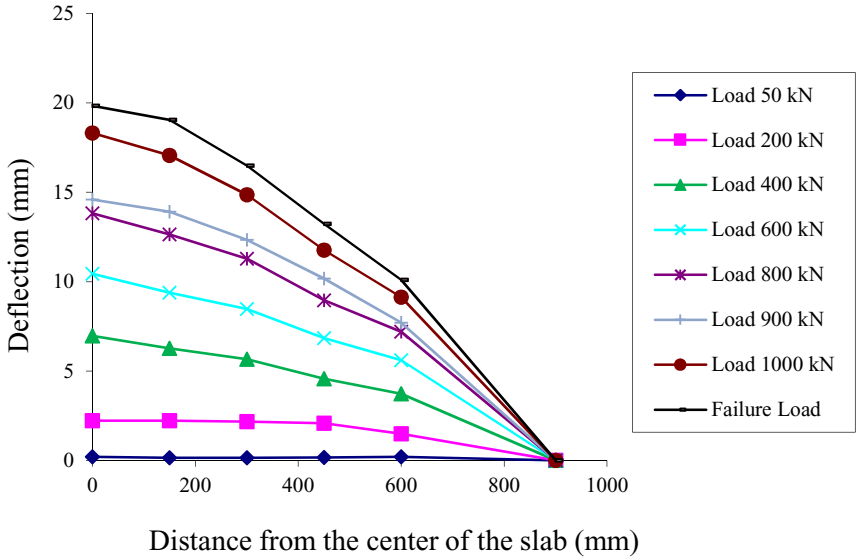

Figure 4.10. Deflection profile for HFR200-0.68/0.2

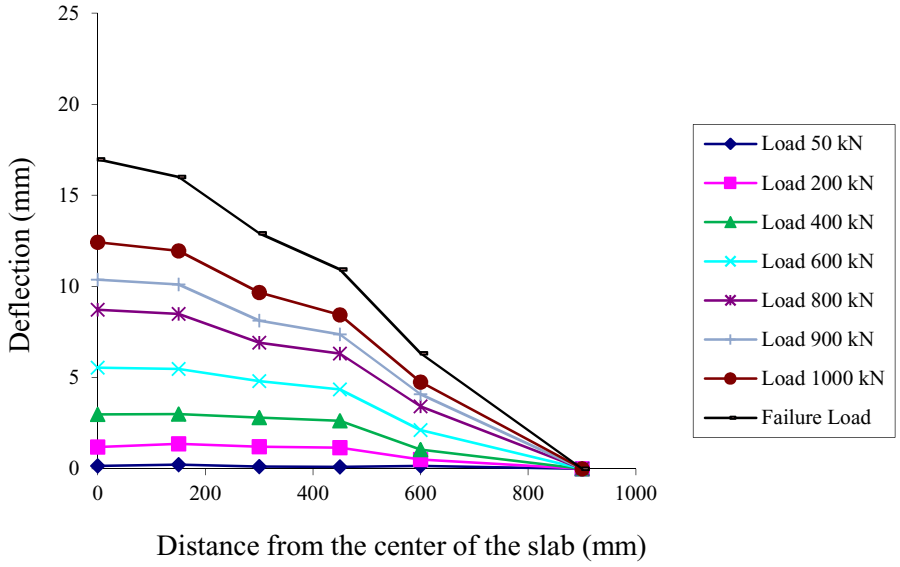

Figure 4.11. Deflection profile for HFR200-0.8/0.2

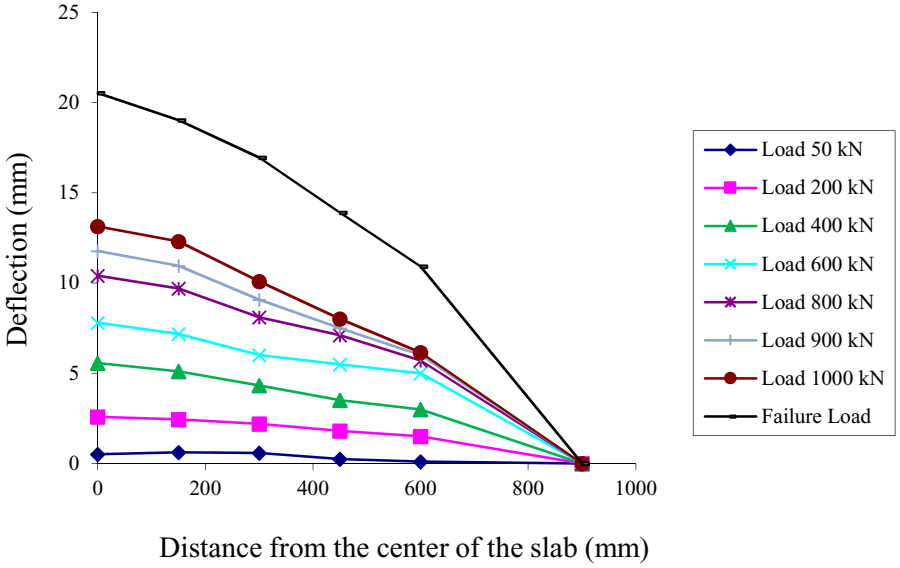

Figure 4.12. Deflection profile for HFR200-0.96/0.2

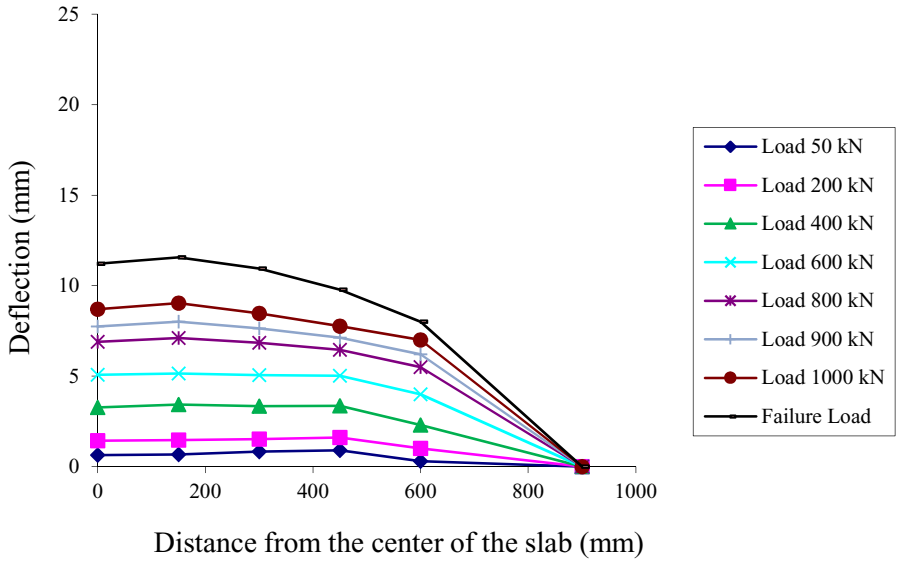

Figure 4.13. Deflection profile for R250

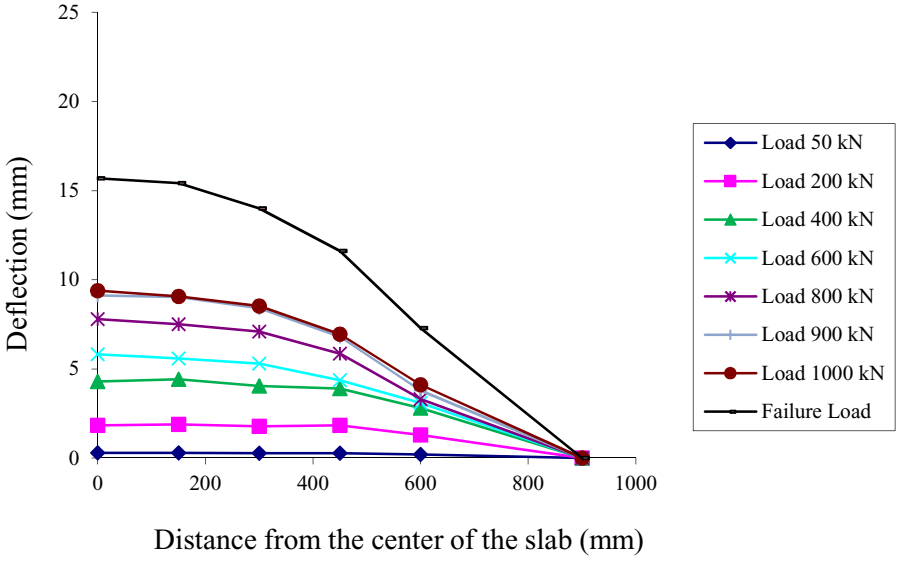

Figure 4.14. Deflection profile for HFR250-0.68/0.2

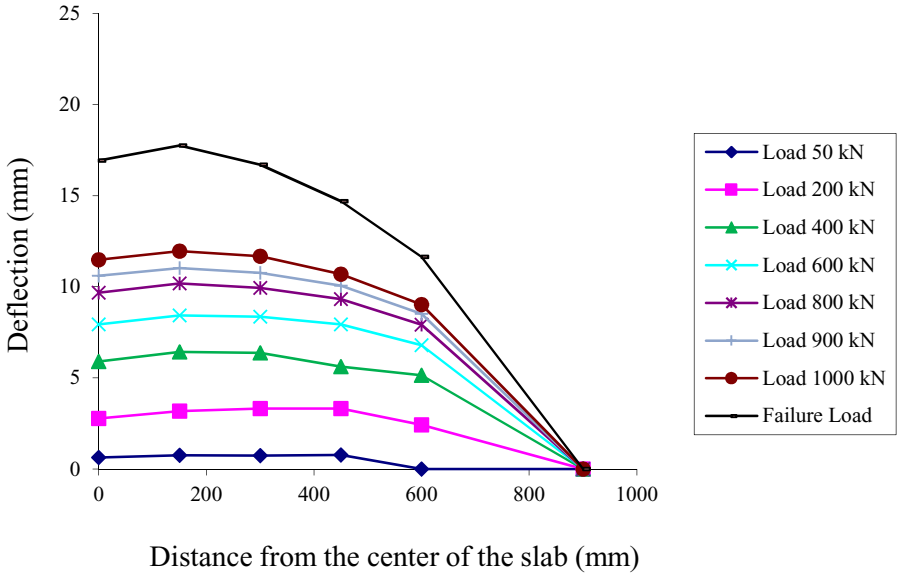

Figure 4.15. Deflection profile for HFR250-0.8/0.2

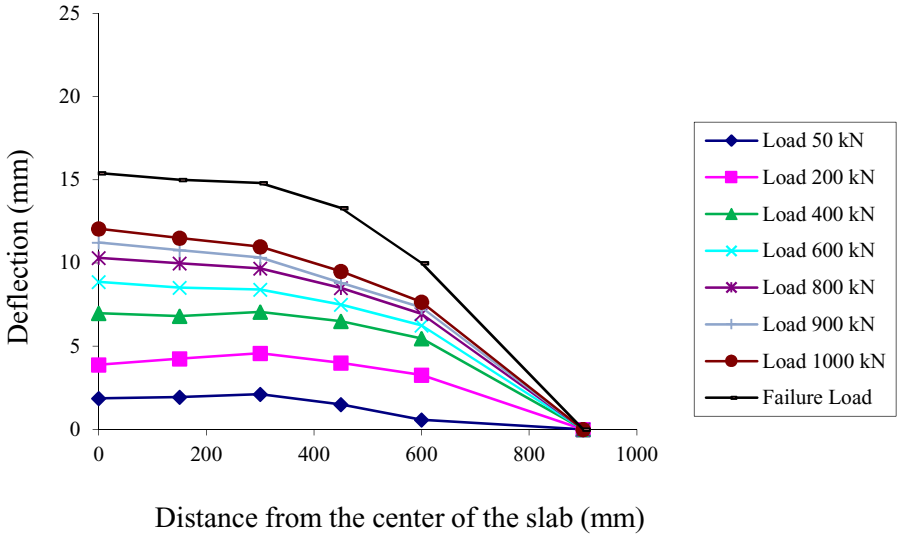

Figure 4.16. Deflection profile for HFR250-0.96/0.2

Adding fibres to the concrete causes less curvature in the test specimens. Figures 4.9 to 4.16 show that the minimum amount of curvature is observed in the slabs containing 0.96% of steel fibres. This behaviour, especially, was more pronounced in the slabs with higher thicknesses.

4.5. Reinforcement Strains

The locations of strain gauges on the reinforcement, as mentioned in Chapter 3, were chosen to find the maximum strains in the bars during the test. In all of the test specimens, tension reinforcement partially yielded before failure occurred. The highest strain in the test slabs occurred below the stub-column, at the center of the slab, where yielding initiated and slightly progressed throughout the tension reinforcement. The load-versus-strain at the center of the slabs is shown in Figures 4.17 and 4.18.

All of the graphs are similar in nature. The slope of the load-strain graphs is high at the first stages of loading; however, the slope gradually decreases as the loading is continued. This could be attributed to the contribution of the concrete in resisting the tensile stresses at the initial stages of loading.

However, the tensile reinforcement started to resist the load after the cracks start to develop and, hence, an increase in reinforcement strains is observed. None of the specimens reached the state of steadily increase in the steel strains at a constant load in all of the gauges in the specimen. This shows that there was no flexure type of failure in any of the specimens.

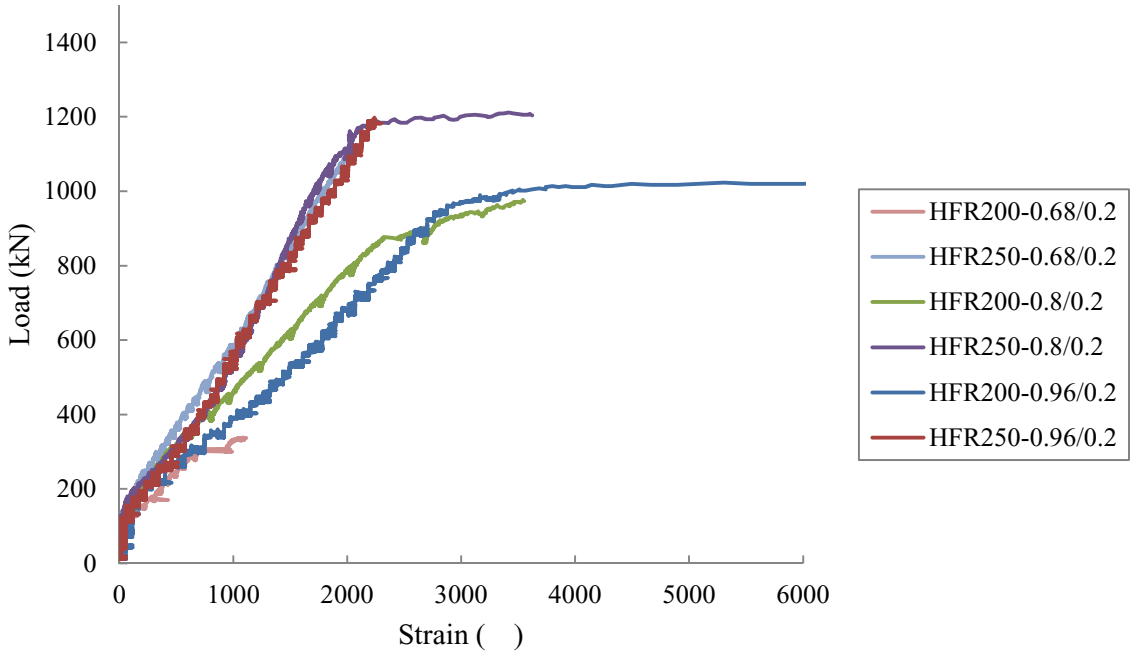

Figure 4.17. Load-steel strain behaviour at the center of the slabs (Gauge no. 1)

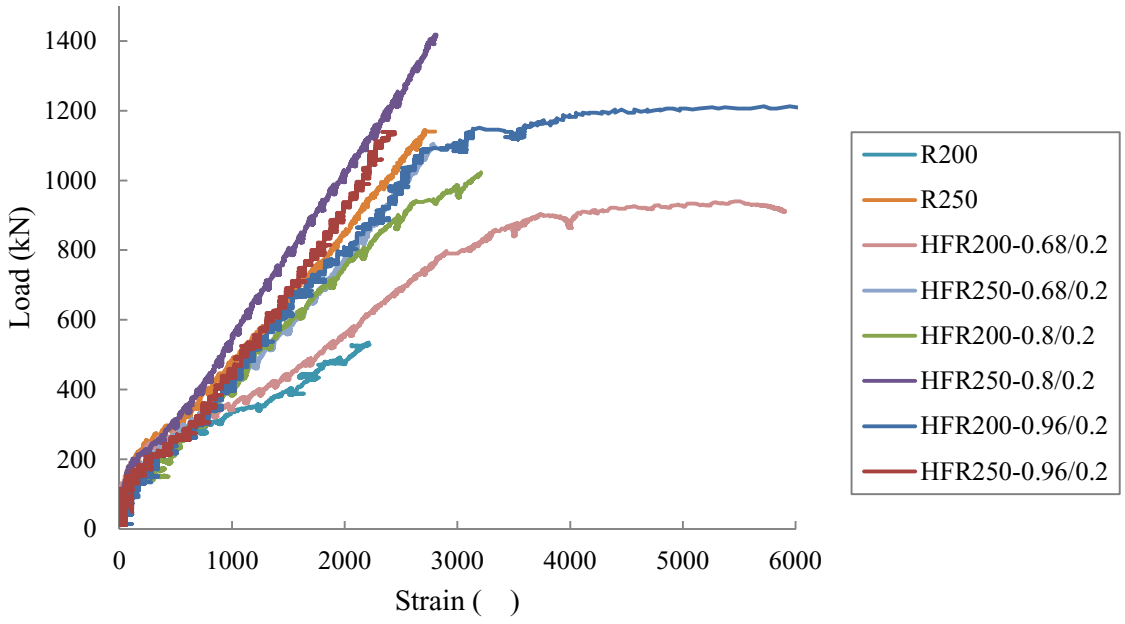

Figure 4.18. Load-steel strain behaviour at the center of the slabs (Gauge no. 4)

According to the graphs, the steel strains decreased at the same corresponding loads by adding fibres to the slabs with different thicknesses. Increasing the amount of fibres from 0.68 to 0.96% caused a reduction in the steel strains, which shows the contribution of fibres in resisting part of the tensile stresses in the HFRC slabs. Addition of fibres up to 0.96%, meanwhile, caused an increase in the first yield load equal to 10 and 25% for the specimens with 200 and 250 mm thickness, respectively.

In all of the slabs, however, increasing the effective depth of the slabs caused an increase in the yield load. The steel strains at other positions of the test slabs are shown in Figures B.1 to B.7 of appendix B. Figures 4.19 to 4.26 show the strain profiles of the tension reinforcement in the test slabs. In most of the test slabs, the readings were obtained almost until the failure occurred. However, in some of the specimens the gauges stopped reading at the loads close to failure.

As shown in Figures 4.19 to 4.22, the contribution of the fibres in extending the yielding throughout the reinforcement was observed. The yielding of the flexural reinforcement extended to a distance almost equal to 400 mm from the center of the 200 mm-thick slabs. According to Figures 4.23 to 4.26, in the 250 mm-thick slabs, meanwhile, the partial yielding did not spread in the slab as much as it did in the 200 mm-thick slabs.

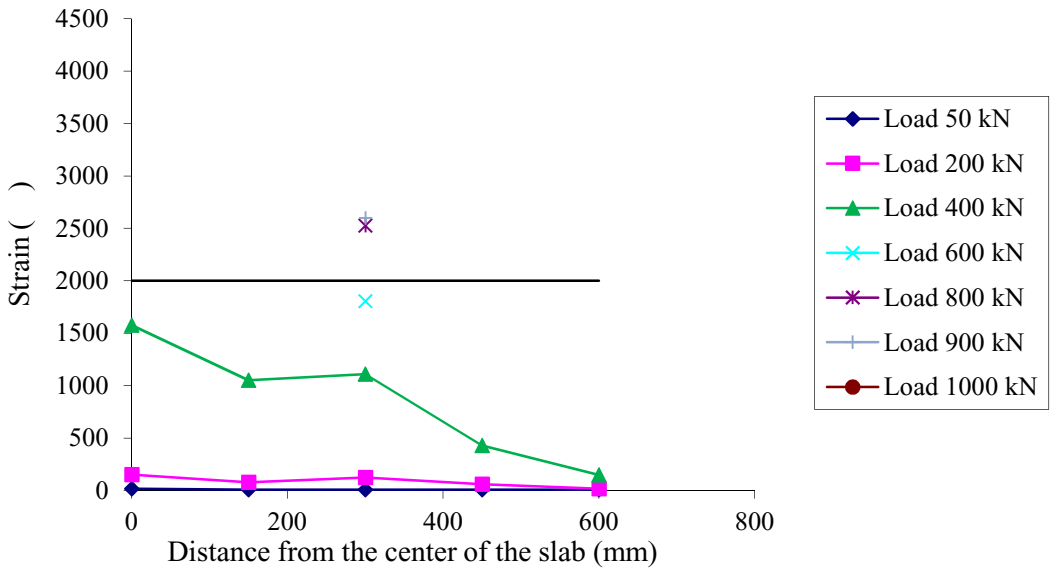

Figure 4.19. Steel strain profile for R200

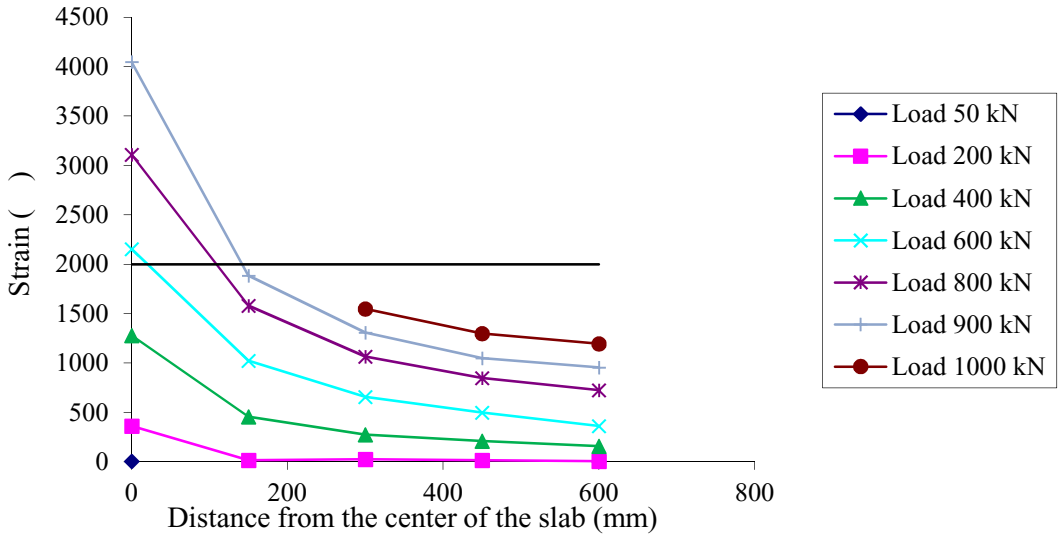

Figure 4.20. Steel strain profile for HFR200-0.68/0.2

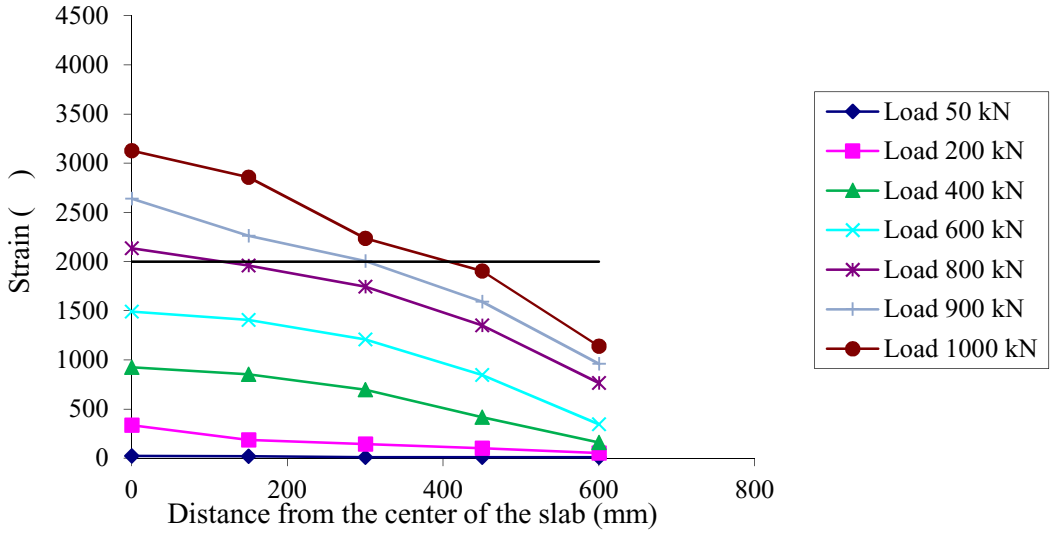

Figure 4.21. Steel strain profile for HFR200-0.8/0.2

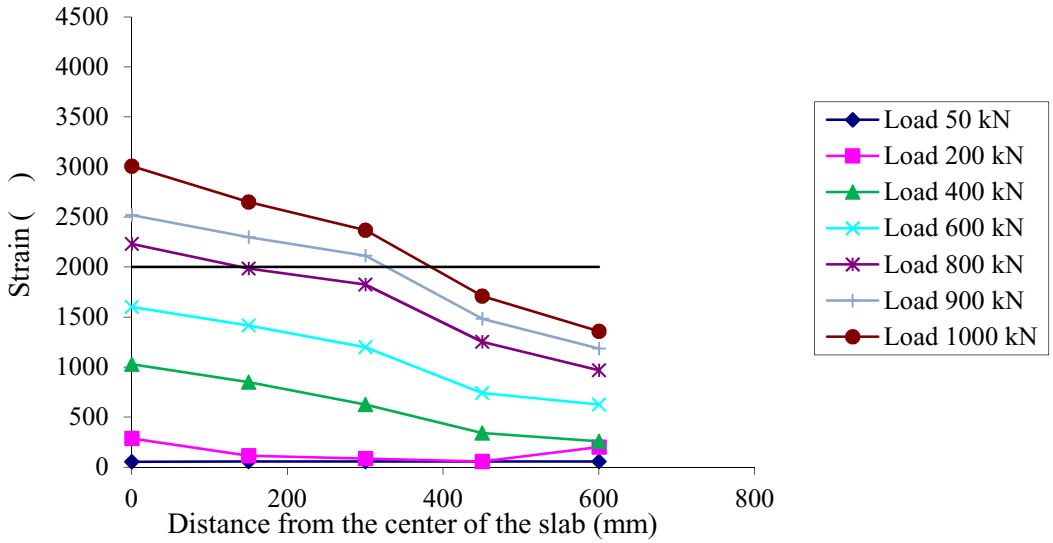

Figure 4.22. Steel strain profile for HFR200-0.96/0.2

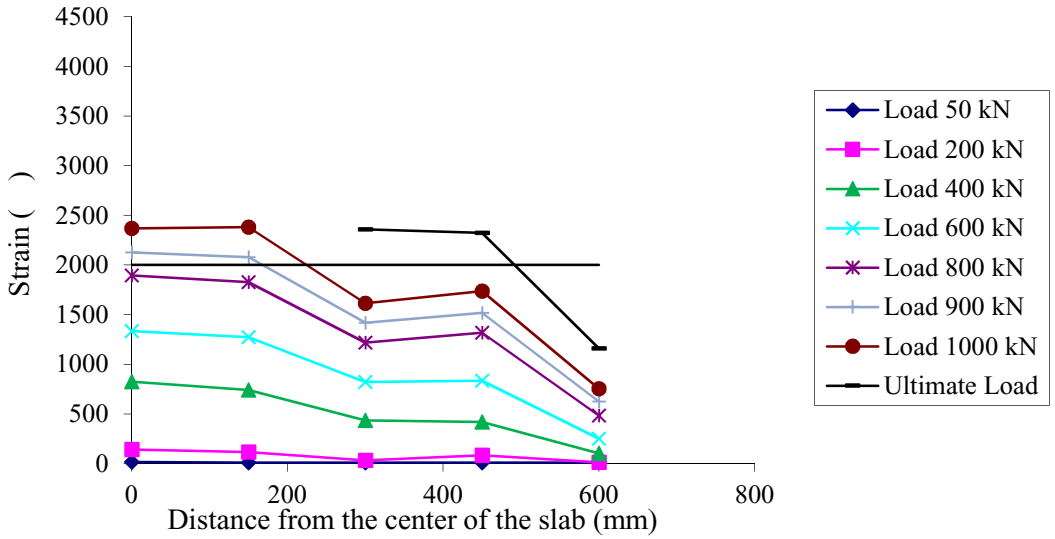

Figure 4.23. Steel strain profile for R250

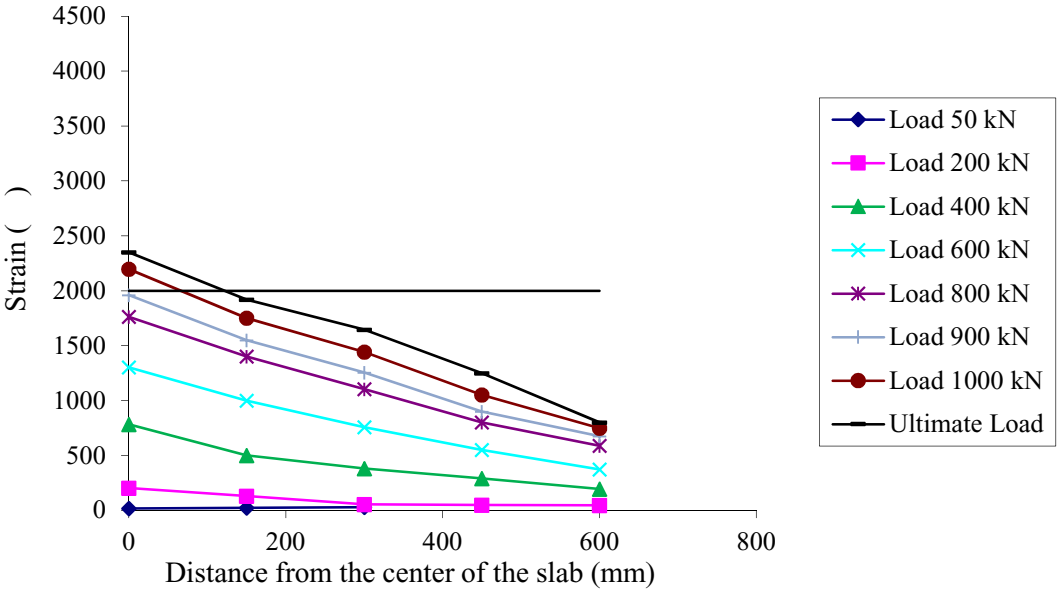

Figure 4.24. Steel strain profile for HFR250-0.68/0.2

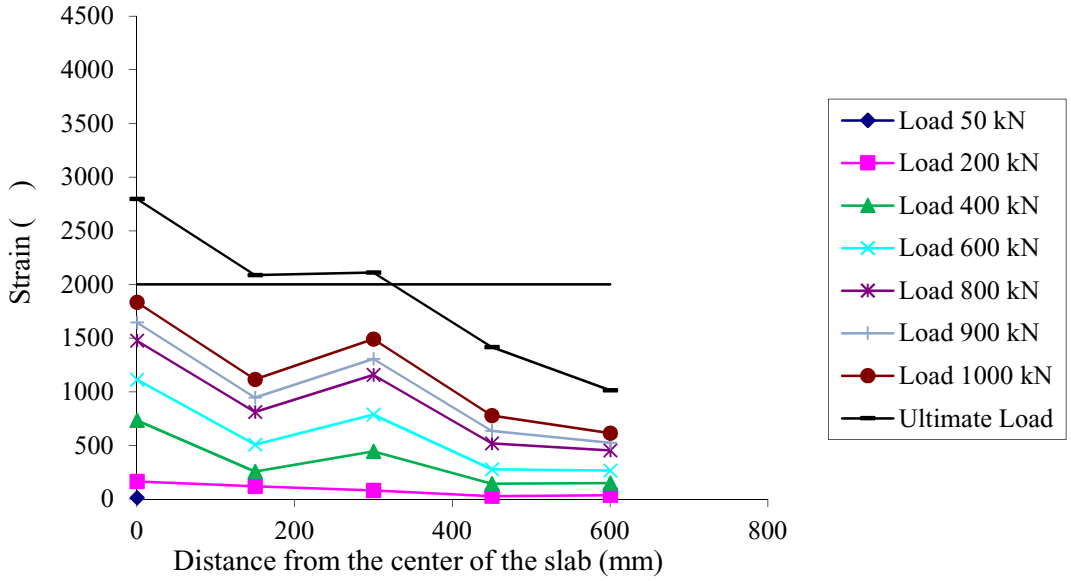

Figure 4.25. Steel strain profile for HFR250-0.8/0.2

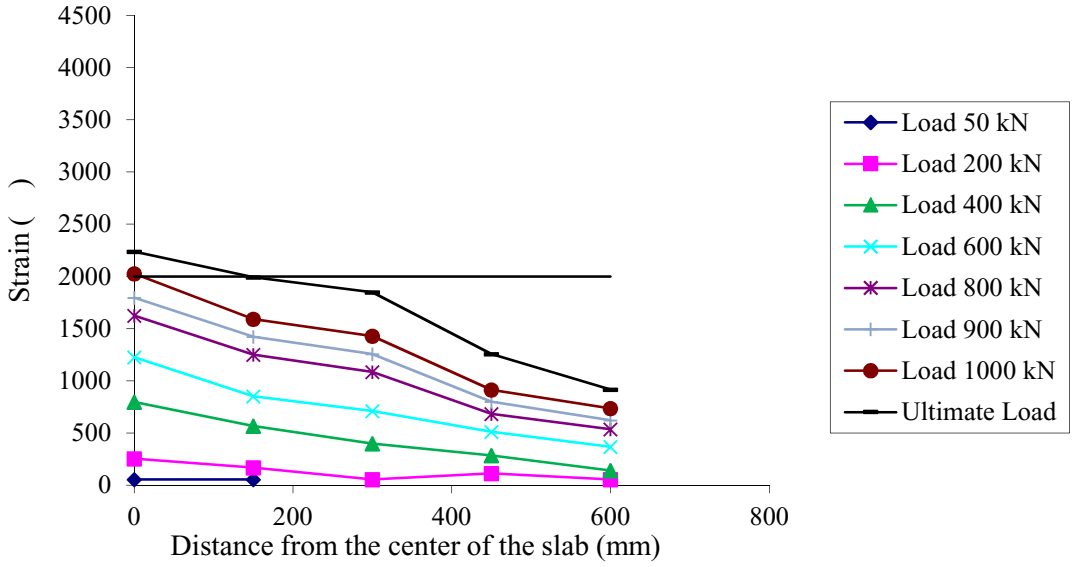

Figure 4.26. Steel strain profile for HFR250-0.96/0.2

Due to the two-way action in the slabs, the maximum bending moments occur at the column face and, as shown in figures 4.19 to 4.26, the maximum strains were observed at the center of the slabs, which is in agreement with the observations of Joo-Ha Lee et al. [17].

In addition, as shown in figures 4.19 to 4.26, the specimens containing hybrid fibres had lower steel strains near the column and at the center of the slabs. The strains in the HFRC specimens containing more fibres were more uniform across the slab width. The presence of the fibres had less influence on the steel strain at the center of the 250 mm-thick slabs, compared to the 200 mm-thick ones.

4.6. Concrete Strains

Concrete strain gauges were located on compression side of the slabs at various distances from the column face, as described in Chapter 3. The positions were selected to measure the distribution of the concrete strain. The gauges were not placed at the column corners because of stress concentration in those areas, which causes the strain gauges to show higher values.

The concrete strain gauges did not reach a strain value of 0.0035 in any of the test specimens. This value is the concrete strain limit according to the CSA code. Furthermore, there was no crushing in the concrete around the column that could be identified by the naked eye.

Table 4.3 shows the concrete strain values at a distance equal to 30 mm from the face of the column for all specimens. The concrete strains at different distances from the column face are also given in Figures B.8 to B.11 of appendix B.

Table 4.3. Maximum concrete strains on the compression side of the slabs

No.	Specimen	Applied load (kN)	Max. concrete strain × 10^{-6}
1	R200	840	1040
2	HFR200–0.68/0.2	968	1335
3	HFR200–0.8/0.2	637	1575
4	HFR200–0.96/0.2	995	2620
5	R250	1092	1380
6	HFR250–0.68/0.2	N/A	N/A
7	HFR250–0.8/0.2	835	1130
8	HFR250–0.96/0.2	1115	2993

The concrete strain profiles are shown in Figures 4.27 to 4.34. As it is shown, the fibres have a considerable effect on the concrete strains in the thinner slabs; however, the effects of the fibres on the concrete strains in the 250 mm-thick slabs are not pronounced. As shown in Figures 4.27 to 4.34 and the same as the steel-reinforcement strains, the concrete strain is inversely proportional to the distance from the center of the slab.

In general, the observations confirm that the contribution of fibres in the 200 mm-thick slabs was more than that in the 250 mm-thick slabs, as the thickness of the test slabs increased, the addition of fibres had fewer effects on the concrete strains.

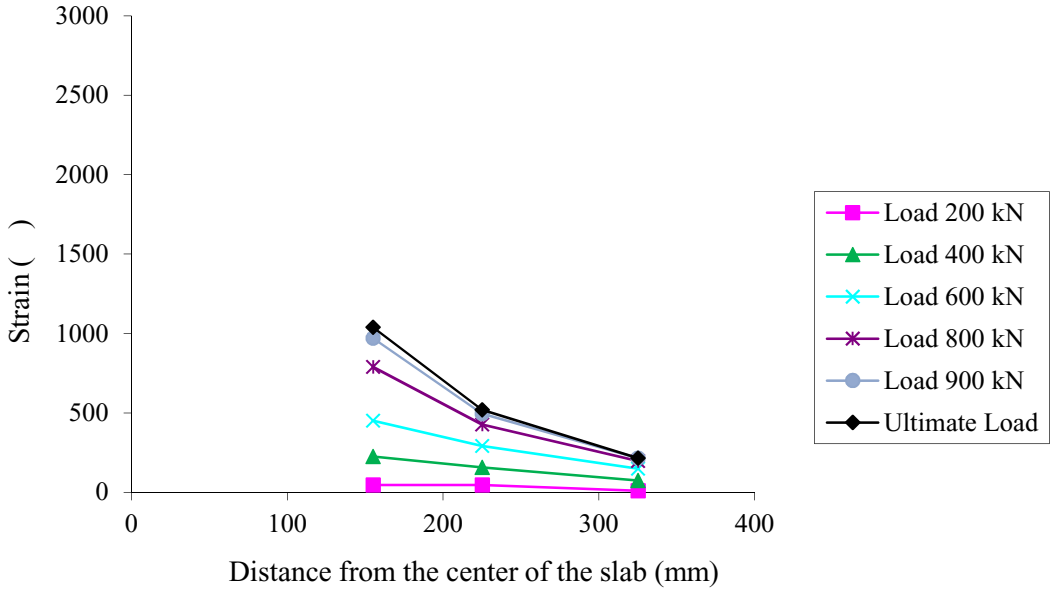

Figure 4.27. Concrete strain profile for R200

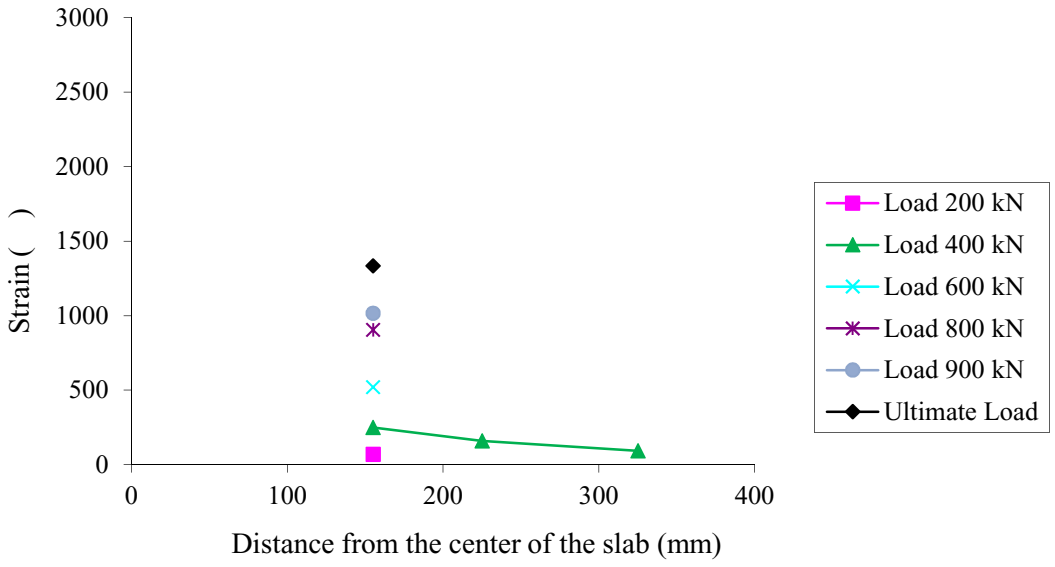

Figure 4.28. Concrete strain profile for HFR200-0.68/0.2

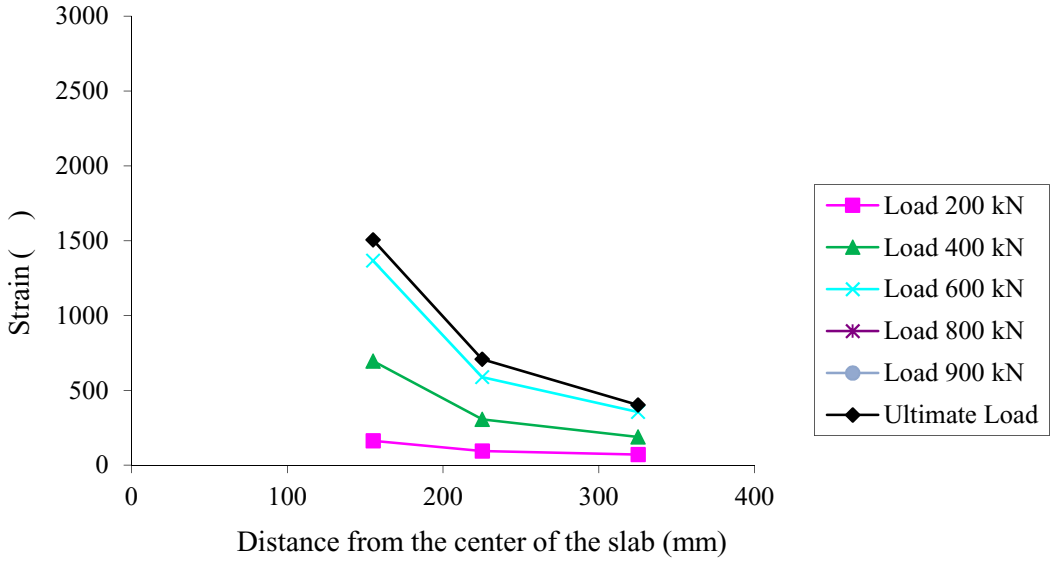

Figure 4.29. Concrete strain profile for HFR200-0.8/0.2

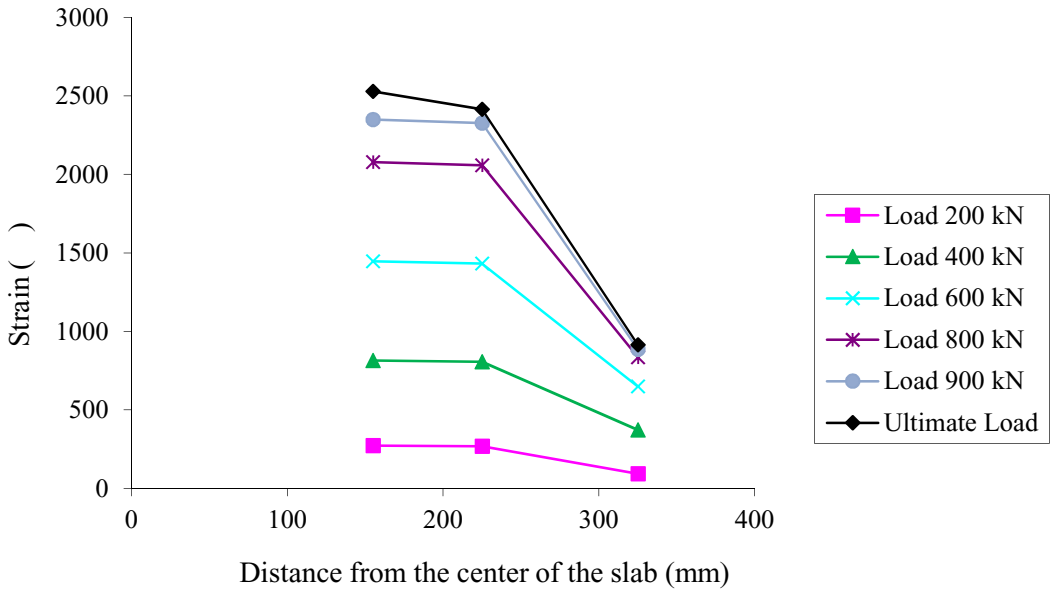

Figure 4.30. Concrete strain profile for HFR200-0.96/0.2

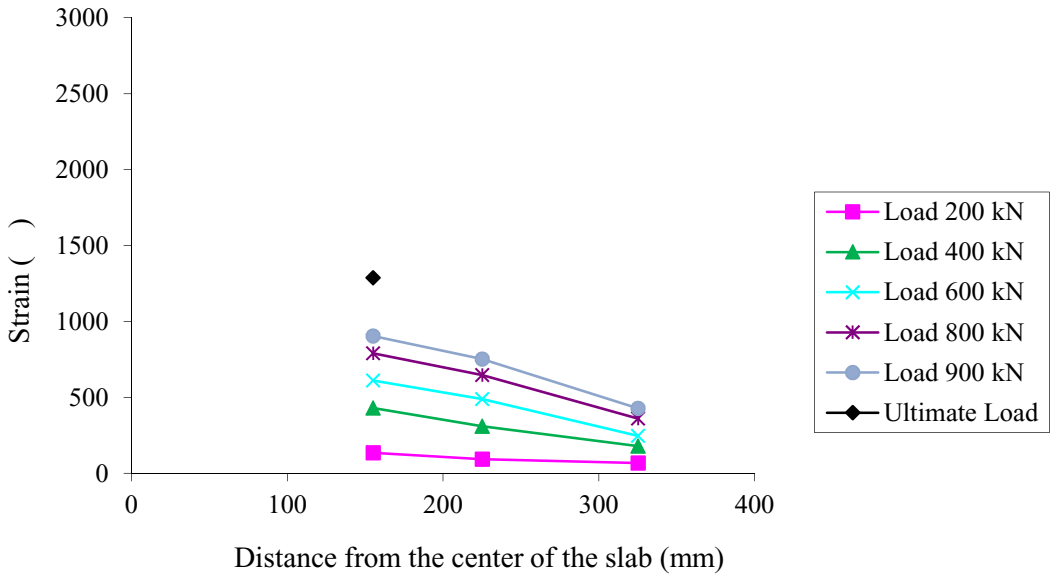

Figure 4.31. Concrete strain profile for R250

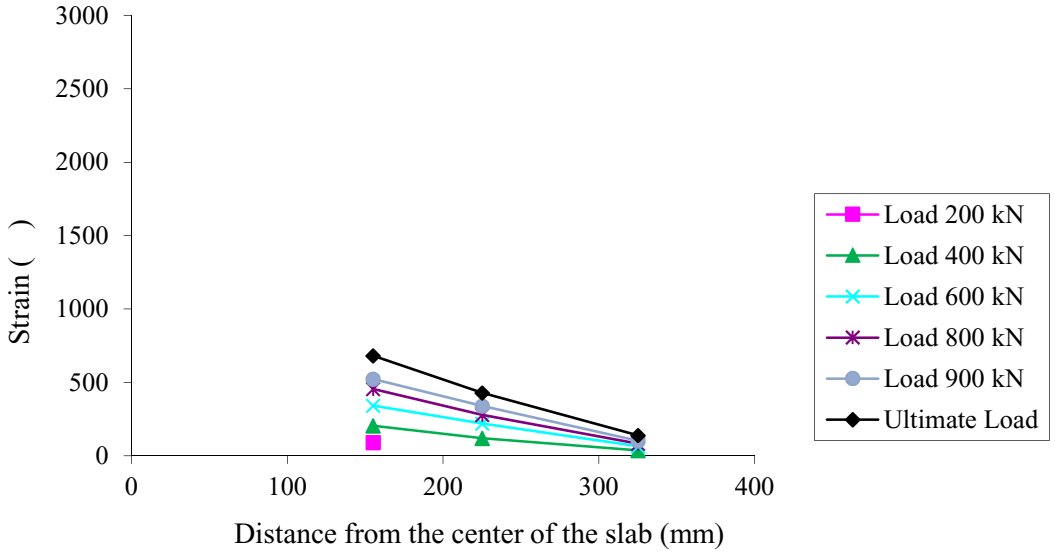

Figure 4.32. Concrete strain profile for HFR250-0.68/0.2

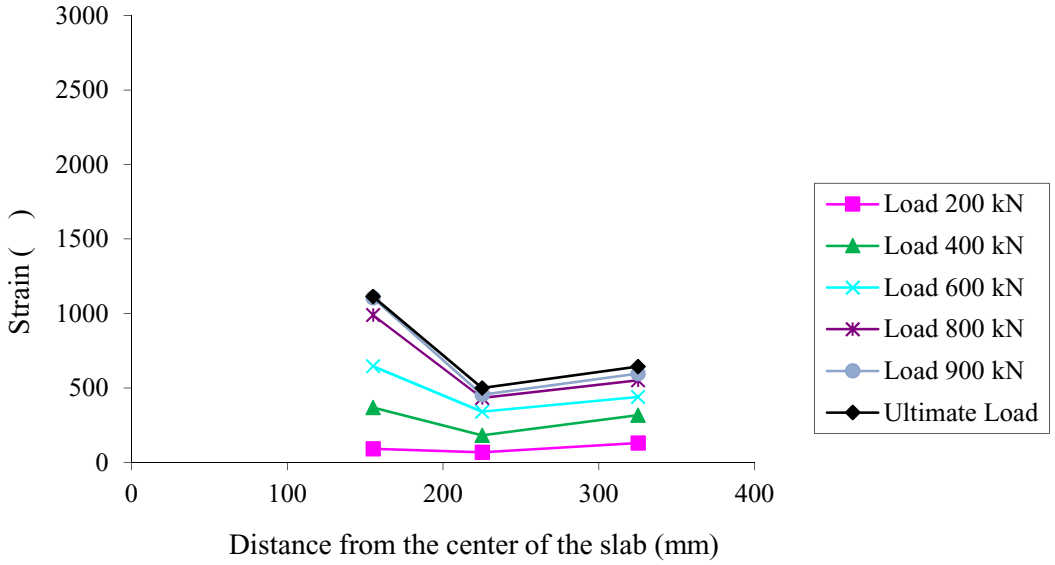

Figure 4.33. Concrete strain profile for HFR250-0.8/0.2

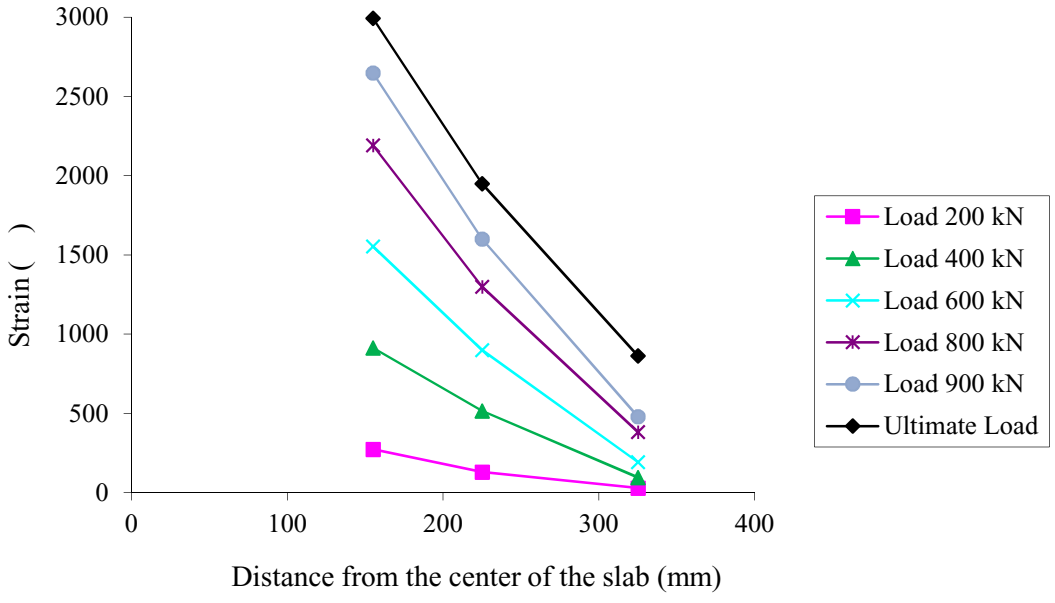

Figure 4.34. Concrete strain profile for HFR250-0.96/0.2

4.7. Post-Punching Behaviour

Post-punching behaviour was monitored and is indicated by the load-deflection curves, as shown in Figures 4.1 and 4.2. After the punching occurred, there is usually a sudden drop in the load-carrying capacity of the slab. According to Figures 4.1 and 4.2, there was a sudden drop in the load, after failure, in the reference slabs. Also, the specimens containing 0.96% fibres had a drop in the capacity after peak load was reached. Both of the reference slabs lost almost 72% of the capacity after punching occurred. The residual strength of the slabs with 0.96% fibres was about 35 and 30%, for the 200 and 250 mm-thick slabs, respectively.

Although test specimens with 0.68 and 0.8% fibres also lost about 70% of the capacity, in both 200 and 250 mm thick slabs, there was a gradual loss of load. This shows a more ductile type of punching failure. The gradual loss of load was more pronounced in the 200 mm-thick slabs than in the 250 mm-thick ones. At failure, the fibres started being pulled out of the concrete and were not able to continue bridging the cracks. The final failure occurred when the concrete was separated in the punching area around the column. Hence, the enhancement in the load-carrying capacity of the slabs, in a post-crack zone, could be attributed to the presence of the fibres.

4.8. Cracking Characteristics

Photographs of the test slabs and crack patterns, at failure, are shown in Figures 4.35 to 4.42. In general, several cracks developed on the tension face of the test specimens as shown in Figures 4.35 to 4.42. Most of these cracks first formed along the

reinforcement which passes through the slab center and at the face of the column stub. As the load was increased, the cracks developed over the entire area on the tension face of the slab. The first visible crack and the cracking patterns were observed by the naked eye and were noted as accurately as possible. Finally, the slabs failed with the occurrence of the final shear crack, as the ultimate load was reached. The specimens failed with the column penetrating through the slabs. It was not possible to determine the exact value of the shear cracking load because slabs were reinforced with two-way bars and an initial shear crack might have remained above the level of the flexural reinforcement; thus, it would not have been visible on the tensile face of the slab. In general, increasing the effective depth of the slabs affects the development of the cracks pattern.

As the load was increased, few new cracks were appeared on the surface of the slabs. Some audible sounds were heard when approaching the ultimate load, which could be due to the fibres being pulled out of the concrete and the separation of the flexural reinforcement mesh from the surrounding concrete.

As mentioned earlier, since the slabs were reinforced with two-way flexural reinforcement, the first shear cracks were not visible as they remained above the level of reinforcement. Nonetheless, as the ultimate load was reached, no punching cone was observed in any one of the slabs around the column area. All of the slabs exhibited a big radius of the punching cone.

Figure 4.35. Crack patterns of the test slab R200

Figure 4.36. Crack patterns of the test slab HFR200-0.68/0.2

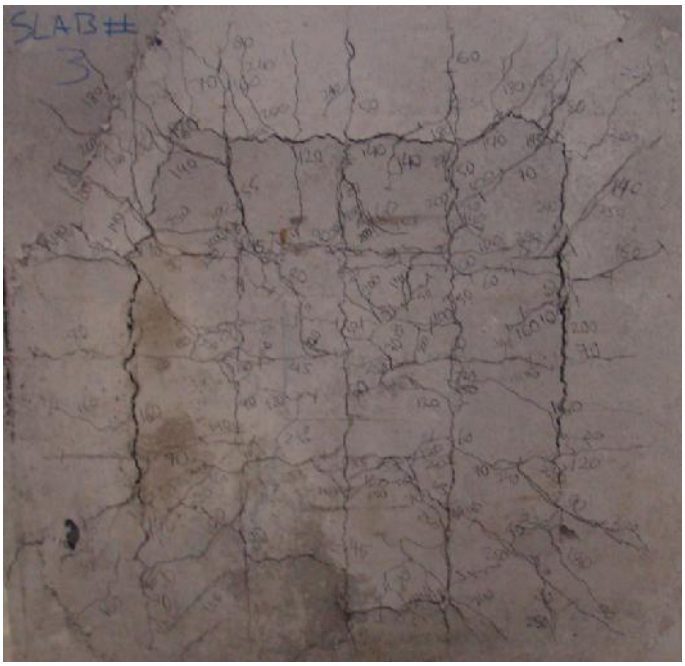

Figure 4.37. Crack patterns of the test slab HFR200-0.8/0.2

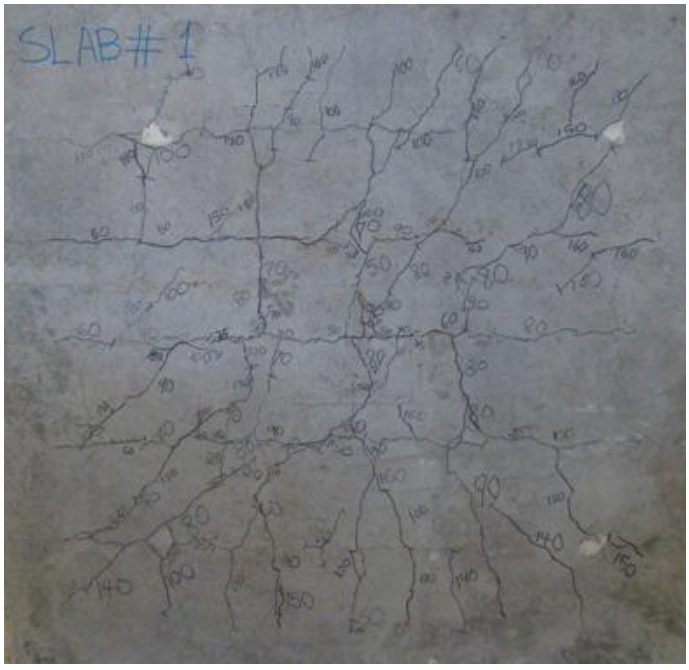

Figure 4.38. Crack patterns of the test slab HFR200-0.96/0.2

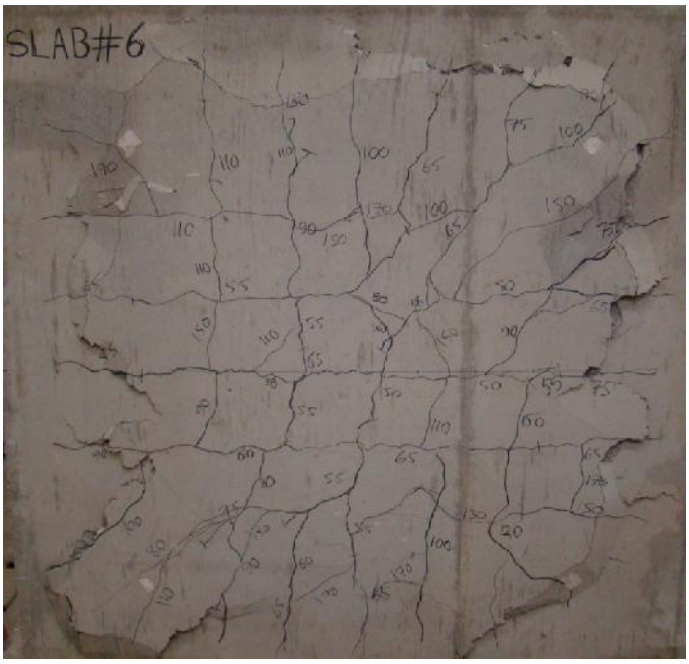

Figure 4.39. Crack patterns of the test slab R250

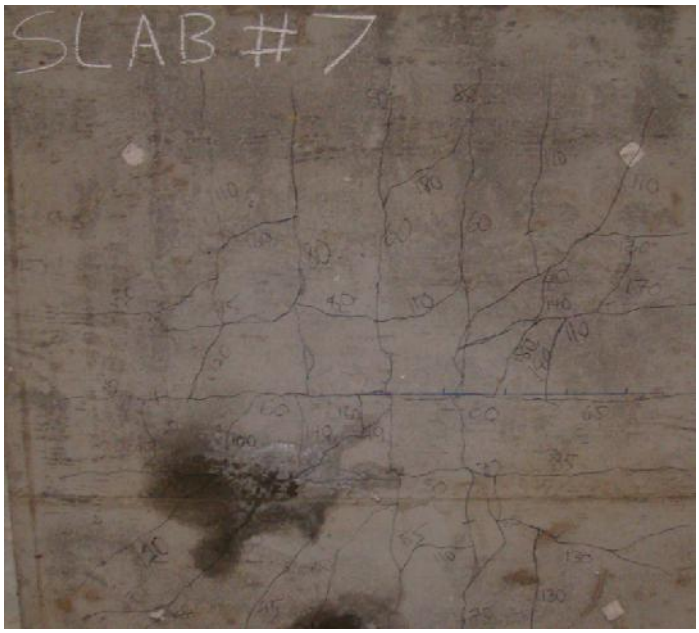

Figure 4.40. Crack patterns of the test slab HFR250-0.68/0.2

Figure 4.41. Crack patterns of the test slab HFR250-0.8/0.2

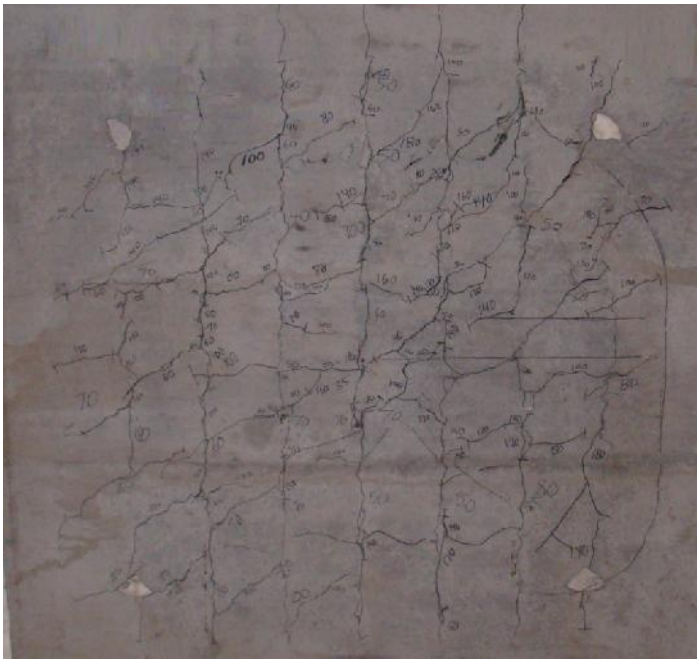

Figure 4.42. Crack patterns of the test slab HFR250-0.96/0.2

The bar spacing was decreased in the thicker slabs to keep the reinforcement ratio constant. In those slabs, the average crack spacing became smaller and the cracking patterns closely matched the reinforcement layout. According to the observations of the crack patterns, the presence of fibres displayed an enhanced performance in cracking control: the test slabs containing more fibres had the smallest cracks around the column head, since the fibres in the concrete matrix bridge the cracks and limit their growth as the load was increased. This observation is in agreement with Joo-Ha Lee et al. [17] for their fibre-reinforced concrete slabs.

4.9. Punching-shear Capacity

The ultimate loads and the corresponding deflections of the test slabs are given in Table 4.1. Comparing the ultimate capacity of the 200 mm-thick HFRC slabs to the reference slabs reveals that the use of fibres up to 0.68% caused an increase in the punching capacity by 15%. Also, increasing the fibre volume fraction up to 0.8 and 0.96% resulted in an increase in punching-shear capacity by 22 and 32%, respectively.

The same trend was observed for the 250 mm-thick slabs. Using 0.68% fibres improved the punching-shear capacity by 20%. An increase in the shear capacity of about 14 and 20% was observed in the slabs containing 0.8 and 0.96% fibres, respectively.

In order to eliminate the effects of the small variation of the compressive strength of the concrete, the punching shear capacity of the slabs is normalized with respect to the square root of the compressive strength, i.e. $\sqrt{f_c}$. The obtained normalized shear strength

is equal to $v = \frac{V}{b_o d \sqrt{f_c}}$. Table 4.4 presents the punching capacity of the test slabs and also the normalized shear strength of the specimens with respect to $\sqrt{f_c}$.

Table 4.4. Normalized shear strength of the slabs w.r.t. $\sqrt{f_c}$

No.	Specimen	Ultimate load (kN)	Shear strength, $\sqrt{f_c}$ (MPa)
1	R200	847.9	0.443
2	HFR200–0.68/0.2	978.1	0.486
3	HFR200–0.8/0.2	1029.9	0.577
4	HFR200–0.96/0.2	1117.6	0.630
5	R250	1147.6	0.394
6	HFR250–0.68/0.2	1375.5	0.451
7	HFR250–0.8/0.2	1300.2	0.481
8	HFR250–0.96/0.2	1386.5	0.516

For the 200 mm-thick slabs, adding 0.68, 0.8 and 0.96% fibres increased the normalized shear strength of the slabs by 10, 31, and 43%, respectively. For the 250 mm-thick slabs, an increase in the normalized shear strength of about 15, 22, and 31% was observed in the slabs containing 0.68, 0.8, and 0.96% fibres, respectively. Hence, increasing the fibre volume fraction has a significant effect on increasing the normalized shear strength of the slabs.

Comparing the slabs with different thicknesses and the same fibre volume fraction, it is evident that the fibres have more pronounced effects on improving the shear strength of the thinner slabs than on the thicker ones. The most effect can be seen by comparing the slabs with 0.96% fibres. The value of the normalized shear strengths are 0.630 and 0.516 for the 200 and 250 mm-thick slabs, respectively. Hence, there is a size effect due to the slab effective depths on the punching strength of HFRC slabs.

4.10. Prediction of Test Results using Existing Equations

Existing equations for predicting the punching shear capacity of SFRC two-way slabs were presented in Chapter 2. The equations were proposed by Narayanan and Darwish [12], Shaaban and Gesund [14], Harajli, Maalouf and Khatib [15], and Hiroshi Higashiyama et al. [22]. Those equations were applied to predict the capacity of the current slabs. The results of the predictions are given in Table 4.5 and shown in Figures 4.43 to 4.46.

The mean values and the standard deviations of V(test)/V(predicted) for the equations proposed are given in Table 4.6. Based on the fibres used in their experimental program, the values of the fibre factor were formed and added to the proposed equations. As shown in the graphs, moreover, the prediction equations which were developed for SFRC slabs are also safe for HFRC two-way slabs and have a greater accuracy in predicting the punching-shear capacity of HFRC samples beside the SFRC ones.

The equations proposed by Shaaban and Gesund [14], and Harajli, Maalouf and Khatib [15] slightly overestimate the punching strength of the HFRC slabs. As shown in Figures 4.44 and 4.45, the equations are particularly unsafe, especially, when used for the 250 mm-thick slabs. The equations gave unsafe predictions for some of the 200 mm-thick specimens. In general, the equations produced the least scatter in the predicted results.

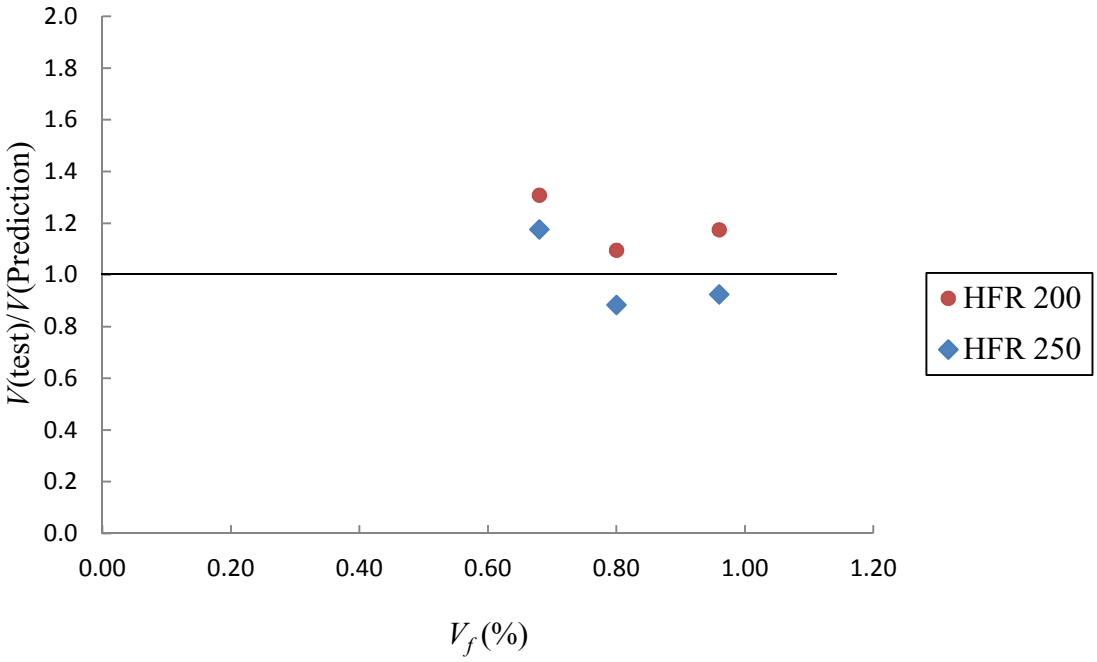

Figure 4.43. $V_{(T.)}/V_{(P.)}$ vs. V_f (%) using Narayanan & Darwish [12]

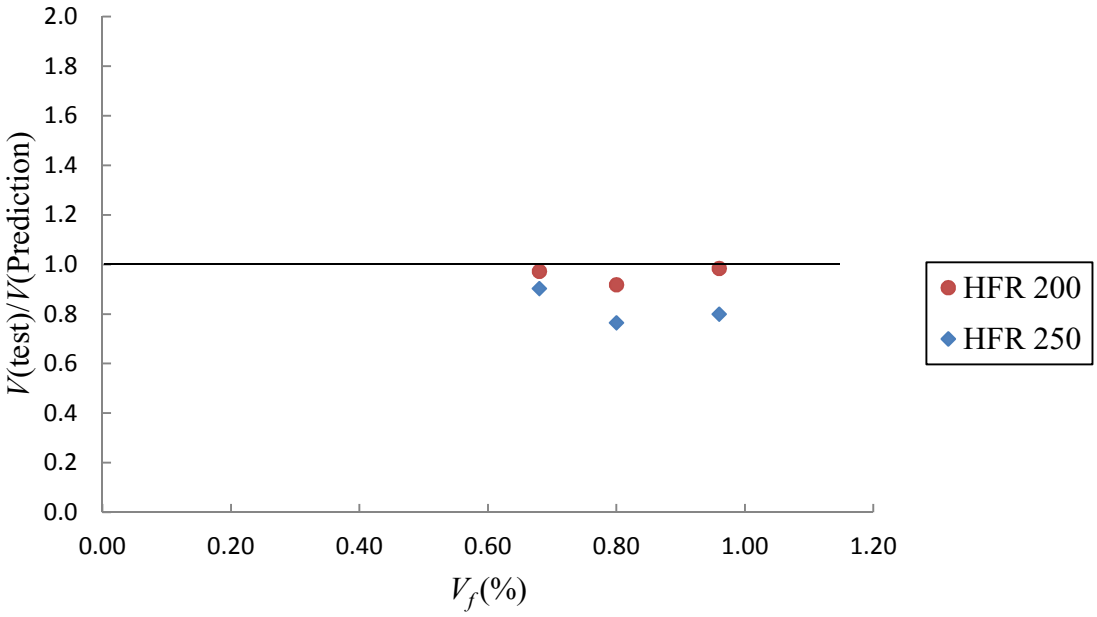

Figure 4.44. $V_{(T.)}/V_{(P.)}$ vs. V_f (%) using Shaaban & Gesund [14]

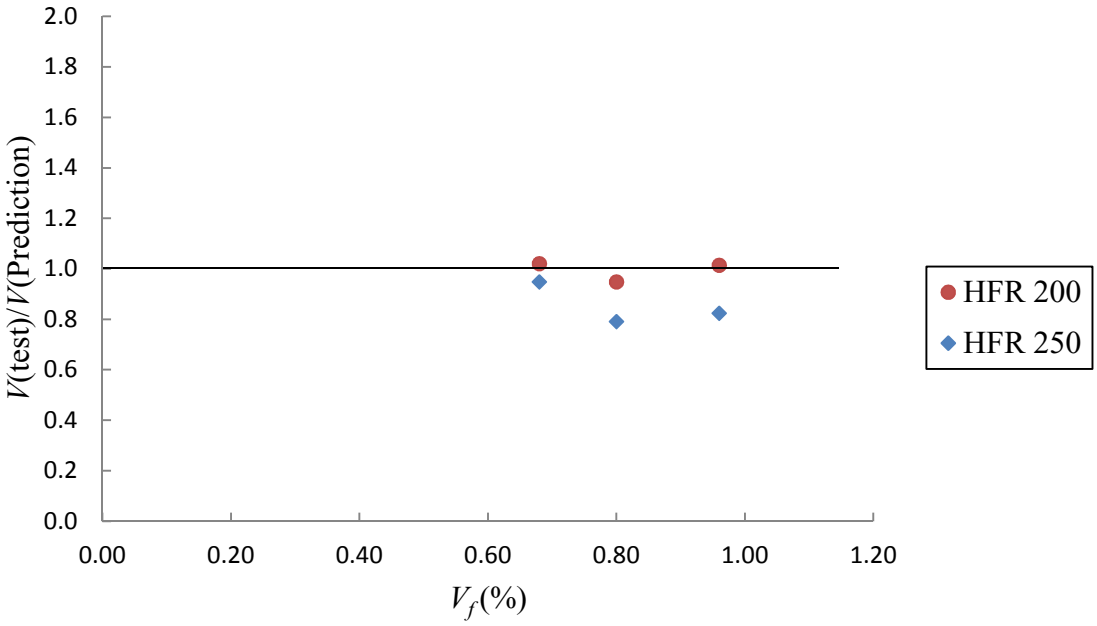

Figure 4.45. $V_{(T.)}/V_{(P.)}$ vs. V_f (%) using Harajli, Maalouf & Khatib [15]

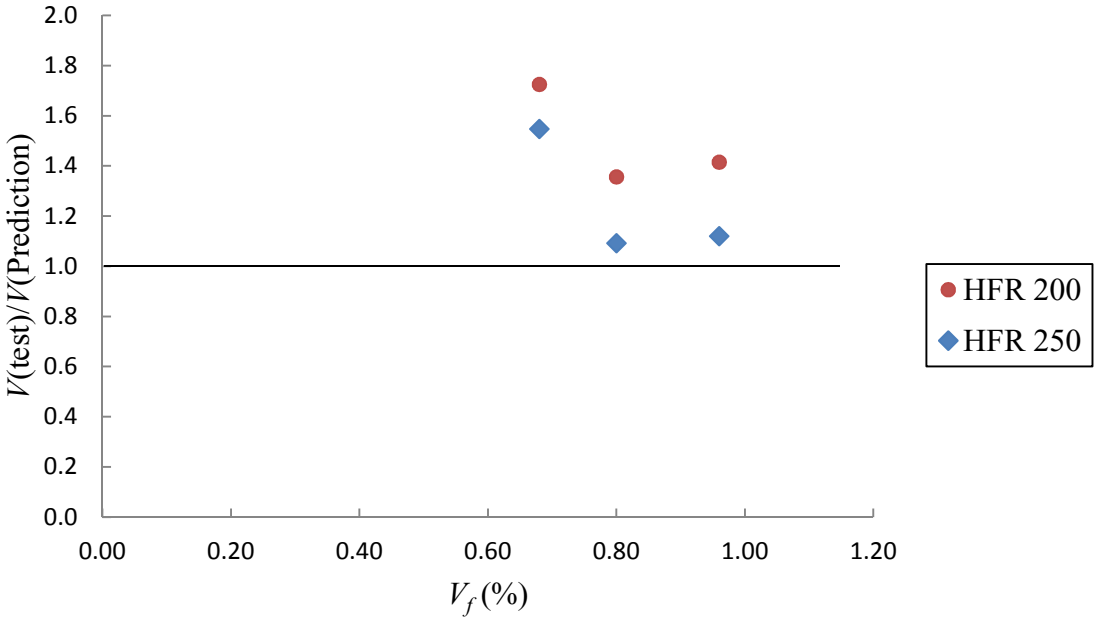

Figure 4.46. $V_{(T.)}/V_{(P.)}$ vs. V_f (%) using Hiroshi Higashiyama et al. [22]

From Figures 4.43 and 4.46, and also from Tables 4.5 and 4.6, it can be concluded that the equation proposed by Narayanan and Darwish [12] gives a safe prediction with least scatter compared to the prediction of Hiroshi Higashiyama et al. [22]. The equation proposed by Hiroshi Higashiyama et al. [22] gave the safest prediction, but it had a large scatter.

As mentioned earlier in Chapter 2 and shown in Figures 2.16 to 2.19, the equations have less accuracy in predicting the capacity of the slabs, in the literature, with higher thicknesses. The prediction of the capacity of the slabs in the current study shows that the 250 mm-thick slabs are mostly in the unsafe region or closer to the unsafe region than the 200 mm-thick slabs. Most of the tested slabs in the literature had small thicknesses and the prediction equations were developed based on the test results that were obtained from the investigations. Thus, it can be concluded that the prediction equations are more accurate for the thinner slabs than the thicker ones. This is also the same trend for the current slabs.

Table 4.5. Test results vs. prediction equations (V_{test} / $V_{predicted}$)

Specimen	Narayanan & Darwish [12]	Shaaban & Gesund [14]	Harajli, Maalouf & Khatib [15]	Hiroshi Higashiyama et al. [22]
R200	1.13	0.84	0.88	1.50
HFR200-0.68/0.2	1.31	0.97	1.02	1.73
HFR200-0.8/0.2	1.09	0.92	0.95	1.36
HFR200-0.96/0.2	1.17	0.98	1.01	1.42
R250	0.98	0.75	0.79	1.29
HFR250-0.68/0.2	1.18	0.90	0.95	1.55
HFR250-0.8/0.2	0.88	0.77	0.79	1.09
HFR250-0.96/0.2	0.92	0.80	0.82	1.12

The mean value of the ratios, V(test)/V(predicted), standard deviations, and coefficient of variation for the current slabs are given in Table 4.6.

Table 4.6. Mean, standard deviation, and coefficient of variation of V(test)/V(predicted)

Values	Narayanan & Darwish [12]	Shaaban & Gesund [14]	Harajli, Maalouf & Khatib [15]	Hiroshi Higashiyama et al. [22]
Mean	1.08	0.87	0.90	1.38
Standard deviation	0.14	0.09	0.09	0.21
Coefficient of variation	0.13	0.10	0.10	0.15

Thus, it seems to be possible to use existing prediction equations for HFRC two-way slabs, which offer a close estimation of the punching-shear capacity of the specimens.

Chapter 5

Conclusions and Recommendations

5.1. Conclusions

An experimental investigation was conducted to investigate the structural behaviour of HFRC two-way slabs. The experimental work was focused on studying the effects of fibre volume fraction and slab effective-depth as the main variables. The behaviour was evaluated in terms of the load-deflection characteristics, stiffness, ductility, energy-absorption, cracking pattern, reinforcement strains, concrete strains, and post-punching behaviour. The experimental results and discussion support the following conclusions:

1. A literature review was carried out on slab-column connections made with steel-fibre-reinforced concrete (SFRC). The major experimental findings were discussed and the data were collected into a databank. The values were screened and only the results

that represent realistic slab-column connections were kept in the databank. The review of the results revealed that there was a large scatter in the data. Also, there was an apparent size effect in the specimens that were tested previously.

2. The existing equations that were proposed to predict the punching-shear capacity of SFRC slabs were evaluated using the collected databank. The predictions of those equations show a significant degree of scatter when compared to the test results. It was found that some of the proposed equations gave unsafe predictions for the slabs. The equation proposed by Hiroshi Higashiyama et al. [22] gave the safest prediction for most of the slabs, having a large scatter.

3. In general, the slabs behaved in a linear elastic fashion up to the formation of the first cracks. The load-deflection graphs show a linear behaviour up to a point that is close to the yield load in the 200 mm-thick slabs. For the 250 mm-thick slabs, the linear load-deflection behaviour was pronounced almost up to the failure load.

4. According to the load-deflection curves, there was no flexural failure observed in any of the test specimens. All of the slabs failed in punching. However, in the slabs containing fibres, the type of failure could be classified as a ductile punching. While the effect of the fibres on the modes of failure is obvious, when comparing the load-deflection curves of the test specimens with different thicknesses, the load-deflection figures show that the presence of fibres in the 200 mm-thick slabs has a more significant effect on the mode of failure than in the 250 mm-thick slabs.

5. The load-deflection curves for the 200 mm-thick slabs show an almost-constant stiffness to the yield load, and at that point the stiffness of the specimens start to gradually

decrease. For the 250 mm-thick slabs, the stiffness remained constant during loading and started to decrease at a point close to the shear capacity.

6. The addition of fibres caused an increase in the stiffness of the 200 mm-thick test slabs. However, the results show that, in the 200 mm-thick slabs, the fibres have more significant effect on the stiffness compared to the 250 mm-thick slabs.

7. The ductility increased by 73% with the addition of fibres for the 200 mm-thick slabs. The addition of 0.8 and 0.96% fibres caused an improvement equal to 153 and 154%, respectively. The ductility also increased when the amount of fibres increased, for all of the 250 mm-thick slabs. The improvement for the 250 mm-thick specimens containing 0.68, 0.8, and 0.96% of fibres was equal to 83, 129, and 157%, respectively.

8. The energy-absorption capacity of the HFRC slabs was also enhanced as the fibre volume fraction was increased. Increasing the amount of fibres to 0.68, 0.8, and 0.96% caused an improvement of about 62, 93, and 116% in the energy-absorption of the 200 mm-thick specimens, respectively. On the other hand, for the 250 mm-thick slabs, an enhancement of 53, 60, and 83% occurred by increasing the amount of fibres to 0.68, 0.8, and 0.96%, respectively. The maximum energy-absorption was observed in the slabs with the highest amount of steel fibres equal to 0.96% by volume. Increasing the effective depth, also, improved the stiffness of the slabs but decreased the ductility and energy-absorption of the specimens.

9. The deflection profiles did not show any specific turning point in the slabs. Also, no linear deflection was observed at any distances from the face of the columns. Instead, a curvature is observed in all of the test specimens. This indicates that the slabs are not rotating as a rigid body in any region, even after the formation of the shear cracks.

10. Adding more fibres to the concrete, then, causes less curvature on the surface of the specimens. The minimum amount of curvature is observed in the slabs containing 0.96% of steel fibres in the concrete mixture, especially in the slabs with higher thicknesses.

11. The flexural reinforcement partially yielded before failure occurred. The highest strain in the test slabs occurred below the stub-column, at the center of the slab. None of the specimens reached the state of steadily increase in the steel strains at a constant load in all of the gauges in the specimen. This shows that there was no flexural type of failure in any of the specimens.

12. The concrete strain gauges did not reach a strain value of 0.0035 in any of the test slabs as the crushing concrete strain limit, according to the CSA 23.3-04 code [31].

13. Several cracks developed on the tension face of the test specimens. Most of these cracks first formed along the reinforcement, which passes through the slab center and at the face of the column stub. The specimens failed with the column penetrating through the slabs with the occurrence of the final shear crack. According to the observations of the crack patterns, the presence of fibres displayed an enhanced performance in cracking control. The test slabs containing more fibres had the smallest cracks around the column head, since the fibres in the concrete matrix bridge the cracks and limit their growth as the load was increased.

14. Some audible sounds were heard when approaching the ultimate load, which could be due to the fibres being pulled out of the concrete and the separation of the flexural reinforcement mesh from the surrounding concrete.

15. Comparing the ultimate capacity of the 200 mm-thick HFRC slabs to the reference slabs reveals that the use of fibres up to 0.68, 0.8, and 0.96% caused an increase in the punching capacity by 15, 22, and 32%, respectively. The same trend was observed for the thicker slabs. Using 0.68, 0.8, and 0.96% fibres improved the ultimate load-carrying capacity of the slabs by 20, 14, and 20%, respectively.

16. Adding fibres had a significant effect on increasing the normalized shear strength of the slabs. For the 200 mm-thick slabs, adding 0.68, 0.8 and 0.96% fibres increased the normalized shear strength by 10, 31, and 43%, respectively. For the 250 mm-thick slabs, an increase in the normalized shear strength of about 15, 22, and 31% was observed in the slabs containing 0.68, 0.8, and 0.96% fibres, respectively. Comparing HFRC slabs with the same fibre volume fraction, the fibres had more pronounced effects on improving the shear strength of the thinner slabs than on the thicker ones. Hence, there is a size effect due to the slab effective depth on the punching strength of HFRC slabs.

17. The equations proposed by Shaaban and Gesund [14], and Harajli, Maalouf and Khatib [15] slightly overestimate the punching strength of the HFRC slabs. The equations are particularly unsafe when used for the 250 mm-thick slabs. The equations also gave unsafe predictions for some of the 200 mm-thick specimens. In general, the equations produced a small scatter in the predicted results. The equation proposed by Narayanan and Darwish [12] gave a reasonably safe prediction with least scatter compared to the prediction of Hiroshi Higashiyama et al. [22] which gave the safest prediction, but it had a large scatter.

18. The prediction equations were developed based on the test slabs in the literature. Most of the slabs had small thicknesses. Thus, the equations gave better

predictions for the 200 mm-thick slabs than the 250 mm-thick ones that were tested in the current study.

5.2. Recommendations for Future Works

1. There is a need to test more slabs containing the combinations of various types of steel and synthetic fibres, to be able to determine the effects of shapes and characteristics of used fibres on the structural behaviour of the test specimens.

2. The effects of concrete compressive-strength, reinforcement-ratio, and the bar spacing on the structural behaviour of two-way slabs should be also investigated.

3. Additional tests are needed to modify existing prediction equations for SFRC in order to produce less scatter in the predictions.

4. A numerical model can be developed to estimate the effects of hybrid fibres on structural behaviour of HFRC two-way slabs.

References

[1] Marzouk, H. and Hussein, A. (1991). "Experimental Investigation on the Behaviour of High Strength Concrete Slabs," ACI Structural Journal, V. 88, No. 6, pp. 701-713.

[2] Swamy, R.N. and Ali, S.A.R. (1982). "Punching Shear Behavior of Reinforced Slab-Column Connections Made with Steel Fiber Concrete," ACI Journal, Proceedings V. 79, No. 5, pp. 392-406.

[3] Theodorokopoulos, D.D. and Swamy, N. (1993). "Contribution of Steel Fibers to the Strength Characteristics of Lightweight Concrete Slab-Column Connections Failig in Punching Shear," ACI Structural Journal, V. 90, No. 4, pp. 342-355.

[4] Alexander, S.D.B. and Simmonds, S.H. (1992). "Punching Shear Tests of Concrete Slab-Column Joints Containing Fiber Reinforcement," ACI Structural Journal, V. 89, No. 4, pp. 425-432.

[5] Yurtseven, A.E. (2004). "Determination of Mechanical Properties of Hybrid Fibre Reinforced Concrete," Master Thesis, Graduate School of Natural and Applied Sciences, Middle East Technical University, Ankara, Turkey, pp. 82.

[6] Yaseen, A. A. (2006). "Punching Shear Strength of Steel Fiber High Strength Reinforced Concrete Slabs," Master thesis, College of Engineering, University of Salahaddin, Erbil, Iraq, pp. 111.

[7] Banthia, N., and Gupta, R. (2004). “Hybrid Fiber Reinforced Concrete (HyFRC): Fiber Synergy in High Strength Matrices,” Materials and Structures, V. 37, No. 10, pp. 707-716.

[8] Cominoli, L., Failla, C., and Plizzari, G. A. (2006). “Steel and Synthetic Fibres for Enhancing Concrete Toughness and Shrinkage Behaviour,” Proc. Int. Conf: Sustainable Construction Materials and Technologies, Pub. UW Milwaukee CBU, pp. 231-240.

[9] Deng, Z., and Li, J. (2006). “Mechanical Behaviors of Concrete Combined with Steel and Synthetic Macro-Fibers,” Journal of Physical Sciences, V. 1, No. 2, pp., 57-66.

[10] ITO, K., Hirasawa, I. and Aichi, I. (1981). “Punching Shear Strength of Steel Fiber Reinforced Concrete Slab,” Transactions of the Japan Concrete Institute, V. 3, pp. 267-272.

[11] Walraven, J., Pat, T. and Markov, I. (1986). “The Punching Shear Resistance of Fiber Reinforced Concrete Slabs,” 3rd Int. Symp. Developments in Fiber Reinforced Cement and Concrete, V. 2, pp. 8-9.

[12] Narayanan, R. and Darwish, I.Y.S. (1987). “Punching Shear Tests on Steel Fiber Reinforced Micro Concrete Slabs,” Magazine of Concrete Research, V. 39, No. 138, pp. 42-50.

[13] Tan, K.H. and Paramasivam, P. (1994). “Punching shear strength of steel fiber reinforced concrete slabs,” Journal of Materials in Civil Engineering, V. 6, No. 2, pp. 240-253.

[14] Shaaban, A.M. and Gesund, H. (1994). "Punching Shear Strength of Steel Fiber Reinforced Concrete Flat Plates,” ACI Structural Journal, V. 91, No. 3, pp. 406-414.

[15] Harajli, M.H., Maalouf, D. and Khatib, H. (1995). “Effects of Fibers on the Punching Shear Strength of Slab-Column Connections,” Cement & Concrete Composites, V. 17, No. 2, pp. 161-170.

[16] McHarg, P.J., Cook, W.D., Mitchell, D. and Yoon, Y.S. (2000). “Benefits of Concentrated Slab Reinforcement and Steel Fibers on Performance of Slab-Column Connections,” ACI Structural Journal, V. 97, No. 2, pp. 225-235.

[17] Lee, Joo-Ha, Yoon, Young-soo, Lee, Seung-Hoon, Cook, W.D., and Mitchell, D. (2008). “Enhancing Performance of Slab-Column Connections,” Journal of Structural Engineering, V. 134, Issue. 3, pp. 448-457.

[18] Hanai, J.B. and Holanda, K.M.A. (2008). “Similarities between punching and shear strength of steel fiber reinforced concrete (SFRC) slabs and beams,” IBRACON Structures and Materials Journal, V. 1, No. 1, pp. 1-16.

[19] Yang, J.M., Yoon, Y.S., Cook, W.D. and Mitchell, D. (2010). "Punching Shear Behavior of Two-Way Slabs Reinforced with High-Strength Steel," ACI Structural Journal, V. 107, No. 4, pp. 468-475.

[20] Nguyen-Minh, L., Rovnak, M., Tran-Quoc, T. and Nguyen-Kim, K. (2010). "Punching Shear Resistance of Steel Fiber Reinforced Concrete Flat Slabs," Procedia Engineering, V. 14, pp. 1830-1837.

[21] Cheng, M.Y. and Parra-Montesinos, G. J. (2010). "Evaluation of steel fiber reinforcement for punching shear resistance in slab-column connections- Part I: Monotonically increased load," ACI Structural Journal, V. 107, No. 1, pp. 101-109.

[22] Higashiyma, H., Ota, A. and Mizukoshi, M. (2011). "Design equation for punching shear capacity of SFRC slabs," International Journal of Concrete Structures and Materials, V. 5, No. 1, pp. 35-42.

[23] Perumal, P., and Thanukumari, B. (2010). "Seismic Performance of Hybrid Fibre Reinforced Beam-Column Joint," International Journal of Civil and Structural Engineering, V. 1, No. 4, pp. 749-774.

[24] Ding, Y., You, Z., and Jalali, S. (2010). "Hybrid Fibre Influence on Strength and Toughness of RC Beams," Composite Structures, V. 92, No. 9, pp. 2083-2089.

[25] Noghabai, K., (2000). "Beams of Fibrous Concrete in Shear and Bending: Experiment and Model," Journal of Structural Engineering, V. 126, No. 2, pp. 243-251.

[26] Kutzing, L., and Konig, G. (2000). "Punching Behaviour of High Performance Concrete Columns with Fibre Cocktails," Leipzig Annual Civil Engineering Report Lacer, V. 5, pp. 253-260.

[27] MU, Bin, and Meyer, C. (2002). "Bending and Punching Shear Strength of Fiber-Reinforced Glass Concrete Slabs," ACI Materials Journal, V. 100, No. 2, pp. 127-132

[28] Ostertag, C. P., and Blunt, J. (2007). "Hybrid Fiber Reinforced Concrete for Use in Bridge Approach Slabs," CBM-CI International Workshop, Karachi, Pakistan.

[29] Hadi, M. N. S. (2008). "An Investigation of the Behaviour of Steel and Polypropylene Fibre Reinforced Concrete Slabs," 7th International Conference Concrete, Dundee, Scotland.

[30] ACI Committee 318, "Building code requirements for structural concrete (ACI 318-11) and commentary (ACI 318M-11)," ACI 318-11, American Concrete Institute, Farmington Hills, Michigan, 2011.

[31] CSA, Canadian Standards Association, "Design of concrete structures for buildings," CSA A23.3-04, Rexdale, Ontario, Canada, 2004.

[32] Zhang, Qi (2006). "Behavior of Two-Way Slabs Reinforced with CFRP Bars," Master Thesis, Faculty of Engineering and Applied Science, Memorial University of Newfoundland, St. John's, Canada, pp. 209.

Appendix A.

Details of the Database

Table A.1. Details of test slabs and results

References	Specimen	Loading area (mm)	Slab thickness (mm)	Average effective depth (mm)	Compressive strength (MPa)	Reinforcement ratio (%)	Fibre volume fraction (%)	Aspect Ratio of fibres	Maximum load (kN)	Mode of failure
Swamy & Ali (1982)	S-1	150	125	100	38.92	0.56	0.0		197	Punching
	S-2	150	125	100	38.4	0.56	0.6	100	243	Punching
	S-3	150	125	100	38.4	0.56	0.9	100	262	Punching
	S-4	150	125	100	38.4	0.56	1.2	100	281	Punching
Theo. & Swamy (1993)	FS-20	150	125	100	37.04	0.37	1.0	100	211	Punching
McHarg et al. (2000)	NU	225	150	110	30	1.1	0.0		306	
	NB	225	150	110	30	2.1	0.0		349	

Yang et al. (2010)	S1-U	225	150	109	37.2	1.18	0.0		301	
	S1-B	225	150	109	37.2	2.15	0.0		317	
	MU1	225	150	109	35.3	1.18	0.0		382	
	MU2	225	150	112	35.3	0.64	0.0		296	
	MB2	225	150	112	35.3	1.36	0.0		282	
Alexander & Simmonds (1993)	P11F0	200	155	134	33.2	0.5	0.00		257	Flexure
	P11F31	200	155	134	35.8	0.5	0.40		324	Flexure
	P11F66	200	155	134	35	0.5	0.85		345	Flexure
	P38F0	200	155	107	35.6	0.62	0.00		264	Flexure
	P38F34	200	155	107	38.4	0.62	0.43		308	Flexure
	P38F69	200	155	107	38.5	0.62	0.87		330	Flexure
Shaaban & Gesund (1995)	SFO-1	63.5	82.5	59.5	33.39	2.03	0.00		90	Punching
	SFO-2	63.5	82.5	59.5	39.05	2.03	0.00		113	Punching
	SFO-3	63.5	82.5	59.5	31.05	2.03	0.00		81	Punching
	SFO-4	63.5	82.5	59.5	31.74	2.03	0.00		95	Punching
	SF2-1	63.5	82.5	59.5	34.5	2.03	0.61		95	Punching
	SF2-2	63.5	82.5	59.5	37.26	2.03	0.61		113	Punching
	SF2-3	63.5	82.5	59.5	29.67	2.03	0.61		72	Punching
	SF2-4	63.5	82.5	59.5	24.84	2.03	0.61			Punching
	SF3-1	63.5	82.5	59.5	37.67	2.03	0.95		108	Punching
	SF4-1	63.5	82.5	59.5	46.78	2.03	1.19		135	Punching
	SF4-2	63.5	82.5	59.5	36.57	2.03	1.19		117	Punching
	SF6-1	63.5	82.5	59.5	22.35	2.03	1.86		99	Punching
	SF6-2	63.5	82.5	59.5	22.08	2.03	1.95		104	Punching
Harajli et al. (1995)	A1	100	55	39	29.6	1.12	0.0		62.5	Punching
	A2	100	55	39	30	1.12	0.45	100	67.6	Punching
	A3	100	55	39	31.4	1.12	0.8	100	77.7	Flexural
	A4	100	55	39	24.6	1.12	1.0	60	68.8	Ductile punching
	A5	100	55	39	20	1.12	2.0	60	62.0	Flexural
	B1	100	75	55	31.4	1.12	0.0		99.3	Punching

	B2	100	75	55	31.4	1.12	0.45	100	114	Punching
	B3	100	75	55	31.8	1.12	0.8	100	117	Punching
	B4	100	75	55	29.1	1.12	1.0	60	117	Punching
	B5	100	75	55	29.2	1.12	2.0	60	145	Punching
Nguyen-Minh et al. (2010)	A0	150	125	105	21.68	0.66	0.00		284	Punching
	A1	150	125	105	22.32	0.66	0.22	80	330	Punching
	A2	150	125	105	23.36	0.66	0.34	80	345	Punching
	A3	150	125	105	25.28	0.66	0.45	80	397	Punching
	B0	150	125	105	21.68	0.66	0.00		301	Punching
	B1	150	125	105	22.32	0.66	0.22	80	328	Punching
	B2	150	125	105	23.36	0.66	0.34	80	337	Punching
	B3	150	125	105	25.28	0.66	0.45	80	347	Punching
	C0	150	125	105	21.68	0.66	0.00		264	Punching
	C1	150	125	105	22.32	0.66	0.22	80	307	Punching
	C2	150	125	105	23.36	0.66	0.34	80	310	Punching
	C3	150	125	105	25.28	0.66	0.45	80	326	Punching
Cheng & Parra-Montesinos (2010)	S1	152	152	126	47.7	0.83	0.0		433	Punching
	S2	152	152	126	47.7	0.56	0.0		379	Ductile punching
	S3	152	152	126	25.4	0.83	1.0	54.5	386	Punching
	S4	152	152	126	25.4	0.56	1.0	54.5	389	Flexure
	S7	152	152	126	31	0.83	1.5	54.5	522	Ductile punching
	S8	152	152	126	31	0.56	1.5	54.5	472	Flexure
Higashiya-ma et al. (2011)	t100-0.67		100	70	24.6	0.85	0.67	48.4	137.5	
	t140-0.67		140	110	24.6	0.54	0.67	48.4	210.2	
	t180-0.67		180	150	24.6	0.40	0.67	48.4	297.6	
	t100-0.72		100	65	42.4	0.91	0.72	48.4	140.8	
	t140-0.72		140	105	42.4	0.57	0.72	48.4	213.2	
	t180-		180	145	42.4	0.41	0.72	48.4	290.7	

	0.72									
	t100-0.91		100	65	21.6	0.91	0.91	48.4	120.8	
	t140-0.91		140	105	21.6	0.57	0.91	48.4	183.1	
	t180-0.91		180	145	21.6	0.41	0.91	48.4	231.2	
	t100-0.63		100	70	27.8	0.85	0.63	48.4	152.3	
	t100-0.94		100	70	31.1	0.85	0.94	48.4	147.9	
	t100-1.03		100	70	30.4	0.85	1.03	48.4	158.9	
Hanai & Holanda (2008)	L1	80	100	80		1.57	0.00		137.2	
	L2	80	100	80		1.57	1.00	54.5	139.5	
	L3	80	100	80		1.57	2.00	54.5	163.6	
	L4	80	100	80		1.57	0.00		192.8	
	L5	80	100	80		1.57	1.00	54.5	215.1	
	L6	80	100	80		1.57	2.00	54.5	236.1	
	L7	80	100	80		1.57	0.75	48.0	182.8	
	L8	80	100	80		1.57	1.50	48.0	210.9	
Narayanan & Darwish (1987)	S1	100	60	40.0	43.28	2.01	0.00	100	86.5	Punching
	S2	100	60	40.0	52.08	2.01	0.25	100	93.4	Punching
	S3	100	60	40.0	44.72	2.01	0.50	100	102.0	Punching
	S4	100	60	40.0	46	2.01	0.75	100	107.5	Ductile punching
	S5	100	60	40.0	52.96	2.01	1.00	100	113.6	Ductile punching
	S6	100	60	40.0	53.04	2.01	1.25	100	122.2	Ductile punching
	S7	100	60	40.0	46.96	1.79	1.00	100	92.6	Ductile punching
	S8	100	60	40.0	45.28	2.24	1.00	100	111.1	Ductile punching
	S9	100	60	40.0	43.52	2.46	1.00	100	111.3	Ductile punching
	S10	100	60	40.0	47.6	2.69	1.00	100	113.3	Ductile punching
	S11	100	60	40.0	29.76	2.01	1.00	100	82.1	Ductile punching
	S12	100	60	40.0	32.4	2.01	1.00	100	84.9	Ductile punching

Table A.2. Test results vs. prediction equations (V_{test} / $V_{predicted}$)

References	Specimen	CSA A23.3-03	ACI 318M-05	BS8110-97	CEB-FIP MC90	JSCE	Narayanan & Darwish [12]	Shaaban & Gesund [14]	Harajli, Maalouf & Khatib [15]	DE Hanai & Holanda [18]	Hiroshi Higashiyama, et al. [22]
Swamy & Ali (1982)	S-1	0.83	0.96	1.44	1.07	1.04	0.94	0.56	0.59	0.95	1.04
	S-2	1.03	1.19	1.78	1.33	1.28	0.73	0.64	0.66	1.11	0.86
	S-3	1.12	1.29	1.92	1.43	1.38	0.76	0.66	0.68	1.16	0.85
	S-4	1.18	1.36	2.05	1.53	1.48	0.85	0.68	0.69	1.19	0.89
Theo. & Swamy (1993)	FS-20	0.91	1.05	1.76	1.34	1.27	0.63	0.53	0.55	0.94	0.77
McHarg et al. (2000)	NU	1.00	1.15	1.36	1.08	0.99	1.08	0.67	0.70	1.14	0.99
	NB	1.14	1.31	1.25	1.00	0.91	1.03	0.76	0.80	1.30	0.91
Yang et al. (2010)	S1-U	0.89	1.03	1.28	0.97	0.88	0.93	0.60	0.63	1.02	0.88
	S1-B	0.94	1.08	1.10	0.86	0.76	0.84	0.63	0.66	1.07	0.76
	MU1	1.16	1.34	1.62	1.25	1.13	1.22	0.78	0.82	1.33	1.13
	MU2	0.87	1.00	1.47	1.14	1.03	1.02	0.58	0.61	0.99	1.03
	MB2	0.82	0.95	1.09	0.84	0.76	0.85	0.55	0.58	0.94	0.76
Alexander & Simmonds (1993)	P11F0	0.66	0.75	1.09	0.85	0.82	0.81	0.44	0.46	0.75	0.82
	P11F31	0.80	0.92	1.37	1.05	0.99	0.97	0.50	0.53	0.87	0.99
	P11F66	0.86	0.99	1.46	1.13	1.07	1.05	0.51	0.53	0.89	1.07
	P38F0	0.89	1.02	1.50	1.16	1.06	0.97	0.59	0.62	1.01	1.06
	P38F34	1.00	1.15	1.75	1.31	1.22	1.08	0.63	0.65	1.09	1.22
	P38F69	1.07	1.23	1.88	1.41	1.31	1.15	0.63	0.65	1.11	1.31
	SFO-1	1.40	1.61	1.34	1.05	1.05	1.05	0.94	0.99	1.60	1.05
	SFO-2	1.63	1.87	1.68	1.25	1.27	1.22	1.09	1.14	1.86	1.27

Shaaban & Gesund (1995)	SFO-3	1.31	1.51	1.23	0.97	0.98	0.98	0.88	0.92	1.50	0.98
	SFO-4	1.51	1.74	1.43	1.13	1.14	1.14	1.02	1.07	1.73	1.14
	SF2-1	1.45	1.67	1.41	1.10	1.09	1.09	0.90	0.93	1.56	1.09
	SF2-2	1.66	1.92	1.68	1.27	1.27	1.25	1.03	1.06	1.78	1.27
	SF2-3	1.19	1.37	1.11	0.88	0.89	0.89	0.73	0.76	1.27	0.89
	SF3-1	1.58	1.82	1.60	1.21	1.22	1.19	0.93	0.96	1.63	1.22
	SF4-1	1.77	2.04	2.00	1.40	1.52	1.32	1.02	1.04	1.79	1.52
	SF4-2	1.74	2.00	1.74	1.32	1.32	1.31	1.00	1.02	1.75	1.32
	SF6-1	1.88	2.17	1.69	1.33	1.42	1.39	1.00	1.01	1.78	1.42
	SF6-2	1.99	2.29	1.78	1.41	1.50	1.47	1.04	1.06	1.86	1.50
Harajli et al. (1995)	A1	1.39	1.61	2.00	1.59	1.41	1.58	0.93	0.98	1.60	1.41
	A2	1.50	1.73	2.16	1.71	1.52	1.09	0.94	0.98	1.63	1.05
	A3	1.68	1.94	2.44	1.93	1.71	1.13	1.01	1.05	1.77	1.04
	A4	1.68	1.94	2.35	1.86	1.71	1.10	0.99	1.02	1.73	1.04
	A5	1.68	1.94	2.28	1.81	1.71	1.01	0.88	0.89	1.57	0.84
	B1	1.37	1.58	1.81	1.43	1.33	1.42	0.92	0.96	1.57	1.33
	B2	1.58	1.82	2.09	1.65	1.54	1.07	0.99	1.03	1.72	1.07
	B3	1.61	1.85	2.13	1.68	1.56	1.00	0.96	1.00	1.68	0.95
	B4	1.68	1.94	2.20	1.74	1.64	1.06	0.99	1.02	1.73	1.04
	B5	2.08	2.39	2.72	2.15	2.03	1.32	1.08	1.10	1.94	1.14
Nguyen-Minh et al. (2010)	A0	1.50	1.73	2.10	1.65	1.69	1.81	1.01	1.05	1.71	1.69
	A1	1.72	1.98	2.42	1.90	1.94	1.46	1.11	1.16	1.91	1.55
	A2	1.75	2.02	2.48	1.96	1.98	1.37	1.12	1.17	1.93	1.47
	A3	1.94	2.23	2.78	2.19	2.19	1.43	1.22	1.27	2.11	1.54
	B0	1.59	1.83	2.23	1.75	1.80	1.92	1.07	1.12	1.82	1.80
	B1	1.71	1.96	2.40	1.89	1.93	1.45	1.11	1.16	1.90	1.54
	B2	1.71	1.97	2.43	1.91	1.94	1.33	1.10	1.14	1.89	1.43
	B3	1.70	1.95	2.43	1.91	1.92	1.25	1.07	1.11	1.85	1.34
	C0	1.39	1.60	1.95	1.54	1.57	1.69	0.93	0.98	1.59	1.57
	C1	1.60	1.84	2.25	1.77	1.80	1.36	1.04	1.08	1.78	1.44

	C2	1.58	1.81	2.23	1.76	1.78	1.23	1.01	1.05	1.74	1.32
	C3	1.59	1.83	2.28	1.80	1.80	1.17	1.00	1.04	1.73	1.26
Cheng & Parra-Montesinos (2010)	S1	1.18	1.36	1.87	1.29	1.39	1.18	0.79	0.83	1.35	1.39
	S2	1.03	1.19	1.86	1.29	1.39	1.08	0.69	0.73	1.18	1.39
	S3	1.44	1.66	1.83	1.44	1.48	0.90	0.84	0.87	1.48	0.93
	S4	1.45	1.67	2.10	1.65	1.70	0.93	0.85	0.87	1.49	1.07
	S7	1.76	2.03	2.31	1.81	1.81	1.09	0.97	0.99	1.72	1.09
	S8	1.59	1.83	2.38	1.87	1.87	1.00	0.88	0.90	1.56	1.12
Higashiya-ma et al. (2011)	t100-0.67	1.53	1.76	2.01	1.58	1.59	0.99	0.94	0.97	1.63	1.14
	t140-0.67	1.21	1.39	1.64	1.29	1.39	0.79	0.74	0.76	1.28	1.00
	t180-0.67	1.05	1.21	1.47	1.15	1.30	0.68	0.64	0.67	1.12	0.93
	t100-0.72	1.33	1.53	2.05	1.48	1.47	0.88	0.81	0.83	1.40	1.11
	t140-0.72	1.00	1.15	1.60	1.15	1.23	0.67	0.61	0.63	1.06	0.93
	t180-0.72	0.83	0.95	1.36	0.98	1.10	0.55	0.50	0.52	0.87	0.83
	t100-0.91	1.59	1.84	2.05	1.61	1.63	0.90	0.95	0.97	1.65	1.05
	t140-0.91	1.20	1.39	1.60	1.25	1.37	0.68	0.71	0.74	1.25	0.88
	t180-0.91	0.92	1.06	1.26	0.99	1.13	0.52	0.55	0.56	0.96	0.73
	t100-0.63	1.60	1.84	2.13	1.68	1.66	1.07	0.98	1.02	1.71	1.23
	t100-0.94	1.47	1.69	1.99	1.57	1.52	0.92	0.87	0.89	1.52	1.05
	t100-1.03	1.59	1.83	2.16	1.70	1.66	0.98	0.93	0.96	1.63	1.11
DE Hanai & Holanda (2008)	L1	1.31	1.51	1.31	1.03	1.07	1.14	0.88	0.92	1.68	1.07
	L2	1.31	1.51	1.32	1.03	1.07	0.73	0.77	0.79	1.49	0.70
	L3	1.42	1.64	1.49	1.15	1.16	0.82	0.74	0.75	1.48	0.69
	L4	1.17	1.35	1.75	1.18	1.34	0.91	0.78	0.82	1.50	1.34
	L5	1.28	1.47	1.96	1.32	1.50	0.81	0.75	0.77	1.47	1.02
	L6	1.51	1.73	2.15	1.45	1.65	1.00	0.78	0.79	1.56	0.99
	L7	1.40	1.61	1.66	1.17	1.27	0.90	0.85	0.88	1.64	0.95
	L8	1.42	1.64	1.92	1.29	1.47	0.88	0.78	0.80	1.56	0.95
	S1	1.33	1.53	1.75	1.27	1.19	1.25	0.89	0.93	1.52	1.19
	S2	1.30	1.50	1.89	1.29	1.29	1.00	0.84	0.88	1.45	1.03

Narayanan & Darwish (1987)	S3	1.54	1.77	2.07	1.48	1.41	1.07	0.96	1.00	1.67	0.98
	S4	1.60	1.84	2.18	1.54	1.48	1.09	0.97	1.00	1.69	0.95
	S5	1.57	1.81	2.30	1.56	1.57	1.13	0.92	0.95	1.62	0.95
	S6	1.69	1.95	2.48	1.68	1.69	1.32	0.96	0.99	1.70	1.01
	S7	1.36	1.57	1.95	1.37	1.33	0.97	0.80	0.82	1.40	0.81
	S8	1.66	1.92	2.17	1.60	1.48	1.14	0.98	1.00	1.71	0.90
	S9	1.70	1.96	2.11	1.63	1.43	1.14	1.00	1.03	1.75	0.87
	S10	1.66	1.91	2.08	1.60	1.42	1.12	0.97	1.00	1.70	0.86
	S11	1.52	1.75	1.73	1.37	1.24	0.94	0.89	0.91	1.56	0.72
	S12	1.50	1.73	1.74	1.37	1.23	0.96	0.88	0.91	1.55	0.73
Mean		1.39	1.60	1.86	1.42	1.41	1.07	0.85	0.88	1.49	1.10
Standard deviation		0.31	0.36	0.40	0.32	0.31	0.26	0.18	0.18	0.31	0.25
Coefficient of variation		0.22	0.23	0.21	0.22	0.22	0.24	0.21	0.21	0.21	0.22

Appendix B.

Detailed Experimental Results

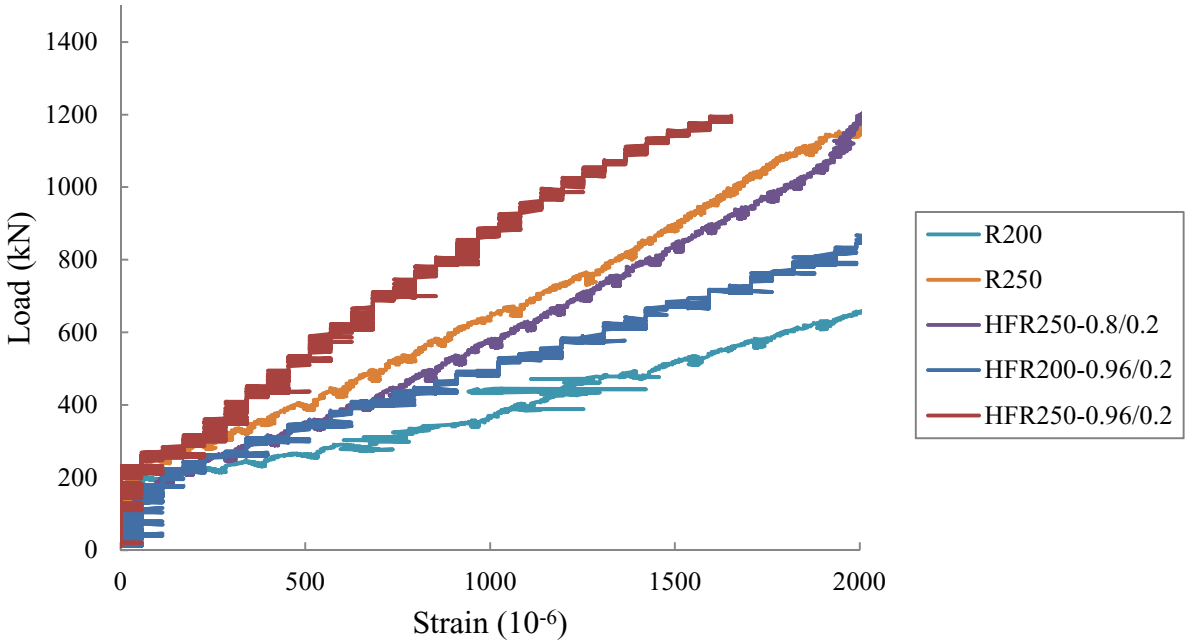

Figure B.1. Load-steel strain behaviour of the slabs (Steel gauge 2)

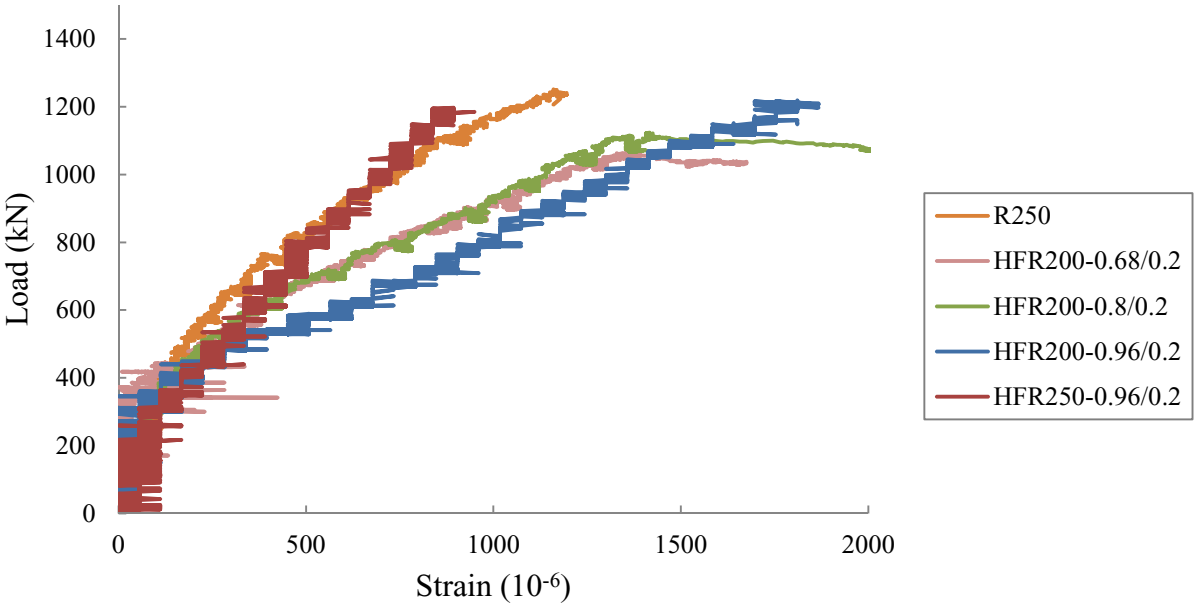

Figure B.2. Load-steel strain behaviour of the slabs (Steel gauge 3)

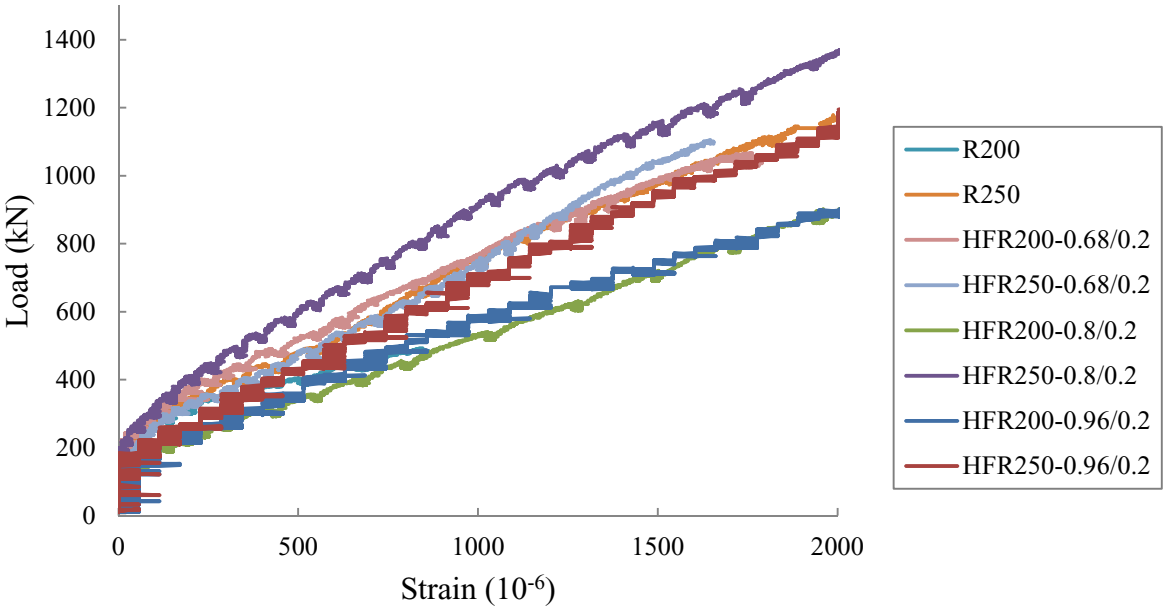

Figure B.3. Load-steel strain behaviour of the slabs (Steel gauge 5)

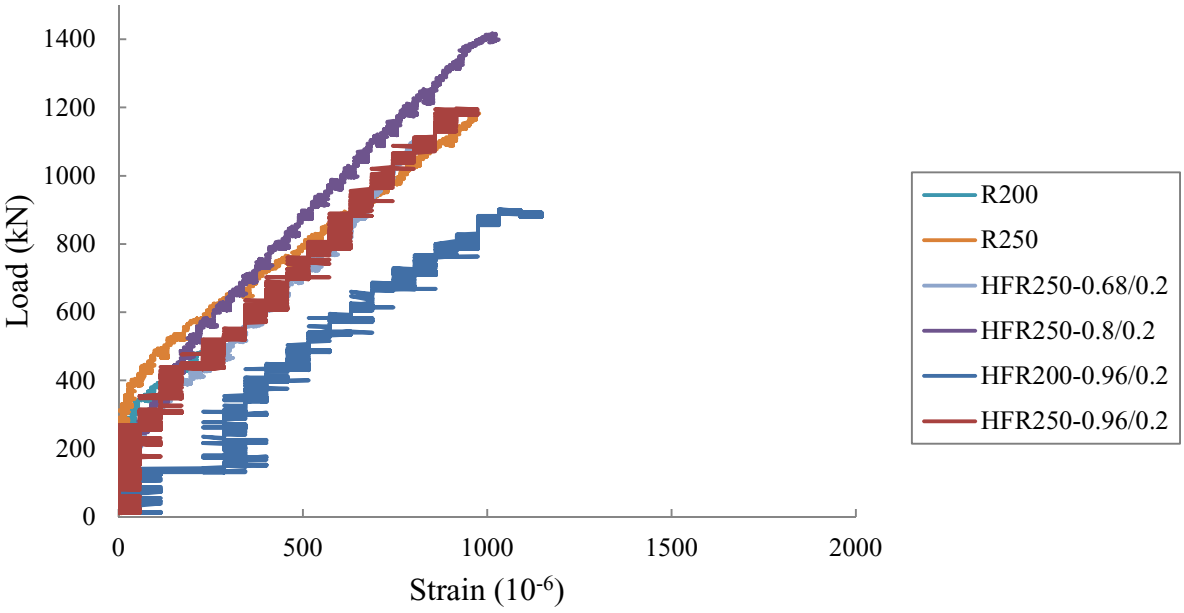

Figure B.4. Load-steel strain behaviour of the slabs (Steel gauge 6)

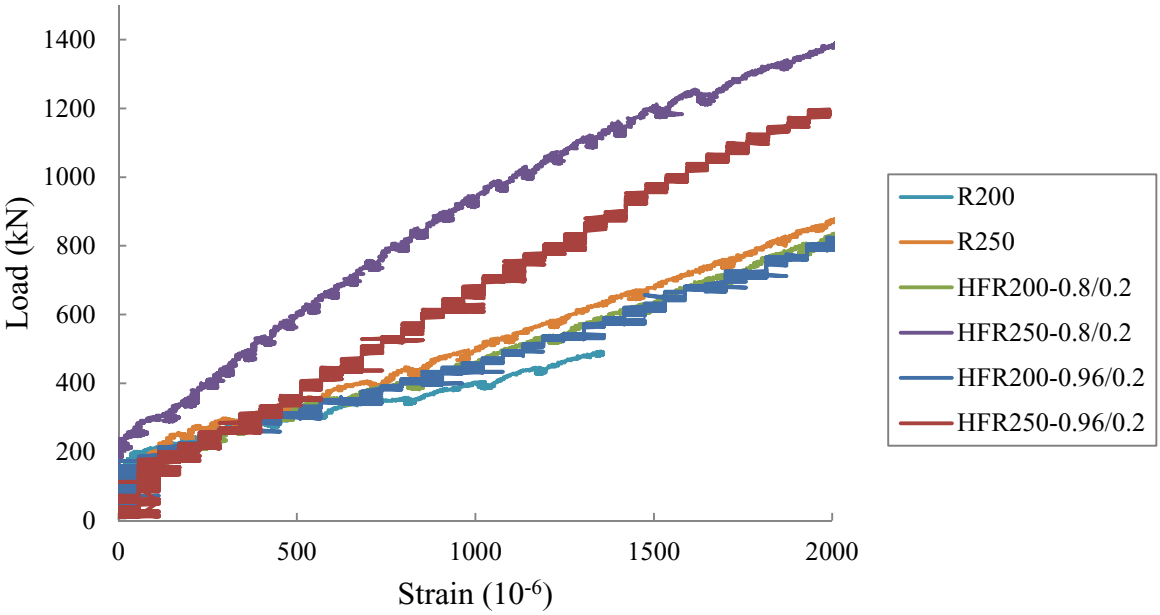

Figure B.5. Load-steel strain behaviour of the slabs (Steel gauge 7)

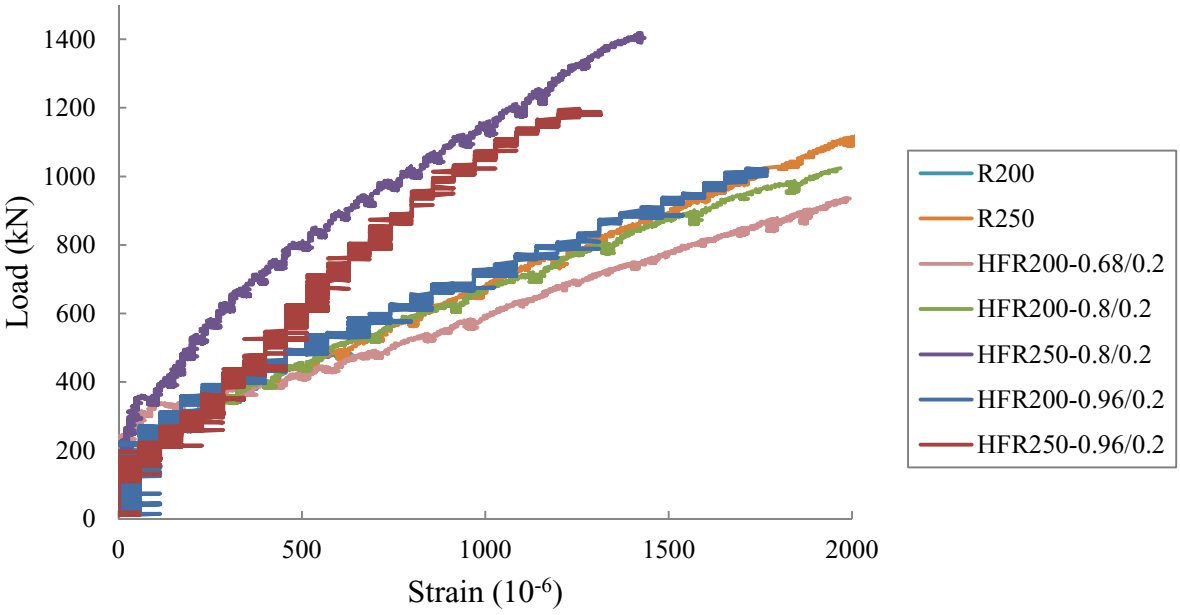

Figure B.6. Load-steel strain behaviour of the slabs (Steel gauge 8)

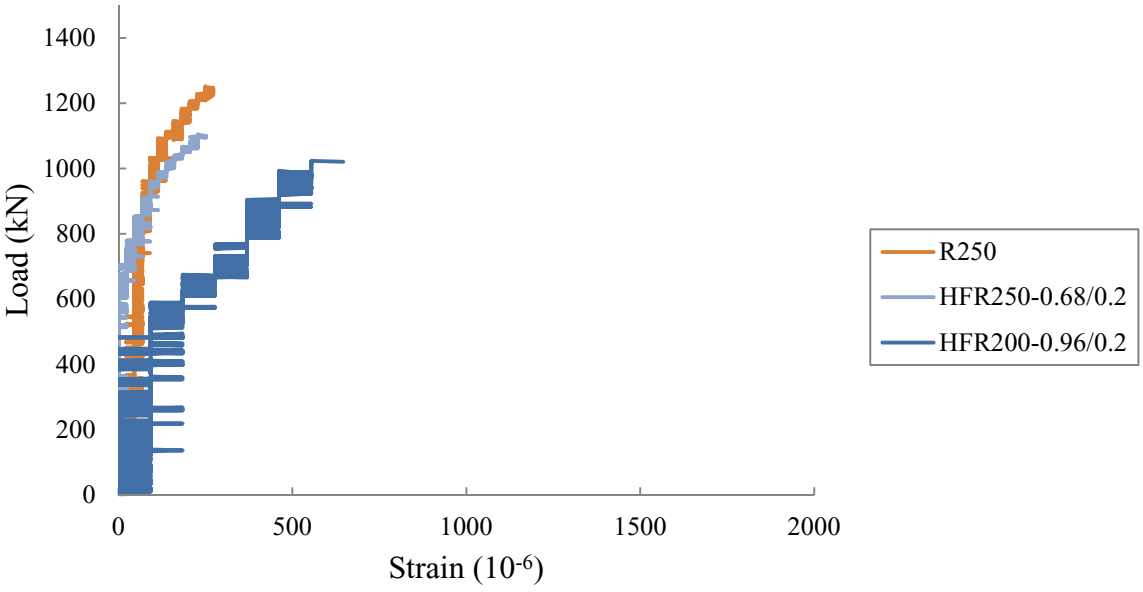

Figure B.7. Load-steel strain behaviour of the slabs (Steel gauge 9)

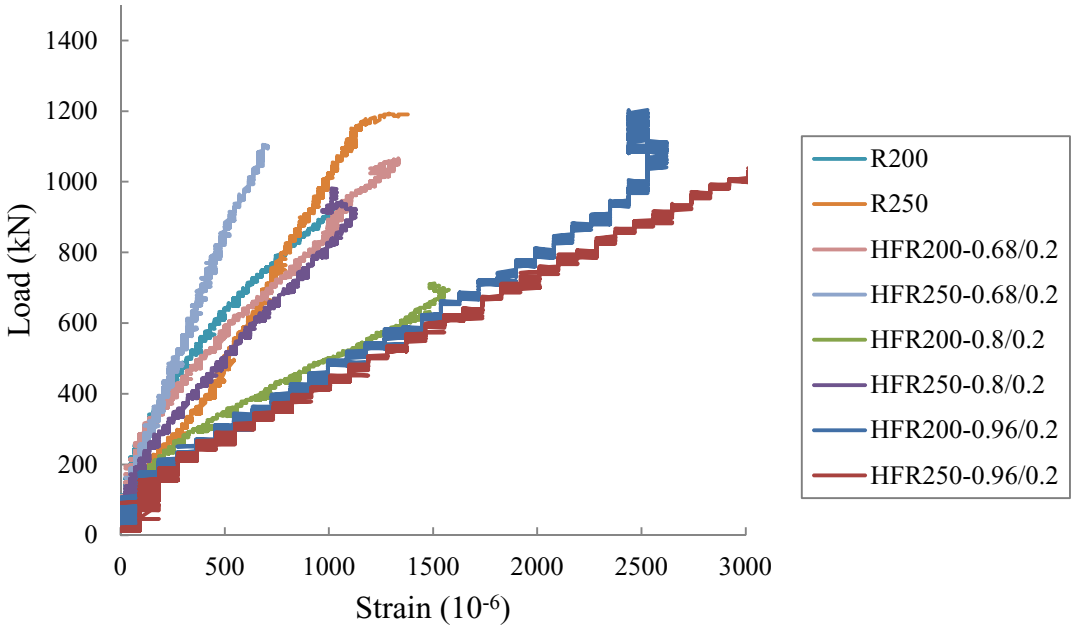

Figure B.8. Load-concrete strain behaviour at 30 mm from the column face

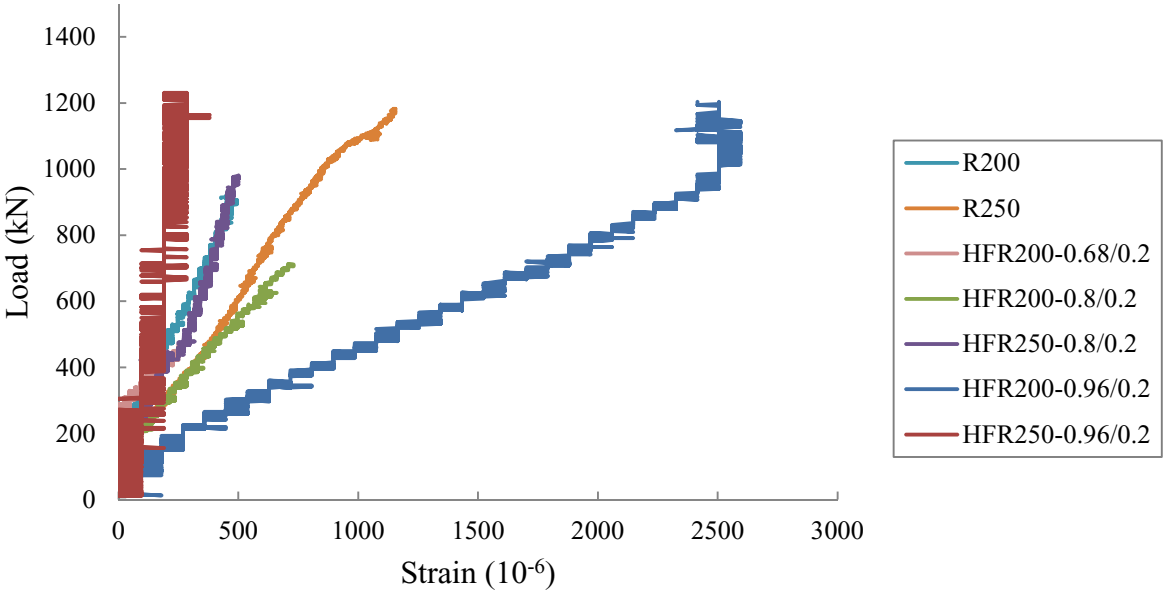

Figure B.9. Load-concrete strain behaviour at 100 mm from the column face

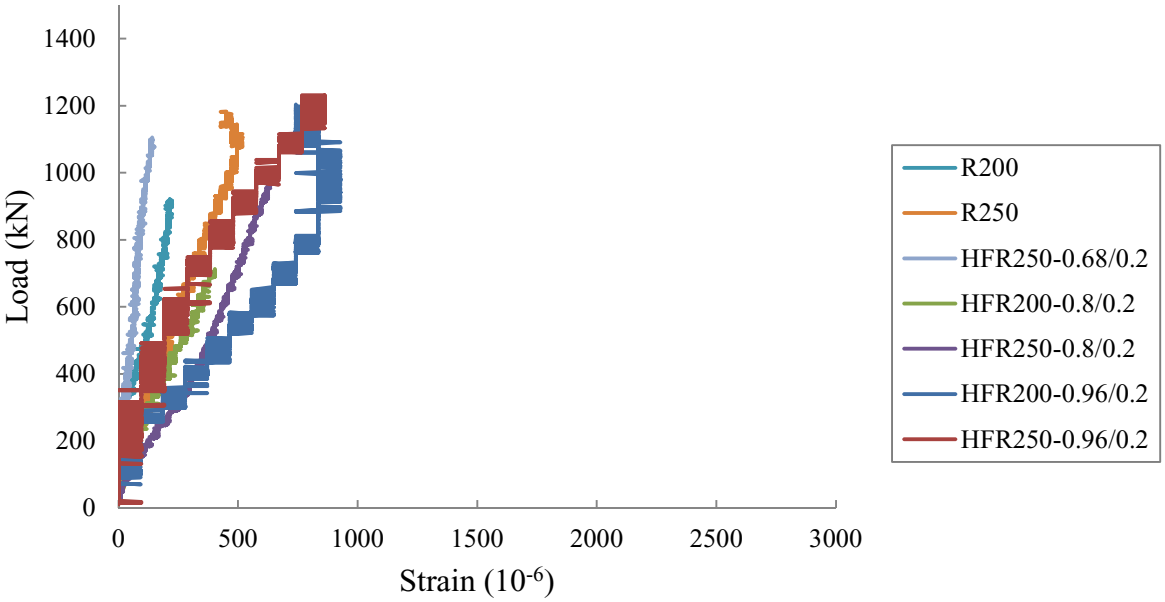

Figure B.10. Load-concrete strain behaviour at 200 mm from the column face

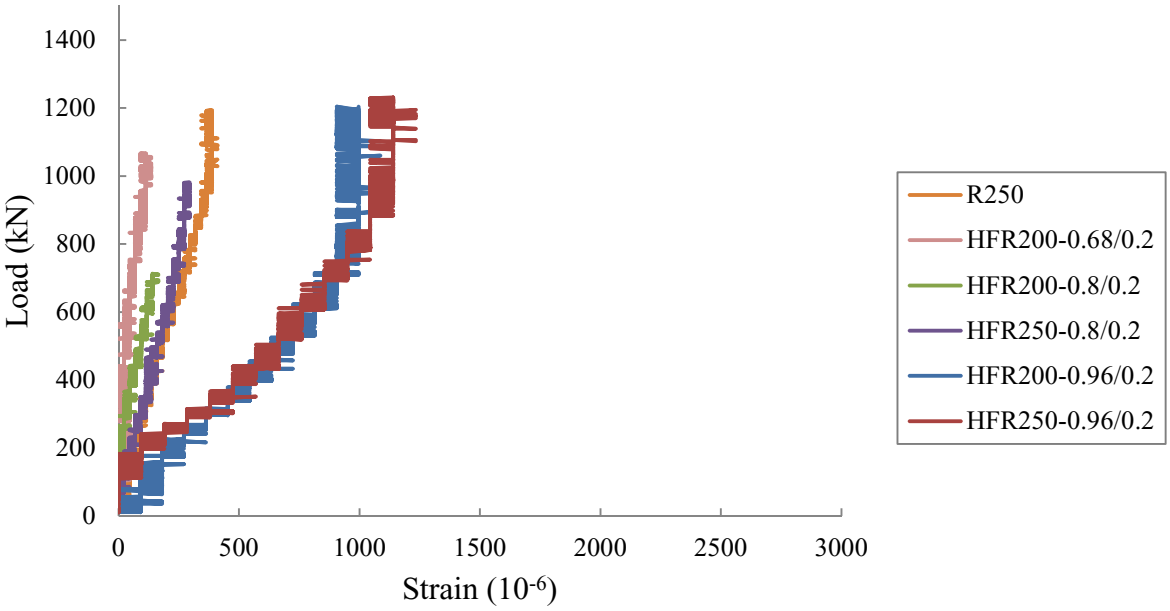

Figure B.11. Load-concrete strain behaviour at 300 mm from the column face